

# NATIONAL ADVISORY COMMITTEE FOR AERONAUTICS

TECHNICAL NOTE 2117

DESIGN AND APPLICATIONS OF HOT-WIRE ANEMOMETERS  
FOR STEADY-STATE MEASUREMENTS AT TRANSONIC  
AND SUPERSONIC AIRSPEEDS

By Herman H. Lowell

Lewis Flight Propulsion Laboratory  
Cleveland, Ohio



Washington  
July 1950

CONN. STATE LIBRARY

JUL 5 1950

BUSINESS, SCIENCE  
& TECHNOLOGY DEPT.

NACA TN 2117

629.1309

Un34

Y3.N215:6/2117





# TABLE OF CONTENTS

	Page
SUMMARY . . . . .	1
INTRODUCTION . . . . .	1
BASIC CONSIDERATIONS . . . . .	3
Basic Instrument . . . . .	3
Nature of device . . . . .	4
Nondimensional correlation of heat losses from wires . . . . .	5
Exposure at oblique incidence . . . . .	8
Behavior of exposed unheated wire . . . . .	9
Radiation losses . . . . .	10
Possible Array Configurations and Uses . . . . .	10
Uses and procedures identical for all arrays . . . . .	10
Single-wire array . . . . .	12
V-array . . . . .	13
Parallel-wire array . . . . .	16
Combination array . . . . .	17
Pyramidal array . . . . .	17
INSTRUMENT DESIGN PROBLEMS . . . . .	18
End losses . . . . .	18
Aerodynamic stress effects . . . . .	21
Impact effects . . . . .	23
Vibration effects . . . . .	24
Oxidation . . . . .	25
Electric stability . . . . .	25
Reconciliation of conflicting requirements . . . . .	26
REALIZED DESIGNS AND CONSTRUCTION . . . . .	30
Evaluation of Materials . . . . .	30
Wire materials . . . . .	30
Support materials . . . . .	34
Mount Details and Assembly . . . . .	35
Mount details . . . . .	35
Wire mounting . . . . .	37
Types in use . . . . .	39
APPARATUS . . . . .	39
Test Tunnel . . . . .	39
Bridge . . . . .	40
Uniform-Temperature Baths . . . . .	41
PROCEDURES . . . . .	42
Mass-Flow or Heat-Loss Measurement . . . . .	42
Angle Data . . . . .	43
Temperature Measurement . . . . .	44



	Page
CALCULATIONS AND CORRECTIONS . . . . .	45
Evaluation of fluid constants . . . . .	45
End losses . . . . .	45
Stress corrections . . . . .	47
EXPERIMENTAL RESULTS AND DISCUSSION . . . . .	49
Calibration and Mass-Flow Determination . . . . .	49
Calibration of single wire normal to stream . . . . .	49
Correlation equations . . . . .	50
Adaptation of generalized correlation for mass-flow- determination applications . . . . .	53
Limitation of $Re^*$ method . . . . .	55
Yaw Characteristics of Angle-Sensitive Arrays . . . . .	56
V-array . . . . .	56
Parallel-wire array . . . . .	56
Temperature Recovery Ratio . . . . .	57
CONCLUSIONS . . . . .	58
APPENDIX A - SYMBOLS . . . . .	59
APPENDIX B - END LOSSES OF WIRES . . . . .	65
APPENDIX C - WIRE STRESS AND SUPPORT DEFLECTION . . . . .	73
Aerodynamic Stress . . . . .	73
Deflection of Wire Support . . . . .	78
REFERENCES . . . . .	81



NATIONAL ADVISORY COMMITTEE FOR AERONAUTICS

---

TECHNICAL NOTE 2117

---

DESIGN AND APPLICATIONS OF HOT-WIRE ANEMOMETERS  
FOR STEADY-STATE MEASUREMENTS AT TRANSONIC  
AND SUPERSONIC AIRSPEEDS

By Herman H. Lowell

SUMMARY

An investigation was made of the design requirements and heat-transfer characteristics of exposed-wire instruments to be used for steady-state measurements at transonic and supersonic speeds. Design criterions, construction details, and typical response behavior are presented.

Several types of instrument were evolved that, in addition to exhibiting the required high stability, are capable of providing steady-state mass-flow, flow-angle, and temperature information of engineering accuracy at total temperatures at least as high as 275° C, Mach numbers at least as great as 2.4, and air total densities at least as great as twice atmospheric. Heat-transfer data for a circular cylinder over at least the Mach number range from 0 to 2.4 may be correlated by addition to the conventional relation among Nusselt, Prandtl, and Reynolds numbers of a factor that is a function of Mach number only. Finally, it is shown that the combination of an air-temperature datum (obtained with a wire), a wire heat-loss datum, and a pressure datum limited to pressures not exceeding static by more than about 20 percent of the velocity head uniquely specifies a steady-state flow.

INTRODUCTION

In connection with the investigation of the behavior of existing compressors and turbines (turbomachines) or of proposed improved components, it is often necessary to obtain a detailed picture of the air flow occurring throughout interblade channels, between stator and rotor cascades, within blade or shroud boundary layers, immediately behind trailing edges of the blades, or within engine ducts.



Demands upon flow instrumentation are severe; even when a device of the pressure-tube or thermocouple type provides accurate data concerning one variable, it is incapable of providing all the required information concerning local flow characteristics.

In principle, the fine wire used as a resistance thermometer or hot-wire anemometer is superior in several respects to either the pressure tube or the thermocouple. A wire or wire array may have very small dimensions and the response time is measured, at most, in milliseconds; moreover, wires are equally useful (at low airspeeds) for temperature, angle, and mass-flow determinations. It appeared probable that wire data (at high airspeeds), if supplemented by pressure information (which could, when necessary and when space limitations did not prohibit, be provided by an integral pressure tube), could be made to yield Mach number information as well as other information despite the unavailability of any additional data concerning a compressible-flow situation.

Previous efforts in the field (prior to about 1940) were largely confined to the speed region below  $10^4$  centimeters per second. Some success was achieved with the idea of using wires to measure both flow rates and angles (references 1 and 2). More recently, investigators, having transferred their efforts from platinum to tungsten wires, have obtained a few mass-flow data at transonic speeds (reference 3) and a very few in the supersonic region; the supersonic data were obtained by Dr. Galen B. Schubauer of the National Bureau of Standards (unpublished results). None of the data, however, have exhibited the required susceptibility to correlation. No investigation seems to have been made of the possibility of using exposed wires as resistance thermometers at high Mach numbers, nor has information been published concerning the use of wires at temperatures substantially above room values.

The problem in the case of the gas turbine is to design an instrument of high stability. It is necessary that the wire have high strength, be free of any tendency toward internal structural alteration, be inert to an oxidizing atmosphere, and be electrically stable. The entire device is required to exhibit freedom from aerodynamically induced vibrations.

An investigation has therefore been made at the NACA Lewis laboratory of the design requirements and heat-transfer characteristics of wire instruments to be used at transonic and supersonic speeds. This inquiry was limited to the development of devices that would be useful under substantially steady-flow conditions and at moderate (below  $275^{\circ}\text{C}$ ) ambient total temperatures. The



1289

heat-transfer correlations are nevertheless applicable to unsteady-state conditions, and the basic designs and design procedures evolved are applicable to anemometry at high temperatures and at mass-flow rates higher than those at which data were obtained.

The report consists of two main groups of subjects. The first group comprises matters of a general nature; it is intended chiefly for possible users of hot-wire instruments who have had no experience with such devices. Dimensionless heat-transfer representation (as applying to anemometry), wire (resistance) thermometry, and possible array configurations and uses are discussed. In addition, a section on instrument-design problems based principally upon work performed at the NACA Lewis laboratory is presented. This section, as well as the sections of the second group, contains material not previously published.

The subjects of the second group are, for the most part, restricted to specific work performed at this laboratory. They include realized instrument designs and construction, descriptions of apparatus employed and of investigation procedures, a brief discussion of the calculations made and corrections employed in the evaluation of data, and a discussion of the experimental results obtained.

The heat-transfer characteristics of several instruments are given at mass-flow rates up to about 24 grams per square centimeter per second ( $1.5 \text{ slugs}/(\text{sq ft})(\text{sec})$ ), air total temperatures of approximately  $36^\circ \text{C}$ , wire temperatures up to about  $300^\circ \text{C}$ , and Mach numbers up to about 2.4 at air total densities at least as great as twice atmospheric. The flow limits and the air temperature were established by the characteristics of the test tunnel rather than by the behavior of the instruments.

Application of the generalized heat-loss correlation obtained to flow situations such that the Mach number distribution is unknown is discussed. In particular, it is shown that the combination of a pressure datum (within certain limits) and wire data uniquely specifies the (steady-state) local flow characteristics.

## BASIC CONSIDERATIONS

### Basic Instrument

The known heat-transfer relations relevant to anemometry are discussed in the following sections.



Nature of device. - A heated object placed in a moving stream of fluid loses heat at a rate dependent upon several variables: identity, pressure, and temperature of the fluid; nature, orientation, and temperature of the object; and mass-flow rate of the fluid. It is clear that by properly fixing all other variables at predetermined or ascertainable values, the mass-flow rate will become the sole factor determining the heat-loss rate.

Accordingly, the investigator who determines the rate of heat loss from the experimental object under properly chosen conditions need merely refer to the predetermined relation between heat-loss rate and mass-flow rate to determine the mass-flow rate. Under such circumstances the object becomes an anemometer.

The conventional anemometer measures wind speed (and often direction as well) rather than mass-flow rate. By simple extension, however, the designation "anemometer" may be retained for high-speed measurements because under compressible-flow conditions the product of density and speed generally takes the place of speed.

Electrically heated fine wires have been used as heat-loss (hence, hot-wire) anemometers for many years. The list of references given herein includes only a fraction of the more than 100 reports now available on hot-wire anemometry.

One of the important variables in connection with heat-loss anemometry is, as previously stated, the temperature of the object. The variation of wire resistance with temperature provides such information. Although in precision resistance thermometry complex relations between resistance and temperature must be employed, it is usually found that, for anemometric purposes, the simple law

$$\bar{\theta}_w = \frac{R-R_0}{\alpha R_0} = \frac{\bar{r}-r_0}{\alpha r_0} \quad (1)$$

is adequate.

(All symbols used in this report are defined in appendix A.)



Nondimensional correlation of heat losses from wires. - The classic investigation of heat losses from wires was made by King (reference 4) in 1913-14. He evolved the following wholly theoretical relation:

$$0.2389i^2r = (k_e + \sqrt{2\pi c_{p,e}\rho V D})(\theta_w - \theta_e) \quad (2)$$

Two important conceptions are embodied in equation (2). The heat-loss rate is dependent upon the square root of mass-flow rate and upon the simple difference of temperature between wire and air (Newton's law of cooling as applied to this situation). In this case,  $\theta_e$  equals the static ambient temperature because King assumed the existence of incompressible flow.

When King attempted to confirm his theoretical result experimentally, he was able to confirm the basic structure of the relation but found it necessary to introduce a number of correction factors principally dependent upon wire temperature.

King's law (equation (2)) when written in the form

$$i^2r = (C_1 + C_2\sqrt{\rho V})(\theta_w - \theta_e) \quad (3)$$

is nevertheless adequate over limited ranges of temperature and pressure provided  $C_1$  and  $C_2$  are experimentally determined. Many users of hot-wire anemometers have therefore employed equation (3) as the basic relation of such instrumentation.

The inherent lack of generality of the relation and, in particular, its lack of precision when the constants  $C_1$  and  $C_2$  are evaluated under one set of conditions (air pressure and temperature and wire temperature) and the wire is used under another set have led to attempts to write a relation that would be valid under widely varying circumstances.

Nusselt (modern discussion in Jakob, reference 5) has previously shown (1909-15) that the most general correlation of heat-transfer data for flow of an incompressible fluid is

$$Nu = U(Gr, Pr, Re, \text{temperature function}) \quad (4)$$



in which  $U$  represents some function (of the variables within parentheses) and the temperature function is the ratio of the absolute temperature of the object (surface) to that of the undisturbed stream.

In equation (4), the several dimensionless groups, with the exception of the temperature function, are understood to be evaluated at the free-stream static temperature, pressure, and speed. The presence of the temperature function theoretically ensures correlation despite the variation of gas properties ( $\mu$ ,  $c_p$ , and  $k$ ) with temperature.

In 1934, Dryden (reference 6) indicated (without providing the derivation of the result) that an additional parameter  $k\Delta\theta/\mu V^2$  is demanded, in general, by dimensional considerations in the case of compressible flow ( $\Delta\theta$  is the difference of temperature between stream and object). A result equivalent to his is obtained in reference 7, where it is shown that the group  $V^2/c_p T$  is of significance;  $T$  is the absolute air temperature in this instance. In every generalized heat-transfer correlation, a function of Prandtl number necessarily appears. Because Dryden's parameter is merely the reciprocal of the product

$$\left(\frac{V^2}{c_p \Delta\theta}\right) \left(\frac{c_p \mu}{k}\right)$$

in which the second factor is the Prandtl number, it is evident that the Dryden parameter and  $V^2/c_p T$  provide essentially the same information if the temperature function is understood to be present when required.

From the fact that

$$c_p = \frac{\gamma R_g}{\gamma - 1}$$

it follows that

$$\sqrt{\frac{V^2}{c_p T}} = \frac{V\sqrt{\gamma-1}}{\sqrt{\gamma R_g T}} = M\sqrt{\gamma-1} \quad (5)$$



When the virtually constant  $\sqrt{\gamma-1}$  factor is ignored, it is patent that the stream Mach number must be added to the parameters originally given by Nusselt.

In general, therefore, the Nusselt number is an unspecified function of Grashof, Prandtl, Reynolds, and Mach numbers and of the temperature function. It has been tacitly assumed that geometrically similar bodies similarly oriented with respect to the stream are being considered. Additional terms or factors are required when those two conditions are not fulfilled; the point is subsequently discussed in connection with oblique flow incidence with respect to a cylinder.

The relative simplicity of the circular cylinder with a reasonably large length-to-diameter ratio and normally exposed to a stream has led a number of investigators to obtain heat-transfer data involving such objects and to attempt to correlate their own data and those of others by using two or more of the dimensionless groups already mentioned.

The specific results of such work are discussed in the section Correlation equations. It is sufficient here to mention the following points:

(1) As indicated in connection with fairly comprehensive discussions by McAdams (reference 8) and Jakob (reference 5) of the mechanism and the peculiarities of heat transfer from such cylinders, such studies have not completely clarified the significance of the Nusselt number itself. The most fruitful concept, particularly at Reynolds numbers below about 1000, is that of the enveloping boundary layer, the mean thickness of which decreases with increasing mass-flow rate. The Nusselt number is therefore a measure of the diminution of relative thickness and hence of the thermal resistance of the mean layer.

(2) Little information has been published concerning the influence of Mach number on the Nusselt number.

(3) No purely forced-convective process can exist; free convection must always accompany forced convection. Accordingly, the Grashof number, which is a measure of the intensity of the free convection, must, in theory, affect even high-speed heat-transfer correlations. Beyond some minimal mass-flow rate, however, the influence of Grashof number changes becomes negligible and correlations can be devised in which the Grashof number is replaced by a



suitable constant. In general, it is impossible to predict the minimal mass-flow rate above which such a procedure is permissible. Jakob (reference 5, pp. 492-493) presents a discussion demonstrating that the square root of the Grashof number can be considered a special case of the Reynolds number; the observation could be used to formulate a rule providing the order of magnitude of the minimal mass-flow rate in a given case. In the present work, Grashof number changes are of negligible importance and are therefore ignored.

(4) A single parameter, the diameter, is sufficient to characterize the geometric properties of a long, smooth, round cylinder normally exposed to a stream. Under such conditions, the Nusselt number has been given by some correlation of the following kind:

$$Nu \equiv \frac{HD_w}{k} \equiv \frac{0.2389i^2r}{\pi k(\theta_w - \theta_e)} = (C_1 + C_2 Re^n) Pr^{0.3} \quad (6)$$

One investigator (reference 5, pp. 559-561) introduced, in addition, a temperature function by which the right expression is multiplied.

(5) The temperature at which the several gas properties are evaluated is arbitrary unless experiment clearly restricts the choice. The usual practice is to evaluate  $\mu$ ,  $k$ , and  $Pr$  at some mean film temperature. The film temperature adopted herein is the arithmetic mean of the wire temperature and the temperature that the wire would attain if unheated. Such a choice is entirely arbitrary unless it is shown that the "best" correlations result from its employment.

Exposure at oblique incidence. - In the foregoing discussion, the assumption was made that the wire is normally oriented to the flow vector. Many applications require orientation at oblique incidence. The question therefore arises as to the effect of such oblique incidence on the Nusselt number.

Numerous investigators (references 1, 3, 4, and 9 to 13, in particular) have attempted to arrive at a generalized, quantitative description of the variation of heat-transfer rate with angle subtended by wire and stream. Such studies have been made at Mach numbers below about 0.4; the results therefore apply only in the case of essentially incompressible flow.

Agreement exists among the investigators for wire-flow vector angles between  $90^\circ$  and about  $25^\circ$ . Within that range, the Nusselt



numbers observed are virtually the same as those that would be observed were the actual flow vectors replaced by the components normal to the wire. At angles smaller than about  $25^\circ$ , the heat loss is greater than that predicted by this rule; the discrepancy and the disagreement among observers increases as the angle decreases. Finally, at the condition of parallelism of wire and flow, the Nusselt number is in the vicinity of 50 to 60 percent of the normal-incidence value.

When wire behavior only at wire-flow vector angles greater than  $25^\circ$  is considered, it is evident that in all such relations as equations (2), (3), (4), and (6) the airspeed  $V$  should be replaced by  $V' = V \cos \phi$ , in which  $\phi$  is the angle between the flow vector and the normal to the wire in the wire-vector plane. The quantity  $V \cos \phi$  is, of course, the effective airspeed. The validity of this substitution at Mach numbers greater than 0.4 is assumed in all discussions herein except where otherwise stated; the soundness of this assumption is unknown.

Behavior of exposed unheated wire. - The temperature assumed by an unheated circular cylinder of high thermal conductivity exposed to a fluid flow is always greater than the static temperature but less than the total. The actual temperature attained under the stated conditions is usually designated the effective temperature and is so designated herein.

Investigations (references 14 and 15) have been made of the variation of the ratio of effective temperature to total or static temperature with Mach and Reynolds numbers. The ratio has been found to be principally a function of Mach number; Reynolds number changes have an almost negligible effect. Numerical values are discussed in the section Temperature Recovery Ratio.

It is sufficient to note that, if Mach number is known or calculable, static and total temperatures may be obtained by using the wire as a resistance thermometer in view of the possibility of experimental establishment of the relation between static and indicated (that is, effective) temperature for a given instrument.

Variation of the effective temperature with  $\phi$  occurs (reference 14), but such variation is not treated in detail in the present report. An additional discussion of the matter is presented in the section Temperature Recovery Ratio.



Radiation losses. - No mention has been made of radiation effects. In general, heat-transfer rates associated with the exposure of heated fine wires to air streams having speeds greater than about 1500 centimeters per second are far higher than any possibly resulting from radiative transfer. At very high temperature levels ( $\theta_w > 800^\circ \text{C}$ ), small radiation corrections are sometimes required; such corrections are assumed negligible herein.

#### Possible Array Configurations and Uses

The term "array" as used herein means one wire or a group of two or more wires arranged in a definite spatial pattern and rigidly held by a suitable series of supports.

The following discussion of array types and uses is limited to steady-state measurements. A fairly comprehensive discussion of the same subject in the case of turbulence measurements is given in reference 16.

Uses and procedures identical for all arrays. - The three principal uses of arrays are the determination of temperature and the measurement of mass-flow rate and of flow direction. Measurements of temperature and of mass-flow rate are made according to essentially fixed procedures regardless of the array type.

In all cases, the quantities  $R_0$  and  $\alpha$  characteristic of each array wire or desired combination are predetermined. The variable  $T_s/T_e$  is then determined as a function of  $M$  by aerodynamic calibration. The orientation of the stream with respect to the array should be that which is to be considered in all subsequent use of the array the principal or mean orientation (generally, normal to a single wire or coincident with an axis of symmetry of a multiple-wire array).

A stream-temperature determination requires a knowledge of  $M$ . The temperature of one or more unheated wires of the array is determined. The stream static and total temperatures are then calculated using the appropriate experimental value of  $T_s/T_e$ . The array orientation must be about the same as that which existed during the calibration.

The following consideration of mass-flow-rate measurement assumes the use of an idealized array consisting of inelastic wires of zero thermal conductivity exposed to the flow of an incompressible fluid.



The necessary modifications of the current simplified treatment are presented in several subsequent sections of the report.

The required initial heat-loss calibration of the array is accomplished by exposure at the principal orientation to a succession of known flows characterized by a wide range of mass-flow rates. In this investigation, constant-temperature operation of the array is usually assumed. A factor of the power input (that is, current) is varied either manually or automatically so as to bring the array to the desired temperature.

The experimental data are used to determine the constants  $C_1$  and  $C_2$  of equation (6), which is restated here in a more explicit form:

$$\frac{Nu_f}{Pr_f^{0.3}} = \frac{0.2389i^2R}{\pi k_f Pr_f^{0.3} (\theta_w - \theta_e) L_w} = C_1 + C_2 Re_f^{0.5} = C_1 + C_2 \left( \frac{GD_w}{\mu_f} \right)^{0.5} \quad (7)$$

No factor  $\cos^{0.5} \varphi$  has here been associated with  $G^{0.5}$ . In fact, if calibration and subsequent data are obtained at the same relative orientation of wire and flow, such a fixed factor can properly be considered to be implicit in  $C_2$ . If the orientation changes, however, it is necessary to retain the explicit factor  $\cos \varphi$  within the parentheses. When an array of two or more wires is considered, the angle will no longer be  $\varphi$ , but rather will be the angle between the flow vector and the principal direction of the array.

The factor  $L_w$  is explicitly retained in equation (7) in order to clarify the following point: The calculated values of  $C_1$  and  $C_2$  will be inversely proportional to the value of  $L_w$  used in connection with a particular wire. The observation is just as true, however, of the value of  $Nu_f$ . The use of an erroneous  $L_w$  in the case of an ideal wire will therefore lead to no error in the value of  $G$ .

The next requirement in the determination of the mass-flow rate of an unknown flow is the measurement of gas temperature. Because incompressible flow has been assumed,  $\theta_e$  equals the static temperature. As before, the power input required to bring the array to a



convenient fixed temperature  $\theta_w$  is then determined. Ideally, the wire temperature need not be the same as that used during calibration.

All quantities appearing in equation (7) are now known with the exception of  $G$ , which is therefore easily calculable. (The gas

properties are supposed evaluated at  $\theta_f = \frac{\theta_w + \theta_e}{2}$ .)

Discussions of flow-direction measurement are subsequently presented in connection with discussions of the respective array types.

Single-wire array. - The single-wire mount consists, of course, of a single wire, two wire supports, and a suitable mounting for the supports. Such a device has the merits of extreme simplicity, ease of construction, and presentation of a minimal drag cross section to the stream. The wire is usually either parallel or perpendicular to the axis of the mounting tube. The array supports are attached to that tube. If the mount axis is considered vertical in the observer's reference frame, reference to a wire parallel to the axis as a vertical wire is convenient; the wire perpendicular to the axis is referred to as a "horizontal wire." Similarly, a horizontal plane is defined as one normal to the mount axis, whereas a vertical plane is one parallel to it.

The power input required to maintain a fixed temperature varies approximately as  $\cos \phi$ , as has been stated; consequently, the variation of input at small angles (normal incidence) will be nearly negligible. For example, a change of  $\phi$  from  $0^\circ$  to  $3.6^\circ$  causes only a 0.1-percent decrease in required input. The single wire at or near normal incidence is therefore very insensitive to flow-direction changes, as is desirable for mass-flow determinations. In the case of a horizontal wire, changes of flow direction within a vertical plane normal to the wire will cause no heat-loss rate change; the same observation applies to the vertical wire and direction changes in the horizontal plane.

A single vertical wire is therefore useless as far as direction determinations are concerned. It can, of course, be used to determine temperatures and mass-flow rates in free streams, within boundary layers adjacent to surfaces nearly parallel to the wire, and within wakes behind blades, the trailing edges of which are roughly parallel to the wire or lie in a vertical plane containing the mount axis.



1289 A horizontal wire may, however, be rotated about the mount axis. In consequence, it can be used to determine the vertical plane in which the flow vector lies. The approximate flow angle is assumed known. The wire is rotated until it and the vertical plane in question subtend an angle of from  $40^\circ$  to  $60^\circ$ . A measurement of power input is made as previously described and the mount then rotated until, at a point roughly  $90^\circ$  from the first position, the same input is required to bring the wire to the fixed operating temperature. The vertical plane of the flow then bisects the horizontal angle subtended by the two wire positions.

The horizontal wire can be used to advantage in a free stream or within a boundary layer adjacent to a surface roughly perpendicular to the mount axis. The method of measuring flow-plane angle described in the preceding paragraph cannot be employed, however, unless the surface is precisely perpendicular to the mount axis.

V-array. - A V-combination consists of two wires (of as nearly equal dimensions as practicable) generally intersecting at an angle of between  $30^\circ$  and  $90^\circ$ .

The plane of the array is usually either horizontal (fig. 1) or vertical. The preferred construction is that which places the center of gravity of the array on the mount axis. In most cases, the bisector of the angle subtended by the wires is normal to the axis.

Such arrays, as well as a pyramidal array, were first suggested and used in reference 1. Wind speed and direction were measured in connection with a meteorological investigation.

A V-array may be used as a single wire by placing the two wires in series; the pair comprise one arm of a bridge. So connected, the array is well adapted to the making of mass-flow measurements. Alternatively, the two wires comprise two adjacent arms of a bridge, which is the preferred connection in the case of yaw-angle determinations when a horizontal array is used. A vertical array is useful for either mass-flow rate or yaw-angle determinations when connected in series. The vertical array is not ordinarily connected otherwise; the point is subsequently discussed, as are the various methods of use and the limitations of both array types.

When connected in series as for mass-flow determination, V-array behavior, as far as the flow component in the array plane is concerned, is nearly the same as that of a single wire running through



the center of gravity of the array parallel to the base of the array triangle. The sensitivity to yaw (undesired in mass-flow measurements) of a horizontal array (or to pitch of a vertical) connected in series may be shown to increase approximately as  $\cot^2 \delta/2$ . The sensitivity in question remains small, however, unless  $\delta/2 < \approx 30^\circ$ . A mass-flow determination will therefore not be inaccurate because of relative inclination of the flow vector and the array bisector if the vector lies in the array plane until such inclination is greater than several degrees.

The consideration of possible error caused by the presence of an out-of-plane component of flow is necessary in a determination of mass-flow rate. A simple analysis may be based on the observation that the array response to such a component is the same as that of each wire acting independently. If a horizontal array is considered, the power input required to maintain a given mean temperature of the wires connected in series may accordingly be shown to vary approximately as  $(\sin^2 \Omega + \cos^2 \Omega \sin^2 \delta/2)^{1/4}$  provided the yaw angle  $\psi$  is small.

The power input required to maintain a series-connected V-array at a fixed temperature varies according to a corresponding law when the pitch angle  $\Omega$  is small and the flow is inclined at an angle  $\psi$  to the array plane. In this instance, however, it is possible to align the array plane with the flow vector by rotating the mount about the axis. The condition of alinement is electrically detectable, as is shown by the following consideration:

By replacing  $\Omega$  by  $\psi$  in the preceding expression, the function

$$u_{\psi, \delta} \equiv \left( \sin^2 \psi + \cos^2 \psi \sin^2 \frac{\delta}{2} \right)^{1/4} \quad (8)$$

is defined.

It is found that

$$\lim_{\psi \rightarrow 0} \frac{\partial u_{\psi, \delta}}{\partial \psi} = \frac{\psi (1 - \sin^2 \frac{\delta}{2})}{2 \sin^{3/2} \frac{\delta}{2}} \quad (9)$$



The relation is not correct when the  $\cos \varphi$  law is not obeyed.

The input power reaches a minimum at  $\psi = 0$ . The minimum point, and hence the flow yaw angle, can be electrically determined. An alternative procedure is to maintain a fixed bridge current; at  $\psi = 0$  the voltage across the array reaches a maximum. In either case, the sharpness of the reversal point increases as  $\delta$  decreases. The sensitivity of the vertical array to pitch-angle changes also increases as  $\delta$  decreases, however, as has been noted.

When the flow vector lies in the plane of a V-array, it is possible to determine  $\Omega$  (when small) approximately by comparing the input powers required by the wires when acting independently. The theory is not presented because the information available is insufficient for application of the technique at transonic or higher speeds (where validity of the simple cosine law is questionable).

The horizontal array is used to measure yaw angle in an altogether different manner. For simplicity and clarity, it will be assumed that the two wires have like dimensions and electric characteristics and that the resistances of the wire supports and the necessary connecting leads are negligible. If each wire becomes one of two adjacent arms of a simple bridge of which the remaining arms are equal resistances, the bridge will be balanced when, and only when, the two array wires have the same resistance, that is, are at the same temperature. If the bridge is so connected that the same current flows through both wires (strictly speaking, at the balance condition only), that condition (equal-resistance) is easily detected by any of a number of conventional instruments.

Because the two wires are now at the same temperature and have the same input powers, the angle between each wire and the flow vector must be the same for both, that is, the relative flow yaw angle is zero. As a first approximation, it can be shown that when this condition is not quite met the bridge output current is proportional to the product  $\psi \cot \delta/2$ . In this instance, the effect is quite linear and a reversal of sign of output occurs at  $\psi = 0$ . Accordingly, the method is basically superior to that previously described for a vertical array. In general, sensitivity is sufficiently high to permit the use of any vertex angle less than about  $120^\circ$  and otherwise acceptable.

The response of any V-array is about the same whether the vertex lies at the upstream or downstream end of the array. In flow situations in which a lateral flow gradient exists, it often



becomes desirable to check the measured flow angle, provided a horizontal array is being used, by rotating the array through approximately  $180^\circ$  and redetermining the yaw angle. If the two so-determined apparent yaw angles differ by more than about  $1^\circ$ , a significant lateral gradient exists and the true direction is very close to the mean of the apparent directions. An X-array is superior in such situations, but is usually prohibitively large; four supports are required.

A V-array may be placed within 0.01 inch of a surface closely parallel to the array plane without serious loss of measurement accuracy; however, for boundary-layer work, a single wire is generally preferable. The chief reason for this preference is that less loss of accuracy results from forward-support wake effect; a second consideration is that it is more difficult to mount two wires in a desired plane than to mount a single wire parallel to a given plane.

A single wire normal to the mount axis can be rotated to a position in which it is parallel to a given surface. In general, the flow vector will not be normal to the wire in such a case. That procedure, of course, cannot usually be employed in the case of a V-array.

Finally, the principal direction of a V-array is the vertex-angle bisector. In general, temperature and mass-flow rate measurements are made when the angle bisector and flow vector have been made to coincide as nearly as is practicable in the given situation.

Parallel-wire array. - A vertical V-array may be used to measure yaw angle, as has been noted, but the accuracy is usually not so high as is desirable. A horizontal V-array is unusable when, for example, a large lateral gradient of flow exists or when wake-angle measurements are desired.

The parallel-wire array was devised to overcome these difficulties. It consists of two wires mounted in the vertical plane containing the mount axis and held in spatial and electric parallelism by two supports. The wires are usually a few (about 5) diameters apart.

The basic principle is the well-known one of the heated wake; earlier forms of the arrangement are discussed in references 2 and 17 to 19. The mean temperature (hence the array resistance) is a maximum when one wire lies directly in the lee of the other, that is, when the localized flow vector lies in the plane of the array.



The wires may be parallel to the mount axis or mounted at some acute angle to it. In either case, the center of gravity of the array is placed on the axis.

A yaw-angle determination is usually made by rotating the mount about the axis until electric indication has been obtained that the resistance of the array is at some maximal value. The bridge current is kept constant. The yaw angle at which the resistance peaks is sharply defined.

Temperature and mass-flow determinations are made in the manner previously described. As before, the array is first rotated until coincidence of flow vector and array plane has been achieved. The initial "zeroing" is of great importance in this case because of the high yaw sensitivity. Mass-flow determinations are accurate when the flow pitch angle is either known, in which case a suitable correction to zero pitch can be applied, or is small.

Combination array. - Certain advantages will subsequently be shown to be associated with the inclination of a wire away from the position of normal incidence. On those grounds, mounting the wires of a parallel-wire array at about  $45^\circ$  to the mount axis is desirable.

The one important adverse effect of the inclination is the considerable increase of pitch sensitivity. In the discussion of V-arrays such arrays were found to be insensitive to direction changes occurring in the respective array planes (when the two wires are connected in series). Combination of the parallel-wire and vertical-V concepts is a simple matter; the result is a vertical V of wire pairs.

The two pairs may be used in combination or separately. The yaw angle is obtained by rotation of the mount, as in a vertical V or a single pair. The sensitivity to pitch during mass-flow-rate determinations is about the same as that of a single vertical wire.

Both the parallel-wire instruments described are particularly useful for wake surveys and for flow measurements near surfaces essentially parallel to the axis of the mount. They are usually not useful near surfaces normal to the axis.

Pyramidal array. - A pyramidal array consists of three or more wires of equal length meeting at an apex and symmetrically disposed about some axis (usually one normal to the mount axis).



Such arrays are very useful whenever the  $\cos \phi$  law is known to hold accurately. For example, if the three wires are oriented along three intersecting edges of an imaginary cube, it can be shown that if the wires are connected in parallel the power input will be virtually independent of flow direction over a substantial solid angle centered about a cube diagonal through the apex. A means of measuring the magnitude of mass-flow rate without regard for direction is therefore available under the hypothetical conditions imposed. Once the magnitude is determined, the direction can be measured by using the individual wires, or the yaw angle can be determined by rotation if two of the wires are symmetrically disposed about a vertical plane through the pyramid apex.

In general, however, the complexity and the size of the pyramidal structure as well as the uncertainties in the current knowledge of oblique-incidence heat-transfer rates at the higher Mach numbers served to postpone investigation of such arrays.

#### INSTRUMENT DESIGN PROBLEMS

The preceding discussions have assumed the existence of ideal anemometers. Explicitly, the assumed instruments were supposed to consist solely of wires having unalterable properties, dimensions, and positions with respect to one another and to the mount tube. Finally, the wires were assumed to have zero thermal conductivity, so that no input power would be lost to the supports. Such instruments, of course, cannot be devised.

From the possible mount details, the available mount and wire materials, and the alternative mounting techniques, the designer must select the optimum combination for a particular application. The optimum combination is that which yields the most accurate flow information after the instrument has been in active use for a protracted period, for example, 20 hours.

Although a wholly quantitative treatment of the design problem is clearly impossible, the following discussion represents an approach to that ideal. Reconciliation of the conflicts among the various findings is discussed after treatments of end losses, aerodynamic stress, impact and vibration effects, corrosion, and electric stability.

End losses. - In the absence of error due to variation with time (or use) of the dimensions or of the physical properties of the wire, the chief source of error is the conductive flow to the



supports of a substantial fraction of the heat released in the wire. The magnitude of that fraction must be known in a given situation to make possible intercomparisons among aerodynamic heat-loss data taken under differing sets of conditions.

The fractional end loss, represented by the symbol  $\xi$ , is defined as the ratio of the heat lost by conduction to that lost directly to the stream. This ratio depends upon the physical properties of the wire and the support materials, the dimensions of the wire and the support, the prevailing local effective mass-flow rate, and the effective ambient temperature and the mean temperature at which the wire is maintained.

Calculation of a fairly precise value of  $\xi$  is subsequently discussed in the section CALCULATIONS AND CORRECTIONS; however, the equations given there are such that the degree and the manner of dependency of  $\xi$  on the values of the several parameters determining it are not apparent. An approximate expression that clearly exhibits the relations sought is developed in appendix B and given here; this expression will be found useful in the making of preliminary estimates:

$$\xi \approx 0.475^{-1/2} \left( \frac{D_w}{L_w} \right)^{3/4} \left( \frac{k_w}{k_f} \right)^{1/2} \left( \text{Re}'_{f,L} \right)^{-1/4} \left( \frac{\theta_{w,\infty} - \theta_{w,b}}{\bar{\theta}_w - \theta_e} \right) (1 - t)^{1/2}$$

$$\left[ 1 - \frac{1}{2(0.475)^{1/2}} \left( \frac{D_w}{L_w} \right)^{3/4} \left( \frac{k_w}{k_f} \right)^{1/2} \left( \text{Re}'_{f,L} \right)^{-1/4} \left( \frac{\theta_{w,\infty} - \theta_{w,b}}{\bar{\theta}_w - \theta_e} \right) \frac{t}{(1-t)^{1/2}} \right]$$

(10)

The value of the expression in brackets differs from 1 by less than 10 percent in almost all cases. The value of the expression  $\left( \frac{\theta_{w,\infty} - \theta_{w,b}}{\bar{\theta}_w - \theta_e} \right)$  usually is nearly 1 when  $\xi \approx 0.1$  (a typical value).

Variation of the product of these two expressions is accordingly a matter of secondary importance; the product may often be taken as 1 with little error.



Minimization of  $\zeta$  may best be accomplished, as inspection of equation (10) indicates, by maximizing the  $L_w/D_w$  ratio and using wire of low thermal conductivity. In view of the presence of the factor  $(Re'_{f,L})^{-1/4}$ , an increase of length at a constant  $L_w/D_w$  ratio will cause a small decrease of  $\zeta$ , so that of two geometrically similar wires the larger will lose relatively less heat to the supports.

Decrease of the support tip diameter and decrease of the support thermal conductivity will result in small decreases of  $\zeta$  through changes in the ratio  $\left( \frac{\theta_{c,\infty} - \theta_{w,b}}{\bar{\theta}_w - \theta_e} \right)$ . Operation at higher mean wire temperatures, through decrease of the quantity  $(1 - t)^{1/2}$ , will similarly affect  $\zeta$ ; this quantity varies approximately as  $(1 + \alpha \bar{\theta}_w)^{-1/2}$ . For example, an increase of mean operating temperature from 200° to 400° C reduces  $\zeta$  under normal conditions by about 6 percent for 20-percent iridium-platinum (as the wire material) or by about 20 percent for nickel. The physical reason for the decrease is that with the rise in resistance of the central portion of the wire a higher fraction of the total power is released within that portion.

In general, errors in the calculation of  $\zeta$  lead to errors in computed flow characteristics that are small but not necessarily negligible. It is important, however, that a distinction be drawn between an incorrect value of  $\zeta$  consistent with a value calculated on the basis of calibration data (and used to correct such data) and an incorrect value of  $\zeta$  inconsistent with a calibration value. If, to take an extreme situation, the calibration situation and the experimental situation are the same, the fact that the calculated value of  $\zeta$  is low by 50 percent in each case (because of use of an incorrect  $k_w$ , for example) has no bearing on the resultant flow measurements. Close similarity of calibration and experimental situations is a guarantee that negligible error will result from uncertainties in  $\zeta$ . As the two differ more widely, greater care is required in the calculation of the end losses. A typical case, involving a fourfold change of flow rate from calibration to experimental situation, was analytically investigated; such a situation could arise as a consequence of limitations of test facilities. In order to avoid an error greater than 0.5 percent in the calculated Reynolds number, as caused by an error in the assumed value of any single parameter, it would be necessary that the magnitudes of the



following parameters be accurate to at least the stated percentages:  $D_w$ , 5.5 percent;  $k_w$ , 11 percent;  $D_p$ , 60 percent;  $k_b$  and  $k_t$ , each 110 percent;  $Re'_{t,b,2}$ , 200 percent. If, however, such errors existed simultaneously, the error in the Reynolds number could be as great as 3 percent so that the permissible deviations are, in general, correspondingly smaller.

Aerodynamic stress effects. - When the wire stress is of the order of  $3 \times 10^8$  dyne centimeter<sup>-2</sup> or greater, the effects upon the dimensions and the properties of the wire are significant and must be quantitatively considered.

When the wire is not exposed, the stress has, by definition, the value  $\sigma_1$ . Upon exposure, the stress is increased; the induced stress is designated  $\sigma_2$ . The resultant stress, called  $\sigma_3$ , is not simply the sum of  $\sigma_1$  and  $\sigma_2$ . The relation among the three stresses and an expression yielding the value of  $\sigma_2$  follow; the derivations are given in appendix C. The errors involved in the use of these relations are discussed in the section CALCULATIONS AND CORRECTIONS.

$$\sigma_3^3 - \sigma_2^3 - \sigma_1^3 = 0 \quad (11)$$

$$\sigma_2 \approx \left[ \frac{L_w^3 (C_D G' V')^2}{6\pi^2 A_w F D_w^2} \right]^{1/3} \quad (12)$$

The quantity  $F$  in equation (12) is the combined flexibility of both supports. In the situation of least complexity, that is, that of a single-wire mount, the wire supports of which consist of frustums of cones rigidly attached to the mount tube, the relation (appendix C)

$$F = \frac{128 L_b^3}{3\pi E_b D_{b,1}^3 D_{b,2}} \quad (13)$$

applies.



A knowledge of the wire dimensions, drag coefficient, mass-flow rate per unit area (taken at a right angle to the wire), flow speed (also taken at a right angle to the wire), and support flexibility is required for a determination of  $\sigma_3$ .

A plot of  $\sigma_3$ , the stress in the wire during operation, as a function of  $\sigma_2$  for several values of the initial stress  $\sigma_1$  is presented in figure 2. At high values of  $\sigma_1$ ,  $\sigma_3$  is nearly independent of  $\sigma_2$  at the lower values of  $\sigma_2$ ; the dependency becomes stronger with increasing  $\sigma_2$ . This significant circumstance will be referred to again.

The value of  $\sigma_3$  may be minimized by decreasing the  $L_w/D_w$  ratio, by decreasing the rigidity of the supports, and by inclining the wire to the stream (equations (11) and (12)). In connection with the first method of minimization, it should be considered that one of the four factors  $D_w$  in the denominator of equation (12) is associated with  $F$ . When equations (12) and (13) are combined, the expression

$$\sigma_2^3 = \frac{1}{64\pi^2} \left( \frac{L_w}{D_w} \right)^3 \left( \frac{D_{b,1}}{L_b} \right)^3 \left( \frac{D_{b,2}}{D_w} \right) (C_D G' V')^2 E_b \quad (14)$$

is obtained. As the mount size varies, the ratios  $L_w/D_w$ ,  $D_{b,1}/L_b$ , and  $D_{b,2}/D_w$  will remain fixed if geometric similarity is maintained for the array and the supports. The ratio  $D_{b,2}/D_w$  is present because the relative rigidity of wires and supports affects the displacement of the wire (from the straight condition) per unit aerodynamic loading. It has already been noted, in effect (equation (11) and fig. 2), that  $\sigma_3$  decreases slowly with decreasing  $\sigma_1$ .

The effects of the steady stress  $\sigma_3$  on the accuracy of measurements are: (1) High stress, by causing slow irreversible deformation, leads to irreversible and uncertain changes in the magnitude of the heat-transfer surface and in the electric characteristics of the wire or even to complete failure; (2) the wire is made more vulnerable to impact and vibrational stresses (subsequently discussed); and (3) a reversible resistance change occurs that is erroneously considered by the observer to be caused by a temperature change (the strain-gage effect).



The adverse effects may be avoided to some extent by proper selection of materials. The wire material should have the highest possible yield point in tension at the desired operating temperature. It is improbable that any material having a room temperature long-time yield point below about  $6.2 \times 10^9$  dyne centimeter<sup>-2</sup> (90,000 lb/sq in.) will be satisfactory for high-speed applications; the figure cited is based upon experience at the NACA Lewis laboratory.

The strain increment accompanying the change from  $\sigma_1$  to  $\sigma_3$  is given by

$$\frac{\Delta L_w}{L_w} = \frac{\sigma_3 - \sigma_1}{E_w} \quad (15)$$

In terms of the strain-resistance factor  $S$ , the fractional resistance change is then given by

$$\frac{\Delta R}{R} = \frac{S (\sigma_3 - \sigma_1)}{E_w} \quad (16)$$

Selection of a material having a low value of the stress-resistance coefficient  $SE_w^{-1}$  is therefore desirable. Unfortunately, the value for 20-percent iridium-platinum is  $2.87 \times 10^{-12}$  centimeter<sup>2</sup> dyne<sup>-1</sup> ( $1.98 \times 10^{-7}$  ohm/ohm/(lb/sq in.)); the material serves very well in strain-gage applications. Tungsten is superior in this respect, exhibiting a value of  $0.44 \times 10^{-12}$  ohm per ohm per dyne centimeter<sup>-2</sup>. On the other hand, tungsten wire, used at higher  $L_w/D_w$  ratios, is usually more highly stressed than is iridium-platinum.

Minimization (by increase of  $\sigma_1$ ) of the quantity  $(\sigma_3 - \sigma_1)$  of equation (15) is the only method other than material selection of minimizing resistance changes caused by stress change.

Impact effects. - A quantitative treatment of instantaneous stresses caused by impacts of stream-borne solid particles is unavailable. An over-simplified analysis yields the exemplary result that a particle having approximately the density of water



and a diameter about the same as that of a 0.0038-centimeter wire can cause a tensile stress of at least  $1.4 \times 10^{10}$  dyne centimeter<sup>-2</sup> (200,000 lb/sq in.) in such a wire when the particle is suddenly brought to rest from an initial speed of 45,000 centimeters per second. No wire used for anemometric purposes has a diameter greater than 0.0038 centimeter.

The probability of a "hit" may be reduced by the reduction of wire length (normally projected to the stream) and diameter. Reduction of wire diameter much below the mean effective particle diameter will not greatly decrease the probability, however, because the sum of the two diameters is the controlling figure in this connection. The most effective way to avoid impacts, of course, is to adequately filter the stream.

The reduction of impact stresses may be accomplished by increasing the wire diameter because the developed stress varies inversely with the square of the wire diameter. Length changes have a relatively minor influence on the developed (impact) stress, whereas the effect of changes of tension is unknown. Impact stresses will not exceed those caused by particles of the maximum size (hence, generally mass) permitted to pass through the filter. Inclination of the wire to the flow, when not contraindicated, is an effective method of stress reduction because the developed stress varies approximately as the square of the component of particle speed normal to the wire.

The selection of materials having high yield points in tension will minimize damage caused by impacts. Although compressive and shear strengths are equally important, all three strengths are sufficiently well correlated to obviate the necessity of separate consideration of each.

Vibration effects. - No attempt has been made to develop quantitative theory whereby predictions could be made of the amplitudes and frequencies of vibrations of the several components of a hot-wire mount. Instead, the approach has been a wholly qualitative one consisting principally of recognition of the fact that a very rigid structure is unlikely to develop significant vibration. In general, then, the mount and supports must be made as rigid as practicable within limitations imposed by other considerations. The wire ratio  $L_w/D_w$  must be minimized and the wire tension  $\sigma_1$  maximized. High tension virtually eliminates wire vibration, a fact that has been confirmed by actual observation.



Because oscillatory stresses associated with any remanent vibration not prevented by the structural rigidity are superimposed on the steady aerodynamic stresses (as well as upon occasional impact stresses), it is desirable to minimize the aerodynamic stresses and to use materials having high fatigue-limited yield points.

Oxidation. - The sensitivity (to flow changes) of an anemometer increases with the temperature difference between wire and fluid. Furthermore, a given absolute change in the fluid temperature will cause an undesired change in the input power required for maintenance of a given wire temperature that is inversely proportional to the mean temperature difference. Otherwise expressed, operation at a high wire temperature minimizes reading changes occasioned by random or other air-temperature changes. High-temperature operation has already been found to decrease  $\xi$ . Finally, the air temperature will often be above  $200^{\circ}\text{C}$ , which, apart from the preceding considerations, requires wire operation at a minimum of about  $350^{\circ}\text{C}$ .

Corrosion (usually oxidation) rates may be minimized, primarily by operation at wire temperatures that are minimal with respect to the considerations mentioned. Noble metals or alloys upon which layers form that are relatively impermeable to oxygen may be employed. Alternatively, suitable barriers of impermeable, nonoxidizing materials may be deposited on the surface of the wire. Finally, the use of metals may be avoided altogether; oxides exist having resistivities falling within a useful range when sufficient impurity content is present.

The only method whereby the effect of a given corrosion rate may be minimized is the use of wire having a maximum allowable diameter - a quantity that varies with many circumstances.

Electric stability. - An invariant correspondence of wire resistance and wire temperature is clearly of basic importance. In terms of the quantities usually dealt with, the  $0^{\circ}\text{C}$  resistance and the temperature coefficient of resistance should be known to about  $\pm 0.05$  percent and should remain fixed within  $\pm 0.1$  percent or better over a period during which recalibration is to be avoided.

Materials having high melting points and high strengths (in the annealed state) will almost invariably exhibit high electric stability. In general, alloys are less susceptible to crystalline growth and other internal changes. Electric changes may be reduced by suitable annealing or partial annealing (normalization). The



magnitudes of the values of resistivity and temperature coefficient of resistance need not usually be considered because, when suitable bridges and galvanometers are employed, virtually all materials otherwise acceptable will be found to exhibit a usefully large change of resistivity per unit temperature. It is inadvisable, however, to attempt to use a material having a temperature coefficient below about 0.0006 per °C because in such cases a given uncertainty of wire resistance change accompanying a particular temperature change is usually a prohibitively large fraction of the small resistance change itself.

Reconciliation of conflicting requirements. - The wire has been chiefly considered as an anemometer - a device that functions because its temperature is raised above the effective ambient. The same wire serves very well as a resistance thermometer, however, and the two functions do not require distinct design considerations.

The  $L_w/D_w$  ratio should be maximized to decrease end losses and minimized to decrease aerodynamic stresses, decrease vibrational amplitudes, and increase frequencies of residual vibration. It has also been found that  $L_w$  should be minimized to decrease the probability of a particle hit, and that  $D_w$  should be maximized to reduce impact stresses and corrosion effects and minimized to decrease the probability of particle impact.

Although establishment of a single quantitative relation that will permit calculation of optimum values of  $L_w$  and  $D_w$  in the absence of quantitative treatments of impact and vibration effects is impossible, typical examples will be given of procedures through which the several conflicting requirements may be, in some degree, reconciled.

Let it be initially assumed that the filtration is perfect; impacts are nonexistent. It is further supposed, in this first example, that vibration has been largely eliminated by the selection of an appropriately high value of  $\sigma_1$ . The wire length and the orientation with respect to the stream are assumed fixed. A value of  $F$  in equation (12) is assumed; the supports have been made as rigid as the requirements of aerodynamic "cleanness" permit. Finally, the wire is to be used at a temperature such that oxidation will not occur. Under these circumstances, the wire material that should be used and the diameter that is most desirable must be selected.



In equation (10), the quantity

$$\left( \frac{\theta_{w,\infty} - \theta_{w,b}}{\bar{\theta}_w - \theta_e} \right) \left[ 1 - \frac{1}{2(0.475)^{1/2}} \left( \frac{D_w}{L_w} \right)^{3/4} \left( \frac{k_w}{k_f} \right)^{1/2} \left( \text{Re}'_{f,L} \right)^{-1/4} \left( \frac{\theta_{w,\infty} - \theta_{w,b}}{\bar{\theta}_w - \theta_e} \right) \frac{t}{(1-t)^{1/2}} \right]$$

may be assumed equal to 1 for the present purpose. Upon solving the modified equation (10) for  $D_w$ , the following equation is obtained:

$$D_w = 0.475^{2/3} L_w \zeta^{4/3} \left( \frac{k_f}{k_w} \right)^{2/3} \left( \frac{1 + \alpha \bar{\theta}_w}{1 + \alpha \theta_e} \right)^{2/3} \left( \text{Re}'_{f,L} \right)^{1/3} \quad (17)$$

As an example, a solution based upon the following figures is given:  $L_w = 0.254$  centimeter;  $\zeta = 0.12$  (a rather high value, but not exceptional); film temperature,  $125^\circ \text{C}$ ; mean wire temperature  $\bar{\theta}_w$ ,  $250^\circ \text{C}$ ; effective ambient temperature  $\theta_e$ ,  $0^\circ \text{C}$ ; and  $\text{Re}'_{f,L}$ , 3000 (corresponding to an airspeed of 2072 cm/sec or 68 ft/sec) at standard pressure and  $0^\circ \text{C}$ .

Initially, the use of 20-percent iridium-platinum is assumed;  $\alpha$  is 0.00085 per  $^\circ \text{C}$  and  $k_w$  is 0.042 (cal/(sec)(cm)( $^\circ \text{C}$ )) ( $2.82 \times 10^{-3}$  Btu/(sec)(ft)( $^\circ \text{F}$ )). In comparison with the value of  $k_w$ ,  $k_f = 0.0000807$  (cal/(sec)(cm)( $^\circ \text{C}$ )).

It is found that  $D_w = 0.0023$  centimeter (0.00091+ in.). The designer would select the nearest available size. The minimum  $L_w/D_w$  ratio would be 110.

The diameter in the case of a different material is easily calculated; the figure will vary with  $\left( \frac{1 + \alpha \bar{\theta}_w}{k_w} \right)^{2/3}$ . For example, the diameter in the case of tungsten would be about 0.00084 centimeter (0.00033 in.). The minimum  $L_w/D_w$  would be 303.



After the wire diameters for various materials have been determined, the wires must be compared on the basis of expected stresses and yield points. The information that is required is the maximum flow velocity to which each wire may be subjected without exceeding a certain fraction of the long-time yield point of the material.

The maximum steady stress should probably be limited to one-half the known long-time yield point of a given material at the operating temperature. A safe margin is afforded by observance of that rule.

By designating the maximum allowable stress  $\sigma_m$  (selected by any such rule), ignoring  $\sigma_1$  in comparison with  $\sigma_3$ , and noting that  $G' = \rho V'$ , the following equation is obtained from equations (11) and (14):

$$V' = \left( \frac{1.5 \pi^3 F}{\rho^2 C_D^2} \right)^{1/4} \frac{D_w \sigma_m^{3/4}}{L_w^{3/4}} \quad (18)$$

Equations (17) and (18) are combined to yield

$$V' = C_4 \sigma_m^{3/4} \left( \frac{1 + \alpha \bar{\theta}_w}{k_w} \right)^{2/3} \quad (19)$$

in which

$$C_4 \equiv 0.475^{2/3} (1.5 \pi^3 F)^{1/4} (\rho C_D)^{-1/2} L_w^{1/4} \zeta^{4/3} \left( \text{Re}'_{f,L} \right)^{1/3} \left( \frac{k_f}{1 + \alpha \theta_e} \right)^{2/3}$$

For the present purpose, the quantity  $(\rho C_D)^{-1/2}$  is considered fixed.

The quantity  $\sigma_m^{3/4} \left( \frac{1 + \alpha \bar{\theta}_w}{k_w} \right)^{2/3}$  may be considered under the conditions of the derivation a "figure of merit" of the wire material.



By using 3.55 as the ratio of the yield points in tension of tungsten and of 20-percent iridium-platinum, the ratio of the figures of merit of the two materials is found to be about 1.05. On the preceding basis, the noble alloy will withstand airspeeds slightly in excess of those to which tungsten may be subjected.

Impact stresses have been ignored in the preceding discussion. Such stresses in the tungsten wire would be over 13 times as great as those in the noble-alloy wire because the square of each diameter is involved. Clearly, if spatial resolution demands permit, the larger (alloy) wire would be employed.

As an additional example, an outline of the analysis required by one other typical situation is considered; no numerical result is given as it would not have the general significance of the result obtained in the previous case.

It is supposed that a wire of specified maximum diameter is to be used to survey a boundary layer. The stream is not free of particles; the maximum allowable diameter is therefore the one chosen. The component of wire length in the direction of flow is limited by the magnitude of the gradient in that direction to a given figure ( $L_m$ ). The lateral gradient is small and the wire-length component in the lateral direction is unspecified. The angle between the stream and the normal to the wire  $\varphi$  should be less than about  $60^\circ$  to prevent the wire from lying, in substantial part, in the wake of the forward support. As previously, the maximum allowable end loss is specified.

The angle  $\varphi$  is either  $60^\circ$ , as a maximum, or is fixed at some lesser value by the relation (from equation (17))

$$\sin \varphi \tan^{1/3} \varphi = 0.475^{2/3} \left( \frac{L_m}{D_w} \right)^{4/3} \left( \frac{k_f}{k_w} \right)^{2/3} \left( \frac{1 + \alpha \bar{\theta}_w}{1 + \alpha \theta_e} \right)^{2/3} \left( \frac{\rho V L_m}{\mu_f} \right)^{1/3} \quad (20)$$

The last quantity in parentheses is the Reynolds number based upon the true airspeed and the length  $L_m$ .



Following the determination of  $\varphi$  and of  $L_w = L_m \csc \varphi$  for each of the materials being considered in a given case, a comparison of materials is made from the point of view of steady stress using equations (11) and (12); the preceding expression for  $L_w$  is used as well as  $V' = V \cos \varphi$ . It is found that

$$\begin{aligned}\sigma_3 &\approx \frac{L_w (C_D \rho V')^{2/3}}{1.5^{1/3} \pi F^{1/3} D_w^{4/3}} \\ &\approx \frac{L_m (C_D \rho V)^{2/3} \csc \varphi \cos \varphi^{2/3}}{1.5^{1/3} \pi F^{1/3} D_w^{4/3}}\end{aligned}\quad (21)$$

In this case it is impossible to state a simple relation that will serve as a figure of merit. The stresses  $\sigma_3$  would be computed for some given high velocity within the desired working range. The several materials of interest would then be assessed on the basis of comparisons among the several ratios  $\sigma_3/\sigma_m$ .

#### REALIZED DESIGNS AND CONSTRUCTION

The considerations governing selection of materials are discussed. The presentation of the salient construction features of mounts is followed by a discussion of wire mounting techniques.

#### Evaluation of Materials

Wire materials. - References 20 to 24 and other publications were consulted to obtain information concerning alloys and elemental metals of possible use in the experimental program. Unfortunately, many materials (many chromium-bearing alloys, for example) that were promising on the basis of strength and corrosion resistance could not be considered because neither thermal conductivity nor electric data were found in the literature. It was considered infeasible to make the thermal-conductivity determinations required to evaluate such materials. Electrical data were easily obtainable, of course, if a given material was available.



The materials finally considered in some detail were tungsten, noble-metal-plated tungsten, and the noble-metal alloys.

It was known that tungsten oxidizes fairly readily; data on the increase of resistance caused by oxidation are presented in figure 3. The curves represent the increase with time of the room-temperature resistance of three typical tungsten wires suspended within a heating jacket and exposed to the atmosphere. Even at the moderate temperature of  $482^{\circ}\text{C}$ , the rate of increase of resistance of the bare wire is about 1 percent per hour. The maximum permissible variation is about 0.005 percent per hour if frequent recalibrations are to be avoided. The remaining curves represent the increase of resistance of two tungsten wires plated with platinum by sputtering and by electroplating. The rate of oxygen diffusion through the plating in each case was such that the plated wires oxidized about as rapidly as bare wire.

Below about  $375^{\circ}\text{C}$ , tungsten resists oxidation (at normal pressure) so that a tungsten wire operating at a mean temperature of  $300^{\circ}\text{C}$  would probably not fail by corrosion. A temperature of  $300^{\circ}\text{C}$  is the maximum allowable because the temperature at the center of a tungsten wire having an  $L_w/D_w$  ratio of 250 will exceed the mean value by more than  $60^{\circ}\text{C}$ . In practice a wire cannot be safely operated at the maximum allowable temperature, for any substantial electric overload will inevitably cause a change in characteristics.

Tungsten wire commercially electroplated with gold or platinum is available. Such material can easily be fastened to suitable supports by routine silver soldering, but the plating serves no other purpose.

Several noble-metal combinations (gold-platinum, silver-platinum, palladium-platinum) were excluded from consideration because of the relatively large rate of decrease of strength with increase of temperature. Rhodium-platinum alloys have insufficient strength even at low temperatures. Alloys containing more than about 10 percent of either osmium or ruthenium could not be used because of susceptibility to oxidation. No information was or is available concerning binary rhodium-iridium alloys; such alloys, as well as ternary alloys based on either rhodium or iridium or both, should be experimentally investigated as their characteristics should be outstanding. One binary alloy (20-percent iridium - 80-percent platinum) and one ternary (5-percent ruthenium - 15-percent rhodium - 80-percent platinum) appeared to



have desirable electric, mechanical, and corrosion-resistant characteristics, on the basis of the published data, and are available from commercial sources.

Published data (with the exception of thermal conductivity) concerning both alloys were checked at this laboratory. The two materials were found to have virtually the same electric properties and corrosion resistances; however, the strength of the ternary alloy was found to be about 20 percent lower than that of the binary. The ternary alloy was not considered after it was found that thermal conductivity data were unavailable; it was felt very unlikely that the thermal conductivity would prove to be sufficiently lower than that of the binary alloy to compensate for the strength difference. Thermal-conductivity data were available (reference 25) for the iridium-platinum alloy.

The results reported herein were obtained with 20-percent iridium - 80-percent platinum. Of the available alloys or elemental metals possessing properties that have been evaluated, no material is believed superior insofar as steady-state anemometric work is concerned.



The relevant characteristics, insofar as they can be assigned numbers, are listed in the following table:

Property	Value	Units	Remarks
Resistivity	$32.9 \times 10^{-6}$	ohm-cm	Dependent upon history of material
Strain-resistance coefficient	6.1	dimensionless	Independent of history of material
Temperature above which oxidation is detectable	750	$^{\circ}\text{C}$	Value correct only for air at normal pressure
Temperature coefficient of resistance	0.00085	$^{\circ}\text{C}^{-1}$	Dependent upon history of material
Thermal conductivity	0.042	cal $\text{cm}^{-1} \text{ } ^{\circ}\text{C}^{-1}$	No measurement made at this laboratory; value correct at both $0^{\circ}$ and $100^{\circ} \text{C}$
Yield point in fully annealed condition	$0.723 \times 10^{10}$ (105,000)	dyne $\text{cm}^{-2}$ (lb/sq in.)	No measurement made at this laboratory on fully annealed material
Yield point in as-drawn condition	$1.00 \times 10^{10}$ (145,000)	dyne $\text{cm}^{-2}$ (lb/sq in.)	Conservative value
Young's modulus of elasticity	$212 \times 10^{10}$ (30,800,000)	dyne $\text{cm}^{-2}$ (lb/sq in.)	Calculated from measured strain-resistance and stress-resistance coefficients

The wire is usually annealed at this laboratory by being brought in open air to a temperature of about  $800^{\circ} \text{C}$  and held there for several minutes. The period is not critical. Such an anneal is not a full anneal but does normalize the material. A decrease in resistance of about 5 percent occurs within the first 3 minutes. A slight change of temperature coefficient also occurs. Changes of



any kind occurring beyond the 3-minute period are small in comparison. The rate of oxidation at  $800^{\circ}\text{C}$  is so low that for all practical purposes the wire composition is unaltered during the annealing.

The linearity of resistance change with temperature is shown in figure 4. The three specimens had been subjected to a 1/2-hour anneal at  $820^{\circ}\text{C}$ . Data at the several temperatures were taken at both increasing and decreasing temperatures. A few points were taken in an entirely random fashion; nevertheless, little scatter and no apparent hysteresis occur. Because straight lines can be drawn through the points, the conclusion is warranted that, to the order of precision required in the present applications, the relation between resistance and temperature is linear.

The stress-resistance coefficient ( $2.87 \times 10^{-7} (\text{ohm})(\text{ohm}^{-1})(\text{cm}^2)(\text{dyne}^{-1})$ ) was found in the usual manner; the resistance was measured while a succession of standard weights was placed on a loading pan supported by the test wire. Excellent reproducibility and linearity were obtained up to the maximum stress to which each specimen was subjected, namely,  $0.430 \times 10^{10}$  dyne centimeter<sup>-2</sup> (62,400 lb/sq in.). The stress-resistance coefficient was the same within experimental error ( $\pm 3$  percent) for both the as-drawn and the annealed (at  $800^{\circ}\text{C}$ ) wires. On the basis of an assumed Young's modulus of  $212 \times 10^{10}$  dyne centimeter<sup>-2</sup>, a strain-resistance coefficient of 6.1 was predicted. The value was later confirmed by experiments made to determine the gage factor (6.0) of strain gages made with the material. As the gage factor is invariably slightly less than the strain-resistance coefficient of the material itself, the assumed value of the modulus must be nearly correct.

Support materials. - The support was required to have high strength, accept silver solder readily, exhibit high electric stability, have a low product of resistivity and temperature coefficient of resistance, oxidize with difficulty, be sufficiently hard to make repeated cleaning practicable, and be capable of being machined or formed. In addition, it was desirable that the thermal conductivity be low.

The commercial nickel-chromium alloy Inconel in the form of welding rod was selected, for it met all of these specifications.

Occasionally it is desirable to have supports, which, although exhibiting rigidity greater than that of Inconel supports, offer the same or even less opposition to local flow. The Young's modulus



of Inconel is about  $214 \times 10^{10}$  dyne centimeter<sup>-2</sup> (31,000,000 lb/sq in.); apparently, no material that is at least equally acceptable in other respects has a higher Young's modulus than alloys in the nickel-chromium series.

One experimental mount was nevertheless constructed using wire supports of (ground) tungsten carbide (6-percent cobalt-bound) cones. The supports were considerably more rigid than the usual Inconel supports despite the smaller cross sections. The electric characteristics were slightly inferior to those of Inconel, however, for although the resistivity is slightly lower than that of tungsten, the temperature coefficient is very high (about 0.006/°C). Such supports should therefore be used only when either conditions of severe vibration prevail at the measuring station or the channel is of such size that supports of minimal cross section are essential. In general, the support resistance will not then be known as precisely as when a nickel-chromium-alloy support is employed (for which the temperature coefficient is usually about 0.00016/°C). Tungsten carbide accepts silver solder readily; furthermore, its extreme hardness makes possible an indefinite support life.

#### Mount Details and Assembly

The realized mounts carrying different arrays are similar to one another with respect to materials, constructional details, and adherence within practical limitations to the design principles previously discussed.

Mount details. - Typical constructional details are illustrated in figure 5. The mount tubes of stainless steel or Inconel are thick-walled wherever the permissible outer diameter is about 0.48 centimeter or greater; the limitation is the substantial fraction of the cross section occupied by the lead wires. The portion at the instrument end is given an approximately streamlined cross section whenever practicable; considered as an approximate ellipse, the minor and major axes of the section have been as small as 0.20 and 0.35 centimeter, respectively, when the supports could be placed in a plane containing the flow vector. The small-sectioned portion is faired into a larger tube; the tube ultimately becomes a round, thick-walled, 1/4-inch-diameter tube that can be accommodated by a standard instrument actuator of NACA design.



The supports, usually of Inconel, consist most frequently of a combination of circular rod and frustum of a cone. The cylindrical portion, about 1.9 centimeters long, has a diameter varying from 0.064 to 0.15 centimeter for the different mounts. The conical portion is tapered from the point of emergence from a commercial porcelain-type cement insulation to a tip diameter of from 0.01 to 0.023 centimeter; the length varies from 0.76 to 1.9 centimeters. The support is usually bent at or near the base (exit point) to place the tip near the desired location. In addition, the tip is often curved in suitable fashion. In some instances, a solid support is replaced by a suitable combination of tubes, making possible the incorporation of a pressure tap. The quantity  $F$  is of the order of  $4.0 \times 10^{-7}$  centimeter dyne $^{-1}$  (0.07 in. lb $^{-1}$ ) for a typical Inconel support. The same support, if fabricated of tungsten carbide, which cannot be inelastically deformed, would have a flexibility of about  $1.48 \times 10^{-7}$  centimeter dyne $^{-1}$  (0.026 in. lb $^{-1}$ ).

The leads are of glass-coated copper. The minimum number is four as a Kelvin bridge requiring two leads per support is used. Each lead is silver-soldered to the support base prior to mount assembly. By the expedient of silver soldering one support into a slot in the end of the mount tube and thereby usually grounding that portion of the circuit, it is possible to reduce the number of lead wires carried within the tube by one. In such a case, the additional lead connection is made to the base of the mount; the two main current-supply leads alone can be handled in this manner.

It is essential that all leads (other than the two furnishing current to the entire bridge) be joined to the respective supports at points within a small fraction of a centimeter of one another to avoid the production of differential thermoelectric electromotive forces.

Standard AN-series connector plugs are used; commercial flexible cable armor connects plug and mount. When a pressure tap is present, a small-diameter tube is brought to the plug along the inside of the armor with the wires; it leaves the plug through a hole drilled at a convenient point (fig. 5). This construction makes it possible to disconnect and to remove plug and armor and thereby to reduce the over-all diameter of the instrument to 0.637 centimeter for insertion into or removal from an actuator without possible damage to the working end.

The variable plug contact resistances have no effect on the bridge relations because of the Kelvin connection. For the same



reason, a cable of indefinitely great length may be used, provided reasonably heavy copper is employed. No lead resistance should be significant ( $\geq 0.03$  percent) in comparison with the minimal value of a bridge arm containing one of the variable resistances.

Wire mounting. - It was previously stated that a wire should be so mounted that a known minimal stress  $\sigma_1$  exists in it apart from other stresses. The entire mounting procedure is described in some detail because satisfactory instrument operation is critically dependent upon wire behavior.

By calibrating the spring of a jig such as that shown along with a micromanipulator in figure 6, the wire may be mounted at a known applied force. It is convenient to wind some 20 or 30 turns on the bobbin. When a mounting is to be performed, a length is brought over the pulleys and attached to the spring-arm clamp. The bobbin may then be turned in a retrograde direction until the tension reaches about  $6.9 \times 10^8$  dyne centimeter<sup>-2</sup> (10,000 lb/sq in.), after which the main clamp is tightened. In the case of iridium-platinum, an annealing current that is sufficient to raise the wire temperature to about 800° C is employed while the wire is held in a horizontal position (bobbin, main clamp, and both pulleys are insulated from the yoke). An annealing period of at least 3 minutes is required for the noble alloy.

Following the anneal, the main clamp is released, the tension adjusted to about  $0.414 \times 10^{10}$  dyne centimeter<sup>-2</sup> (60,000 lb/sq in.), and the clamp retightened.

The wire jig is always attached to a micromanipulator. In many cases, a second jig and manipulator are required, as for mounting a V-wire. One or both of the manipulators are adjusted to bring the wire to the proper position with relation to the supports. The wire should just touch the supports. In the case of a single wire, a mixture of flux and finely ground 650° C silver solder is applied under the stereoscopic microscope to the junction farther from the jig spring. At this point, either an electric or a torch method of heating the prong tip may be used. The alcohol torch, fine-tipped and fed by oxygen under several pounds pressure, is excellent for the work. The flame should be perhaps 3 centimeters in length; it can hardly be too fine.

The flame tip is directed at the wire support between the mount and the junction. Under no circumstances can it be allowed to play on the wire or the joint itself. When the support has become locally



heated to a moderate red heat, the flame tip is brought nearer the joint until the joint - by conduction only - has been brought to a moderate red. It is nearly impossible to melt the solder too quickly. Several seconds use of the flame is adequate. The wire on the joint side should now be melted through at a distance of about 0.5 centimeter from the joint. This procedure transfers the spring load to one support. Next, the joint at the support nearer the spring should receive solder and the same flame treatment. The wire can then be melted through on that side; the spring arm should be caught by the operator or a rubber stop to prevent damage. Alternately, the spring arm may be pushed toward the pulley and the melting accomplished or, in this case, a pair of scissors can be used. The jig is then removed from the work area.

Under the microscope each free wire end is seized, preferably by a reverse-action pair of tweezers. In the process of engagement, the pair of tweezers is advanced toward the proper support so that the free end is never under tension. Finally, a half-loop is made of the free wire and the piece is moved back and forth (transverse to the wire axis) until the free end breaks off.

If this procedure is followed, the wire will be rigidly fastened to the supports under a stress about one-half that originally produced by the spring action of the jig. A stress of about  $0.212 \times 10^{10}$  dyne centimeter<sup>-2</sup> (30,000 lb/sq in.) can therefore be achieved in this fashion; by the use of more elaborate schemes, this figure can be doubled if necessary. The difficulty of wire mounting increases, however, more rapidly than does the final stress. In the case of tungsten, higher stresses are easily achievable and are desirable.

In the case of a parallel pair of wires, wherein both wires are attached (in spatial and electric parallelism) to the same pair of supports, the only problem is that of holding the wires on the jig. For this purpose, an auxiliary pulley is added to the spring arm. When a continuous length of wire has been attached to the jig, the course being from bobbin through clamp, over first and second pulley, and then over the spring-arm pulley and back to the clamp, the forces on the two wires will, of necessity, remain equal. If each main pulley is plurally grooved to a depth of about 0.005 centimeter, using a groove interval of about 0.013 centimeter, the spacing of the wires can be varied in 0.013-centimeter steps, the two being held to true parallelism.

When a mount carries more than one wire or parallel pair, the wires or pairs are simultaneously positioned. The precise soldering



procedure varies with the configuration. The basic techniques remain the same, namely, to solder as quickly and with as little heat and solder as practicable and to transfer spring force to that support farther from the spring arm prior to application and heating of solder at the remaining joint of a given wire. In most instances involving a wire array, a support to which is to be attached a plurality of wires is either actually or effectively more rigid than each of those that carry a single wire. It is therefore best to attach the wires to the single-wire supports prior to attachment to the multiple-wire support, for through such a procedure the final wire stresses are more easily established at high values.

Types in use. - Several typical mounts in current use are shown in figures 7 to 9. A photograph of the working end of a horizontal V-array that was combined with a total-pressure tap is shown in figure 7. Upon suitable calibration, the tap may be used to indicate a pressure less than static by rotating the instrument through  $180^\circ$  about the axis; the calibration will be followed if the radial-flow component is not too great. The dimensions are typical of a 0.0038-centimeter wire array; the entire working end is scaled down for the smaller wires.

A parallel-wire array is shown in figure 8. The 0.0020-centimeter wires are separated by about 0.013 centimeter (center to center) and are inclined at about  $45^\circ$  to the horizontal plane. A total-pressure tap is incorporated.

A double parallel-wire array is shown in figure 9. Each pair is similar to the array of figure 8. No pressure tap has been provided; the central support could have been designed to serve this purpose.

## APPARATUS

### Test Tunnel

A conventional wood converging-diverging nozzle was used for the investigation and calibration of the arrays. The cross section is rectangular, the width is constant at 7.62 centimeters, and the throat height is 10.16 centimeters.

Instrument bosses are located along the center line of one or the other of the plane sidewalls at positions such that flows at eight fixed Mach numbers ranging from 1 to 2.4 are available when



the tunnel is being operated at a sufficiently high pressure ratio. Subsonic data are obtained at the throat at subcritical pressure ratios.

Dried, felt-filtered air is supplied through a plenum chamber having an inside diameter of 91 centimeters. It is shown in reference 26 that large changes of relative humidity have small but detectable effects on hot-wire heat-loss rates. It would have been impossible to obtain substantially shock-free flow at supersonic speeds without at least partial desiccation. Accordingly, the relative humidity, as measured at room temperature and atmospheric pressure, was kept below 5 percent.

No evidence of shock formation at Mach numbers below 2.2 was ever observed when the total temperature exceeded 35° C. Oblique shock formation occasionally became evident beyond Mach numbers of 2.2. The Reynolds number range for Mach numbers beyond 1.5 was restricted by limited heater capacity.

#### Bridge

The circuit of the bridge employed is given in figure 10. For all functions other than the determination of the ratio of two array resistances (for example, arms of a V), the circuit is that of a Kelvin double bridge.

The switch arrangements are such that lead and contact resistances are either compensated by the Kelvin connection or are in series with the high-resistance arms of the bridge. In either case, no appreciable error results.

A 1.0-ohm four-terminal resistor is used as the fixed reference arm. The variable arms consist of commercial decade units of high stability.

Suitable means are provided whereby the effective galvanometer sensitivity may be altered or the galvanometer as well as the wire removed from the circuit when no reading is being taken. The switch contacts are so arranged that the galvanometer is connected to the circuit only after initiation of current flow in the wire or is disconnected from the circuit prior to interruption of the flow of wire current.



One use of the bridge is the determination of the resistance of an unheated array or an array heated by the passage of a fixed current.

A second use of the bridge is the conventional one of hot-wire anemometry; that is, provision of a sensitive and accurate means of determining whether the resistance of a heated array agrees with some fixed predetermined value.

The third use of the bridge is that of determination of the ratio of the resistances of members of an array (for example, the arms of a V). Such a determination may be an original one or a subsequent one required to make possible a decision as to whether a ratio has remained fixed at the original value (as during rotation of a heated V exposed to a stream).

Bridge operations are subsequently discussed in the section PROCEDURES.

#### Uniform-Temperature Baths

The electric characteristics of the supports as fabricated and of the mounted wires have been determined by the use of ice baths and a molten-salt uniform-temperature bath based on National Bureau of Standards practices.

The purpose of each bath is the provision of a reasonably extensive zone over which the temperature is virtually constant and in which the temperature is accurately known. The support and wire resistances at 0° C are obtained by measuring those quantities while the mount is immersed in the melting-ice bath. The temperature coefficient of the wire or of the supports is then obtained by noting the resistance of the wire or supports while the mount is immersed in the salt bath at an appropriate temperature, usually about 300° C. In each case, a closely fitting metallic protection tube is used.

In the case of the resistance of the supports, it is convenient (before wire mounting) to attach a shorting bar of negligible resistance to each pair of supports; the position is the same as that of the wire (or pair) that is to replace the bar. In an array resistance measurement, the known resistance (at the appropriate temperature) of the supports in series with the array is subtracted from the total resistance.



The salt-bath temperature is uniform to within a deviation undetectable by use of an exploring thermocouple over the central 60 or 70 cubic centimeters of the bath. A 650° C mercury thermometer readable to  $\pm 0.1^\circ$  C is used for routine work; the thermometer must be checked from time to time against a platinum-platinum - rhodium thermocouple.

The temperature assumed by the wire in either bath differs negligibly, after a suitable waiting period, from the bath temperature. The salt-bath temperature is routinely determined to better than  $\pm 0.25^\circ$  C; the internal consistency of the readings is higher. The over-all accuracy is therefore sufficient for the present application.

## PROCEDURES

### Mass-Flow or Heat-Loss Measurement

The experimental procedures required to make measurements of heat losses from a wire under known flow conditions and to make mass-flow determinations in unknown flow regions are similar.

Total temperature and pressure and exit pressure of the test tunnel are assumed to have been adjusted to the desired values. In general, the array must be exposed to a succession of mass-flow rates at each of a succession of Mach numbers; the total temperature may, according to simple theory, be permitted to vary widely, but in practice must usually be held within certain narrow limits (which was the case in the present work) if the amount of computational labor involved in the reduction of data and presentation in non-dimensional form is not to be unduly large.

Array resistances, temperature coefficients of resistance, dimensions, and behavior when unheated and exposed to flows at various Mach numbers must have been previously determined. From this information the ratio  $T_e/T_t$  has to be determined as a function of Mach number.

An array mean operating temperature (up to about 500° C for iridium-platinum) is chosen and the resistance calculated. The bridge variable-arm settings required to ensure bridge balance (at the sum of the resistances of the selected array and supports) are made.



The array is exposed to the stream at the desired immersion depth and orientation. Current is then permitted to flow through the array and the magnitude adjusted until bridge balance has been attained. The magnitude of the current is determined.

Because the flow conditions are known, the Mach number and therefore the effective temperature are known. All quantities required for the calculation of  $Nu_f/Pr_f^{0.3}$  in the idealized relation equation (7) are then known. The practical calculation of the end-loss correction factor required in the case of a real wire having finite rather than zero thermal conductivity is subsequently considered in the section CALCULATIONS AND CORRECTIONS.

In a mass-flow determination, the heat-loss determination must be preceded or accompanied by a flow-angle determination (discussed previously in the section Possible Array Configurations and Uses and subsequently in the section Angle Data). Knowledge of the flow yaw angle permits the array to be oriented with respect to the stream approximately as it was oriented with respect to the calibration flow. Successive measurements of effective temperature and of heat loss at a selected array temperature are then made as discussed elsewhere.

A pressure reading is made at the same time if the instrument is equipped with an appropriate tap and tube.

Although the Nusselt number can be calculated at this point (the necessary end-loss correction having been made), the calculation of mass-flow rate cannot, in general, be continued according to equation (7). The required algebraic procedure is presented in the section Adaptation of generalized correlation for mass-flow-determination applications.

#### Angle Data

The yaw angle of the flow (with respect to some arbitrary direction) can be measured, as discussed in general terms in the section Possible Array Configurations and Uses, by a single horizontal V, or by a vertical parallel pair.

The required procedure in the case of the single wire or horizontal V has been described in sufficient detail.

In the case of the use of either a vertical V, vertical parallel pair, or the array of figure 9 in the determination of



yaw angle, the procedure has been outlined in the section on array configurations. An unimportant difficulty in practice is that of combining the mass-flow and angle determinations. The bridge arms are set for the desired array operating temperature. The array is then oriented so that the principal direction coincides with the estimated vertical plane of the flow. In the case of an array having two arms, the arms are placed in series. The array current is adjusted to the value required to balance, approximately, the bridge.

The mount is then rotated while the current remains fixed until the direction of change of bridge output voltage reverses. At that point the array plane and the vertical plane containing the flow vector coincide. If a parallel-pair array is being used, a recheck of the current required for bridge balance is often required. In the case of a vertical V (of single wires), no such check is necessary because the Nusselt number will not vary rapidly with yaw angle.

#### Temperature Measurement

Temperature measurements have been previously considered; it has been remarked that each array is usable as a resistance thermometer. The procedure in practice is first to align the array with the flow (in yaw). A current ranging from 3 milliamperes for the smallest wires and lowest air flows to 15 milliamperes for the largest wires and highest air flows is then permitted to pass through the wire. The bridge is balanced by adjustment of the variable arms and the total resistance of array and supports is calculated. After the deduction of the resistance of the supports (virtually independent of temperature in the case of Inconel), the array temperature is computed by the use of equation (1). Finally, the effective temperature is converted to static (or total).

The preceding discussion neglects two possible sources of error, namely, strain-gage effect and the conduction of heat to or from supports immersed in portions of the stream flow at effective temperatures differing from the mean value characteristic of the region in the vicinity of the wire. The correction for strain-gage effect is discussed later in the section Stress corrections. The second source of error has been negligible so far. The required theory may be obtained by a slight modification of the end-loss treatment presented in appendix B; however, it is not given herein.



## CALCULATIONS AND CORRECTIONS

Evaluation of fluid constants. - Throughout the calculations, the properties of air have been generally evaluated at the mean film temperature, which is defined as the arithmetic mean of the local effective temperature and the object temperature. A slight departure from the stated practice occurred in the evaluation of air properties in connection with heat transfer from the supports to the stream. For reasons of simplicity, and with no significant loss of accuracy, it was decided in that instance to use the total rather than the mean temperature, as previously defined.

The air thermal conductivity, viscosity, and Prandtl number were evaluated at the film temperature as so defined.

End losses. - The principal correction required in connection with all wire devices is the elimination of the effects of end losses on the absolute values of the heat-transfer coefficients.

The necessary theory, which essentially is a modification of earlier treatments, is given in appendix B. The approximations made, as stated in appendix B, do not adversely influence the exactitude of the treatment.

All heat-loss data presented herein were corrected for end loss when such correction had a significant effect on the magnitudes of the data reported. The following relation determined the correction:

$$Y \left( \frac{1}{1 + \xi} - t \right)^{1/2} - \frac{(1 - t)}{(1 - t) - \left( \frac{1}{1 + \xi} - t \right)} + B \left( \frac{1}{1 + \xi} - t \right) = 0 \quad (22)$$

The several parameters are defined by the following equations:

$$Y \equiv \frac{L_w}{D_w} \left[ \frac{0.238912 \bar{r}}{\pi k_w (\bar{\theta}_w - \theta_e)} \right]^{1/2} = \frac{L_w}{D_w} \left( \frac{k_f}{k_w} \right)^{1/2} Nu_f^{1/2} \quad (23)$$



$$t \equiv \frac{\bar{\theta}_w - \theta_e}{\bar{\theta}_w + \alpha^{-1}} \quad (24)$$

$$B \equiv \frac{0.2389 i^2 r}{1.54 k_b^{1/2} k_t^{1/2} D_b \left( \text{Re}'_{t,b,2} \right)^{0.3} (\bar{\theta}_w - \theta_e)} \quad (25)$$

When  $\xi$  has been calculated by the use of equation (22), the Nusselt number is calculated according to a modified equation (7), which becomes

$$0.2389 i^2 r = \pi k_f \text{Nu}_f (\bar{\theta}_w - \theta_e) (1 + \xi) \quad (26)$$

The quantities  $B$ ,  $\text{Nu}_f$ ,  $\left( \text{Re}'_{t,b,2} \right)^{0.3}$ ,  $t$ ,  $Y$ , and  $\xi$  are dimensionless. The conversion factor 0.2389 calorie per second per watt that appears in the previous equations is present because the product  $i^2 r$  has the dimensions watts per unit length whereas the thermal conductivities  $k_f$ ,  $k_p$ ,  $k_t$ , and  $k_w$  are normally assigned the dimensions calories per unit length per second per  $^\circ\text{C}$ . The factor 1.54 is a pure number. The calculation of  $\xi$  requires computation of  $B$ ,  $t$ , and  $Y$ .

When a given instrument is being calibrated all the required quantities are immediately available. In an experimental situation, however, neither the total temperature nor the local mass-flow rate is initially known and it is therefore impossible immediately to determine  $k_t$  and  $\text{Re}'_{t,b,2}$ . The magnitude of  $\xi$  is not critically dependent upon  $B$  (which essentially determines the temperature at the ends of the wire), however, and because  $B$  varies only as  $k_t^{-1/2} \left( \text{Re}'_{t,b,2} \right)^{-0.3}$  it follows that the use of reasonable estimated values of these quantities will lead to virtually the final value of  $\xi$  upon first calculation. In this connection, the quantities  $k_e$  and  $\mu_e$  may be initially used in place of  $k_t$  and  $\mu_t$ , respectively. If desired,  $k_t$  and  $\text{Re}'_{t,b,2}$  may be recalculated after the first approximation of the local-flow conditions has been obtained.



The over-all error in the calculated value of  $\xi$  in any given case is estimated to be less than 5 percent. On the other hand, the internal consistency of calibration data and experimental data will be of a higher order than that figure appears to imply, inasmuch as errors in  $\xi$  are primarily of a systematic rather than an accidental nature.

In the present end-loss treatment, an assumption is made that the ratio of effective to total temperature is the same for both wire and supports. Otherwise expressed, such an assumption is equivalent to the ignorance of Reynolds number effects on the ratio in question. The experimental data available are insufficient to form a basis of determination of the validity of the assumption.

In the absence of a difference of effective temperature between wire and support, no end effects exist when temperatures are being measured and no end-loss correction need be made.

Stress corrections. - Despite all precautions, hot-wire instruments are rather susceptible to damage. No data are presented herein that were obtained with any wire which for any reason whatever exhibited an irreversible change of resistance amounting to more than about 0.1 percent between checks of that quantity. Temperature-coefficient changes as great as 0.2 to 0.3 percent occurred between checks and were tolerated.

As has been pointed out, reversible deformations of the wire cause changes of total heat-transfer rates associated with the corresponding changes of the exposed surface area. Such changes are patently negligible.

The accompanying resistance change, to the contrary, is not necessarily negligible.

In the case of the current data the required calculated corrections would have been of smaller magnitude than the figure of precision of the measurements. Such reversible strain-gage effects were therefore ignored.

Calculation of the stress change (occasioned by aerodynamic loading) and of the associated resistance change has been briefly discussed in the section Aerodynamic stress effects. Use of the relations presented (equations (11), (12), (13), (15), and (16)) in a few typical cases led to  $\Delta R/R$  values small enough to warrant ignorance; however, the magnitudes of the errors involved in such calculations must be considered.



Because of the nature of the assumptions made in the derivation of equation (12) (appendix C) and the rather large uncertainties in the values of  $C_D$  and of  $F$  in any given case, it is questionable that the value of  $\sigma_2$  is known to better than  $\pm 10$  percent.

The value of  $C_D$  is actually obtained by multiplying the incompressible value ( $C_{D,n}$  in fig. 11) by the ratio of the compressible coefficient to the incompressible (fig. 11); the values have been taken from references 27 and 28. The procedure is not rigorously correct but yields values of  $C_D$  probably correct to better than  $\pm 10$  percent. The underlying assumption is that the variations of  $C_D$  reported for various Mach numbers were, to a first approximation, uninfluenced by the relatively small changes of Reynolds number occurring over the speed ranges in question.

The calculated value of  $\sigma_3$  varies slowly with  $\sigma_2$  at low values of  $\sigma_2$  (and high values of  $\sigma_1$ ) and approximately as  $\sigma_2$  at the higher values of  $\sigma_2$  (that is, those considerably greater than  $\sigma_1$ ). The greatest error in  $\sigma_3$  is therefore about 10 percent if the uncertainty in  $\sigma_1$  is ignored.

The possible error in the difference  $(\sigma_3 - \sigma_1)$  is of greater importance than the error in  $\sigma_3$ , inasmuch as  $(\sigma_3 - \sigma_1)$  determines the change of wire characteristics. At currently employed values of  $\sigma_1$  (about 20 percent of the room-temperature yield points of the wire materials used), the uncertainty of  $(\sigma_3 - \sigma_1)$  probably is usually less than  $\pm 2.1 \times 10^8$  dyne centimeter<sup>-2</sup> ( $\pm 3000$  lb/sq in.) at any absolute stress up to about  $3.4 \times 10^9$  dyne centimeter<sup>-2</sup> (50,000 lb/sq in.). Whenever substantial (greater than 0.0025 cm) differential bending of supports can occur due to unequal aerodynamic loading or use of unmatched supports of insufficient rigidity, the errors will be greater.

Substantiation of equations (11) and (12) should be accomplishable by exposing a wire to flows characterized by a range of Reynolds numbers at nearly constant Mach number and total temperature. If the Reynolds number range is not great enough to affect conceivably the ratio of effective to total temperature, any apparent variations of effective temperature can be tentatively ascribed to resistance changes caused by variation of tensile stress. Recently, a few data were obtained with a standard-mount, single-wire combination in an attempt to substantiate quantitatively the theory as well as the preceding considerations concerning the over-all precision of calculations of stress changes.



No significant change of resistance of an iridium-platinum wire could be detected while the air-flow characteristics were varied in the manner indicated. The value of  $\sigma_1$  was about  $1.4 \times 10^9$  dyne centimeter<sup>-2</sup> (20,000 lb/sq in.). The negative result was interpreted as signifying that either the true resistance change was as predicted by theory (in this case, not quite detectable) or was smaller by some unknown decrement. Such tests should be repeated at low  $\sigma_1$  values and high  $L_w/D_w$  ratios.

Accordingly, the theory probably sets an upper bound to the resistance change as well as to the absolute steady stress under given conditions.

## EXPERIMENTAL RESULTS AND DISCUSSION

### Calibration and Mass-Flow Determination

In the following paragraphs, typical data obtained with a single wire normal to the stream are considered along with the utilization of such information. The behavior of a more complex array is similar for a fixed orientation with respect to the stream although the values of the dimensionless constants of the equations will, in general, be different from those applying to the single wire.

Calibration of single wire normal to stream. - Results of a series of heat-loss experiments made with the same 0.0038-centimeter-diameter wire over a period of about 1 month are presented in figure 12. The air temperature varied between 23° and 45° C. The wire temperature was fixed at 290° C. A systematic change of  $Nu_f/Pr_f^{0.3}$  with Mach number can be observed.

Data taken at several wire temperatures are presented in figure 13. The total air temperatures varied between about 25° and 50° C. The uncertainties of the thermal conductivity of air and of viscosity are not thought to be sufficiently great to account for the increase of  $Nu_f/Pr_f^{0.3}$  at decreasing wire temperatures.

The deviations are in a direction such that the inference is possible that the mean wire temperatures actually are higher than the assigned values. For example, if all mean wire temperatures actually were about 3° C higher than the assigned values, the several curves would coincide. No source of such large errors could be found, however.



Correlation equations. - In order to correlate the data of figures 12 and 13 properly, a more complex relation than that of equation (7) is required. In view of the change of  $Nu_f/Pr_f^{0.3}$  with Mach number, it is necessary to introduce in the manner subsequently indicated a wholly empirical function designated  $f_1$  and dependent solely upon Mach number. The value of  $f_1$  is arbitrarily taken to be 1 at a Mach number of 1.

The spread of the data of figure 13 with wire temperature can be eliminated by the adoption of a temperature function in the manner indicated in the section Basic Instrument. In the absence of variable air-temperature data, however, the exponent of any temperature ratio so employed would be quite arbitrary. When such data become available, it should not be difficult to exhibit heat-loss data over wide ranges of air temperature, wire temperature, Reynolds number, and Mach number as a single-valued function in view of the regularity of change of nondimensional heat-loss rate with change of wire temperature. Because a difference of temperature  $(\bar{\theta}_w - \theta_e)$  of at least  $150^\circ\text{C}$  is required if reasonably reliable heat-loss data are to be obtained, the maximum allowable effective air temperature will be about  $275^\circ\text{C}$ ; this value is based on the conservative maximum allowable operating wire temperature of  $500^\circ\text{C}$  and the usual difference (approximately  $70^\circ\text{C}$ ) between  $\theta_{w,c}$  and  $\bar{\theta}_w$ . The air temperature is unlimited by any factor other than wire behavior and the existence of suitable calibration facilities; the mounts have been successfully subjected to high-temperature flows. For the present, however, the air temperature is assumed to remain within perhaps  $\pm 50^\circ\text{C}$  of some reference value and the wire temperature is assumed to vary by not more than  $\pm 25$  percent (in terms of the value on the centigrade scale). Under such conditions adoption of a temperature function is unnecessary.

A correlation of the data of figure 12 of the type

$$\frac{Nu_f}{Pr_f^{0.3}} = C_1 + C_2 \left( Re'_{f,w} \right)^{0.5} f_1 \quad (27)$$

is accordingly indicated, for the several curves apparently converge to a common zero-flow intercept on the  $Nu_f/Pr_f^{0.3}$  axis.



Actually, however, it is impossible to determine either from the data of figure 12 or from other similar data obtained at this laboratory whether such a correlation or one of the following type represents a correct description of the data:

$$\frac{\text{Nu}_f}{\text{Pr}_f^{0.3}} = \left[ C_1 + C_2 \left( \text{Re}'_{f,w} \right)^{0.5} \right] f_1 \quad (28)$$

In view of the fact that it is unnecessary as well as impossible to distinguish between the two possible correlations because of the smallness of the constant  $C_1$  in comparison with  $C_2 \left( \text{Re}'_{f,w} \right)^{0.5}$  for Reynolds numbers greater than about 30, equation (27) has been arbitrarily adopted as the description of these and similar data because of its relative simplicity.

According to equation (28),  $f_1$  could be defined as the ratio of the Nusselt number at a particular Mach number to that at a Mach number of 1.0 and the same Reynolds number. Such a definition, although not rigorously applicable in the case of equation (27), is convenient as an approximation to the precise denotation.

No attempt has been made to establish a quantitative theoretical basis for  $f_1$ . Qualitatively, it appears reasonable that the function, whatever its nature in the subsonic regime, should exhibit rough over-all symmetry about a point at a Mach number of 1.0 on a plot of  $f_1$  against Mach number (fig. 14). This observation stems from the consideration that the fluid flow over a substantial portion of the surface of a wire at a given supersonic free-stream speed is roughly equivalent to that at some subsonic free-stream speed because of the presence of a bow wave at the supersonic speed. The correspondence requires further investigation but is partly confirmed by the circumstance that  $f_1$  has nearly the same value at pairs of Mach numbers connected by the well-known normal shock relation

$$M_2^2 = \frac{1 + \frac{\gamma-1}{2} M_1^2}{M_1^2 - \frac{\gamma-1}{2}}$$



in which the subscripts 1 and 2 refer to the conditions prior and subsequent to the shock, respectively.

The function  $f_1$  as well as certain other functions to be discussed is shown in figure 14. Although the values plotted are probably nearly correct, modification will possibly be required as additional data are obtained. Furthermore, some evidence (not presented herein) exists that indicates that the shape of the curve is modified by orientation of the wire at an acute angle to the stream. Qualitatively, such an effect should exist at supersonic speeds because of the flow-field modifications accompanying the shock configuration associated with the forward support (or supports, in the case of certain multiple-arm arrays). In any case,  $f_1$  must currently be experimentally determined for each array.

Comparison of the data of figures 12 and 13 with published data on a quantitative basis is impossible because no similar information has been released. The equation of the line  $M = 0.375$  is

$$\frac{Nu_f}{Pr_f^{0.3}} = 0.16 + 0.468 Re_f^{0.5} \quad (29)$$

The use of

$$\frac{Nu_f}{Pr_f^{0.3}} = 0.35 + 0.47 Re_f^{0.52} \quad (30)$$

is recommended in reference 8 (equation (4a), p. 222) in the Reynolds number range from 0.1 to 1000 at low Mach numbers. Because equation (30) represents the best curve through many data points obtained by a number of investigators, it should be reliable.

The value 9.80 for the variable  $Nu_f/Pr_f^{0.3}$  at an  $Re_f^{0.5}$  value of 18 is obtained from equation (30); equation (29) yields 8.58+ at the same  $Re_f^{0.5}$  value. The difference is partly ascribable to the fact that the data of figure 12 do not extend to the very low Mach numbers at which  $f_1$  certainly exceeds the value corresponding to  $M = 0.375$ .



Furthermore, no entirely satisfactory method has been employed at this laboratory for the measurement of wire diameter. The diameter used in the calculations is possibly in error by several percent. Accordingly, it is felt that the agreement between equations (29) and (30) is fairly good.

Adaptation of generalized correlation for mass-flow-determination applications. - Because introduction of a function of Mach number to effect correlation of heat-loss data obtained at different Mach numbers has been found necessary, the question of the utilization of such data arises. It will now be shown that the combination of an indicated pressure, an effective temperature, and a heat-loss datum uniquely specifies the local steady-state flow characteristics. The flow direction is assumed to be either known or determinable.

The quantities

$$\rho^* \equiv \frac{p_1}{R_g T_e} \quad (31)$$

and

$$\text{Re}^*_{f,w} \equiv \frac{\rho^* a_e D_w}{\mu_f} \quad (32)$$

are defined.

Then,

$$\text{Re}_{f,w} = \text{Re}^*_{f,w} \frac{\rho V}{\rho^* a_e} \quad (33)$$

Furthermore,

$$f_2 \equiv \frac{\rho V}{\rho^* a_e} = \frac{p_g}{p_1} M \sqrt{\frac{T_e}{T_s}} \quad (34)$$

is defined.



From equations (33) and (34),

$$\text{Re}_{f,w} = \text{Re}^*_{f,w} f_2 \quad (35)$$

The immediate significance is that separation has been effected of  $f_2$ , the factors of which are dependent solely upon Mach number, and of  $\text{Re}^*_{f,w}$ , experimentally determinable without reference to the Mach number.

Combination of equations (27) and (35), permissible because  $\text{Re}'_{f,w} = \text{Re}_{f,w}$  in this case, yields

$$\begin{aligned} \frac{\text{Nu}_f}{\text{Pr}_f^{0.3}} &= C_1 + C_2 \left( \text{Re}^*_{f,w} \right)^{0.5} f_1 f_2^{0.5} \\ &= C_1 + C_2 \left( \text{Re}^*_{f,w} \right)^{0.5} f_3 \end{aligned} \quad (36)$$

in which

$$f_3 \equiv f_1 f_2^{0.5} = f_1 \left[ M \frac{p_s}{p_1} \left( \frac{T_s}{T_e} \right)^{-1/2} \right]^{0.5} \quad (37)$$

Now  $f_3$  is a function of Mach number alone; it is experimentally determined prior to any mass-flow measurement.

Accordingly, the Mach number and mass-flow rate may be obtained by the following procedure:

(a) The experimental data and equations (26) and (32) are used to calculate  $\text{Nu}_f$  and  $\text{Re}^*_{f,w}$ .

(b) Equation (36) is used for the calculation of  $f_3$ .

(c) The experimental relation between  $f_3$  and  $M$ , represented by equation (37), is used to determine  $M$ .



(d) Equation (34) and the value of  $f_2$  corresponding to the obtained value of  $M$  are used to calculate  $\rho V$ .

Limitation of  $Re^*$  method. - The method is clearly applicable regardless of the value of the exponent of  $Re_{f,w}$ .

In practice, the procedure will yield a well-defined value of  $f_3$  only when the indicated pressure  $p_i$  exceeds the static  $p_s$  by, at most, about 20 percent of the velocity head. In figure 14, values of  $f_3$  are plotted for three cases. The case in which the known pressure is the static pressure is that for which  $p_s/p_i = 1.0$ . A second curve is given that corresponds to the use of a pressure tap having the constant recovery coefficient of 0.5 so that

$$\frac{p_s}{p_i} = \frac{1}{1 + 0.5 \left( \frac{p_t}{p_s} - 1 \right)} \quad (38)$$

The total pressure upstream of any shock configuration has been used here because the nature of the device is unspecified and calculation of the total-pressure loss across any shock is therefore impossible. The third curve corresponds to the use of a hypothetical total-pressure tube that indicates true total pressure under all conditions. The corrections at Mach numbers below 1.4, for any real total-pressure tube, would be small.

It is patent that the prescribed procedure will fail completely in the third case; it will be unsatisfactory in the second. The physical reason for the situation appears to be that, with a pressure which is itself nearly invariant with Mach number, neither the change of Nusselt number with Mach number nor the change of effective temperature with Mach number is sufficiently great to define the point on the Mach number scale at which the heat loss is occurring. Otherwise stated, the principal determiner of Mach number must be a pressure that varies substantially with Mach number, that is, a pressure approaching the true static pressure. Considered from the point of view of Reynolds number variations,

$$Re^*_{f,w} = \frac{p_i a_e D_w}{R_g T_e \mu_f}$$

must be strongly dependent upon Mach number.



Because total-pressure taps have already been added to two types of mount, static-pressure taps may be added as well. The outlined procedure is one of very general usefulness, as it is necessary only that the indicated pressure roughly approximate the static pressure.

#### Yaw Characteristics of Angle-Sensitive Arrays

V-array. - Figure 15 presents the yaw characteristics of a V-wire having a  $90^\circ$  apex angle. Galvanometer deflection has been entered as a function of angle of deviation from the point of zero deflection. These data were obtained for a succession of  $M$  values, the total pressure and wire and air total temperatures remaining fixed throughout. It is apparent that: (1) The plots are straight lines that would all pass through the common origin had they not been, except for the lowest one, displaced upward to exhibit their characteristics more clearly; (2) the lines have roughly equal slopes, indicating constant sensitivity over the flow range in question; and (3) the characteristics at high supersonic speeds are the same as at low speeds.

The over-all accuracy of a determination of angle should be considered to be about  $\pm 0.5^\circ$ . This value would be smaller for a V-wire having, for example, an apex angle of  $45^\circ$ .

The linearity of response has been predicted in the section on the V-mount for the subsonic case. No theory is available for the supersonic case, but evidently the same relation holds, that is, the bridge output current or voltage is linearly dependent upon the angle  $\psi$  at small angles.

Parallel-wire array. - Figure 16 shows the yaw characteristics of a typical parallel-wire mount; in this case the array consisted of two 0.0025-centimeter-diameter wires 0.25 centimeter long separated by about 0.013 centimeter and oriented at about  $45^\circ$  to the stream.

For yaw applications, a bridge output meter having a small period, for example, less than 0.1 second, is very desirable but was unavailable; the sensitivity requirements are high. The galvanometer used had a period of 3 seconds; the point of deflection-movement reversal was accordingly less certain than the inherent tolerance of the array and there is therefore some scatter in the data points. The over-all accuracy of an angle determination should be considered as about  $\pm 0.5^\circ$ .



The deflections are presented as a function of angle of deviation from direction of maximum deflection for several different Mach numbers. Again, the characteristics are essentially independent of  $M$ , although there is a slight increase of sensitivity with increase of  $M$ . Supersonic results are unavailable, but no reason exists to suppose that the array behavior would be different in that region.

The accuracy with which flow angles can be determined is indicated in figure 17. In the first case, the Mach number was held at 0.457 and the mass-flow rate varied over a wide range. In the second case, the Mach number was varied from a low value through the transonic range and the section pressure held constant. The density varied slightly, of course, as the static temperature varied with  $M$ . The shift of the angular zero position was small in each case. There are reasons based on experiment for believing that the test-tunnel air-flow direction varies slightly and it must be considered that the errors are total values, that is, wire plus tunnel.

#### Temperature Recovery Ratio

In figure 18, the current knowledge of  $T_t/T_e$ ,  $T_e/T_t$ , and  $T_s/T_e$  is presented for air (Prandtl number  $\approx 0.74$  and  $\gamma = 1.4$ ) in the case of normal exposure of a circular cylinder.

The German data (reference 15) were obtained at somewhat higher Reynolds numbers and, although of interest, are not strictly comparable to those obtained at this laboratory. Other subsonic data (reference 14) are in substantial agreement with the subsonic portions of the curves of figure 18.

In figure 19, preliminary data pertaining to the question of variation of the ratio  $T_e/T_t$  with the angle between a supersonic stream and the normal to the wire are presented. Such effects are significant and in view of the surprising lack of symmetry of the results about the  $0^\circ$  point end effects (exposure to post-shock cone flow) are pronounced.

These results indicate that when an array of wires not all of which are normal to the stream is used, the array temperature ratio  $T_e/T_t$  as well as the heat-loss characteristics must be determined.



### CONCLUSIONS

An investigation was made of the design requirements and heat-transfer characteristics of wire instruments to be used as hot-wire anemometers and resistance-wire thermometers at transonic and supersonic speeds. The following conclusions were drawn from the results:

1. Fine-wire instruments of proper design may be used to obtain accurate air temperature, mass-flow rate, and flow-angle data over at least the total temperature range from  $0^{\circ}$  to  $275^{\circ}$  C, at Mach numbers ranging from 0 to at least 2.4, and at air total densities at least as great as twice atmospheric. The stability of such devices may be made sufficient for engineering use.

2. Heat-transfer data for a circular cylinder over at least the Mach number range from 0 to 2.4 may be correlated by addition to the conventional relation among Nusselt, Prandtl, and Reynolds numbers of a factor that is a function of Mach number only.

3. Thermometric and power-input data obtained with such instruments together with a pressure datum having as an upper limit a pressure exceeding static pressure by about 20 percent of the velocity head uniquely specify a local flow situation regardless of the lack of other information concerning Mach number.

Lewis Flight Propulsion Laboratory,  
National Advisory Committee for Aeronautics,  
Cleveland, Ohio, January 12, 1950.



## APPENDIX A

## SYMBOLS

Symbols used only in appendixes B and C are defined where used and are not listed.

A	cross-sectional area, $\text{cm}^2$
$A_{b,2}$	cross-sectional area of wire support at point of wire attachment, $\text{cm}^2$
a	speed of sound, $\text{cm sec}^{-1}$
B	$\frac{0.2389 \cdot 10^{12} \bar{r} L_w}{1.54 k_b^{1/2} k_t^{1/2} D_b \text{Re}'_{t,b,2}{}^{0.3} (\bar{\theta}_w - \theta_e)},$ nondimensional (1.54 is a pure number)
$C_D$	drag coefficient for circular cylinder normal to stream
$C_{D,n}$	drag coefficient for circular cylinder normal to stream under incompressible-flow conditions
$C_1, C_2, \dots$	constants defined in text
$c_p$	specific heat of air at constant pressure, $\text{cal gram}^{-1} \text{ } ^\circ\text{C}^{-1}$
D	diameter, cm
$D_{b,1}$	diameter of wire support at base, cm
$D_{b,2}$	diameter of wire support at point of wire attachment, cm
E	Young's modulus of elasticity, $\text{dyne cm}^{-2}$
F	flexibility of wire support or pair of supports, deflection per unit force, $\text{cm dyne}^{-1}$
$f_1$	ratio of Nusselt number at given Mach number to that at Mach number of unity at fixed Reynolds number (definition approximate; defined quantitatively by equation (27))



$$f_2 \quad \frac{\rho V}{\rho^* a_e} = \frac{p_s}{p_i} M \sqrt{\frac{T_e}{T_s}}$$

$$f_3 \quad f_1 f_2^n = f_1 \left[ M \frac{p_s}{p_i} \left( \frac{T_s}{T_e} \right)^{-1/2} \right]^n \quad \text{in which } n \text{ is usually } 0.5$$

G mass-flow rate per unit area, gram cm<sup>-2</sup> sec<sup>-1</sup>

Gr Grashof number

H heat-transfer coefficient, cal cm<sup>-2</sup> sec<sup>-1</sup> °C<sup>-1</sup>

$$H_f \equiv \frac{0.2389 i^2 \bar{r}}{\pi D_w (\bar{\theta}_w - \theta_e) (1 + \xi)}$$

i wire current, amperes

k thermal conductivity, cal cm<sup>-1</sup> sec<sup>-1</sup> °C<sup>-1</sup> (refers to air when subscript e, f, or t used)

L length, cm

L<sub>m</sub> maximum allowable (projection of) wire length in direction of flow (see text), cm

M Mach number

Nu Nusselt number HD/k

$$Nu_f \equiv \frac{0.2389 i^2 \bar{r}}{\pi k_f (\bar{\theta}_w - \theta_e)} \quad \text{ideally, or} \quad \frac{0.2389 i^2 \bar{r}}{\pi k_f (\bar{\theta}_w - \theta_e) (1 + \xi)} \quad \text{if end}$$

losses occur

$$Nu''_f \equiv \frac{0.2389 i^2 \bar{r}}{\pi k_f (\bar{\theta}_w - \theta_e)}$$



Pr	Prandtl number
p	fluid (air) pressure, dyne cm <sup>-2</sup>
P <sub>i</sub>	pressure indicated by measuring device, inherent error of which (taking either true total or true static as a reference) is function of Mach number only, dyne cm <sup>-2</sup>
R	wire resistance, ohms
Re	Reynolds number
Re <sub>f,w</sub>	$= \frac{\rho V D_w}{\mu_f} \quad (\text{when primed, replace } V \text{ by } V')$
Re <sup>*</sup> <sub>f,w</sub>	$= \frac{\rho^* a_e D_w}{\mu_f}$
Re' <sub>t,b,2</sub>	Reynolds number of flow based upon support tip diameter at point of wire attachment, upon mass-flow rate per unit area component normal to support tip at same point, and upon total temperature
Re' <sub>f,L</sub>	Reynolds number of flow based upon wire length L <sub>w</sub> , upon mass-flow rate per unit area component normal to wire, and upon mean film temperature
R <sub>g</sub>	gas constant for air, erg gram <sup>-1</sup> °K <sup>-1</sup>
r	wire resistance per unit length, ohms cm <sup>-1</sup>
$\bar{r}$	$\equiv L_w^{-1} \int_0^{L_w} r \, dx, \quad \text{where } x = \text{distance along wire}$
S	strain-resistance factor of wire material, resistance change per unit resistance per unit strain $\frac{L_w}{R} \frac{\Delta R}{\Delta L_w}$



T	absolute temperature, °K
t	$\frac{\bar{\theta}_w - \theta_e}{\bar{\theta}_w + \alpha - 1}$
U	general function ( $U_{\psi, \delta}$ is defined by equation (8) of the text)
V	fluid velocity, cm sec <sup>-1</sup>
Y	$\frac{L_w}{D_w} \left[ \frac{0.2389 i^2 r}{\pi k_w (\bar{\theta}_w - \theta_e)} \right]^{1/2}$ , nondimensional
$\alpha$	temperature coefficient of resistance of wire material, °C <sup>-1</sup>
$\gamma$	ratio of specific heats
$\delta$	angle between two wires of array, radians
$\xi$	ratio of heat lost by conduction to supports to that lost directly to fluid stream
$\theta$	temperature, °C
$\theta_{w,b}$	temperature at intersection of wire and support, °C
$\theta_{w,c}$	temperature at center of wire, °C
$\theta_{w,\infty}$	temperature virtually identical with $\theta_{w,c}$ (see appendix B), °C
$\mu$	viscosity, poise
$\rho$	fluid density, gram cm <sup>-3</sup>
$\rho^*$	$= \frac{P_i}{R_g T_e}$ , gram cm <sup>-3</sup>



$\sigma$	stress, dyne cm <sup>-2</sup>
$\sigma_1$	wire stress prior to aerodynamic loading, dyne cm <sup>-2</sup>
$\sigma_2$	aerodynamically induced wire stress, dyne cm <sup>-2</sup>
$\sigma_3$	wire stress during aerodynamic loading, dyne cm <sup>-2</sup>
$\sigma_m$	maximum allowable operating wire stress (see text), dyne cm <sup>-2</sup>
$\phi$	angle between flow vector and normal to wire in plane of wire and vector, radians
$\psi$	angle in plane normal to mount axis between projec- tion of flow vector on that plane and either vertex angle bisector of V-array or projection, on same plane, of wire neither orthogonal nor parallel to mount axis, radians
$\Omega$	angle between flow vector and plane normal to mount axis, pitch angle, radians

## Subscripts:

b	wire support
c	center
D	drag
e	effective - with reference to temperature attained by unheated body in fluid stream
f	mean film value, based on arithmetic mean of object and effective temperatures.
i	indicated
L	wire length
m	maximum allowable value
n	incompressible-flow conditions
p	pressure



s	static
t	total
w	wire
0	evaluated at 0° C
∞	pertaining to ideal condition of no end loss

Superscripts:

n	general exponent
'	based on flow component normal to object
"	not corrected for end loss
*	reference state (as defined in text)

The bar ( $\bar{\phantom{x}}$ ) denotes mean value.



## APPENDIX B

## END LOSSES OF WIRES

The steady-state case of a one-dimensional heat flow is elementary and has been given by numerous writers for different situations. The chief purpose of the treatment herein is the reorganization of the material with the aim of expressing the loss in a manner that will facilitate estimates and will expedite the making of precise computations. The results are expressed in a generalized form and the finiteness of the thermal conductance of the support is considered. Initially, the treatment is that of reference 12.

The differential equation (B1) connecting the direct loss to the air stream, the conduction from the volume element in question, and the joulean heat developed locally is

$$0.2389 i^2 r_0 (1 + \alpha \theta_w) = (\theta_w - \theta_e) \pi k_f Nu_f - k_w A_w \frac{d^2 \theta_w}{dx^2} \quad (B1)$$

in which  $r_0$  is the resistance in ohms per centimeter at  $0^\circ \text{C}$  and  $x$  is the distance along the wire.

This equation may be written

$$\frac{d^2 \theta_w}{dx^2} - \beta \theta_w = -\beta_1 \quad (B2)$$

in which

$$\beta \equiv \frac{\pi k_f Nu_f - 0.2389 i^2 r_0 \alpha}{k_w A_w} \quad (B3)$$

and

$$\beta_1 \equiv \frac{\pi k_f Nu_f \theta_e + 0.2389 i^2 r_0}{k_w A_w} \quad (B4)$$



The variation of  $k \text{Nu}_f$  along the wire is ignored; the resulting error is negligible.

By utilizing the boundary conditions  $d\theta_w/dx = 0$  at wire center and taking the origin there (so that  $\theta = \theta_b$  at  $x = l$ , defining  $l \equiv L_w/2$ ), the solution is found to be

$$\theta_w = \theta_{w,\infty} - (\theta_{w,\infty} - \theta_{w,b}) \frac{\cosh \beta^{1/2} x}{\cosh \beta^{1/2} l} \quad (\text{B5})$$

in which

$$\theta_{w,\infty} = \frac{\beta_l}{\beta} = \frac{\pi k_f \text{Nu}_f \theta_e + 0.2389 i^2 r_0}{\pi k_f \text{Nu}_f - 0.2389 i^2 r_0 \alpha}$$

It is of considerable practical as well as theoretical interest that  $\theta_{w,\infty}$  is equal to the equilibrium temperature the wire would assume if there were no end losses. Furthermore, the difference between the temperature at the center of even a short wire and the quantity  $\theta_{w,\infty}$  is small.

Thus

$$\theta_{w,\infty} - \theta_{w,c} = \frac{\theta_{w,\infty} - \theta_{w,b}}{\cosh \beta^{1/2} l} \quad (\text{at } x = 0) \quad (\text{B6})$$

In practical situations,  $\beta^{1/2} l$  is seldom less than 6 and is usually greater; hence,  $\cosh \beta^{1/2} l > 200$ . It will be shown that  $\theta_{w,b} \approx \theta_e$  and therefore  $\theta_{w,\infty}$  and  $\theta_{w,c}$  differ by at most  $2^\circ \text{C}$ . The difference is usually negligible. (That fact would be of great importance in the case of a fine-wire thermocouple stretched between two supports. The present treatment would not be rigorously correct in such a situation because of the difference between the thermal conductivities of the two materials, but the basic observation would still be valid. In the case of a fine-wire thermocouple, of course,  $\theta_e$  and  $\theta_{w,\infty}$  are virtually the same because joulean



DESIGN AND APPLICATIONS OF HOT-WIRE ANEMOMETERS  
 FOR STEADY-STATE MEASUREMENTS AT TRANSONIC  
 AND SUPERSONIC AIRSPEEDS  
 By Herman H. Lowell

Page 67, equation (B9) should read as follows:

$$0.2389 i^2 r_0 (1 + \alpha \bar{\theta}_w) = \pi k_f Nu_f (\bar{\theta}_w - \theta_e) + \frac{\beta^{1/2} k_w A_w}{l} (\theta_{w,\infty} - \theta_{w,b}) \tanh \beta^{1/2} l$$

(B9)



heating may be neglected. The source of conduction error is the immersion of the supports in regions having temperatures other than  $\theta_e$ .)

The mean temperature is now obtained as follows:

$$\begin{aligned}\bar{\theta}_w &= \frac{1}{2l} \left[ \int_{-l}^l \theta_{w,\infty} dx - \int_{-l}^l \frac{(\theta_{w,\infty} - \theta_{w,b}) \cosh \beta^{1/2} x}{\cosh \beta^{1/2} l} dx \right] \\ &= \theta_{w,\infty} - \frac{(\theta_{w,\infty} - \theta_{w,b})}{\beta^{1/2} l} \tanh \beta^{1/2} l\end{aligned}\quad (B7)$$

Because  $\beta^{1/2} l \geq 6$ ,  $\tanh \beta^{1/2} l \approx 1$ . This approximation is valid for values of  $\beta^{1/2} l$  as small as 3.5; therefore,

$$\bar{\theta}_w = \theta_{w,\infty} - \frac{(\theta_{w,c} - \theta_{w,b})}{\beta^{1/2} l} \quad (B8)$$

Simmons and Beavan, who presented the theory just given (reference 12), showed that  $R = R_0 (1 + \alpha \bar{\theta}_w)$ , in which  $R_0 \equiv L_w r_0$ ; the identity follows directly from the observation that the resistance per unit length is a linear function of temperature.

Upon taking the derivative of the expression for  $\theta_w$ , the rate of heat loss to each support is found to be

$$\beta^{1/2} k_w A_w (\theta_{w,\infty} - \theta_{w,b}) \tanh \beta^{1/2} l$$

Therefore, the following equation can be written:

$$0.2339 i^2 r_0 (1 - \alpha \bar{\theta}_w) = \pi k_f \text{Nu}_f (\bar{\theta}_w - \theta_e) + \frac{\beta^{1/2} k_w A_w}{l} \tanh \beta^{1/2} l \quad (B9)$$



The quantity

$$\xi \equiv \frac{k_w A_w (\theta_{w,\infty} - \theta_{w,b}) \beta^{1/2} l \tanh \beta^{1/2} l}{l^2 \pi k_f \text{Nu}_f (\bar{\theta}_w - \theta_e)} \quad (\text{B10})$$

is defined. It is the ratio of heat lost by conduction to the supports to that lost directly to the air stream.

The ratio  $\xi$  may also be written

$$\xi = \frac{k_w}{k_f} \left( \frac{D_w}{L_w} \right)^2 \text{Nu}_f^{-1} \left( \frac{\theta_{w,\infty} - \theta_{w,b}}{\bar{\theta}_w - \theta_e} \right) \beta^{1/2} l \quad (\text{B11})$$

making only the previous approximation that  $\tanh \beta^{1/2} l = 1.000$ .

It is notable that the parameter  $\beta^{1/2} l$  has the following physical significance: It is given by the ratio of the difference  $(\theta_{w,\infty} - \theta_{w,b})$  to the difference  $(\theta_{w,\infty} - \bar{\theta}_w)$ ; therefore it is a dimensionless measure of the degree of departure of the wire temperature from the ideal condition of uniformity. Under the preceding circumstance  $\beta^{1/2} l = \infty$ . Such a situation virtually exists whenever the ratio  $L_w/D_w$  or  $\text{Nu}_f$  is very large or when  $k_w$  is very small.

It is a simple matter to transform the earlier expression for  $\beta$  in such a way as to obtain

$$\beta^{1/2} l = \left( \frac{k_f}{k_w} \right)^{1/2} \frac{L_w}{D_w} \text{Nu}_f^{1/2} \left[ 1 - \frac{(\bar{\theta}_w - \theta_e)(1 + \xi)}{(\alpha^{-1} + \bar{\theta}_w)} \right]^{1/2} \quad (\text{B12})$$

It then becomes possible to combine equations (B11) and (B12) to obtain

$$\xi = C_3 \left[ (1 - t) - t\xi \right]^{1/2} \quad (\text{B13})$$



in which

$$C_3 \equiv \left( \frac{k_w}{k_f} \right)^{1/2} \frac{D_w}{L_w} Nu_f^{-1/2} \left( \frac{\theta_{w,\infty} - \theta_{w,b}}{\theta_w - \theta_e} \right) \quad (B14)$$

By expanding the bracket in equation (B13), the following equation is obtained:

$$\xi = C_3 (1 - t)^{1/2} \left[ 1 - \frac{t\xi}{2(1-t)} - \dots \right] \quad (B15)$$

By replacing  $\xi$  where it appears in the right-hand expression by  $C_3 (1 - t)^{1/2}$ , the relation

$$\xi = C_3 (1-t)^{1/2} \left[ 1 - \frac{C_3 t}{2(1-t)^{1/2}} - \dots \right] \quad (B16)$$

is deduced.

In equation (27), the presence of the factor  $f_1$  complicates the relation between Nusselt and Reynolds numbers. For the present purpose, however,  $f_1$  is considered fixed at a value such that  $C_2 f_1 Pr_f^{0.3}$  has the value 0.475, which is a representative mean value for the Mach number range investigated.

Under that circumstance and with  $C_1$  permitted to vanish,

$$Nu_f^{-1/2} \approx 0.475^{-1/2} \left( Re'_{f,w} \right)^{-1/4} \quad (B17)$$

$$\approx 0.475^{-1/2} \left( \frac{D_w}{L_w} \right)^{-1/4} \left( Re'_{f,L} \right)^{-1/4}$$

Upon replacing  $Nu_f^{-1/2}$  in equation (B14) by the second approximate equivalent, equation (10) is obtained.



Equation (26) follows directly from the preceding solution of the differential equation for the heat flow to and from a given portion of the wire and from the definition of  $\Gamma$ . Equation (22) remains to be obtained; the initial step consists of a statement of the following relation:

$$\theta_{w,b} = \frac{\Gamma \theta_{w,\infty} + \theta_e}{\Gamma + 1} \quad (B18)$$

in which

$$\Gamma \equiv \frac{1.02 k_w D_w^2 \beta^{1/2}}{k_p^{1/2} k_t^{1/2} D_b \left( \text{Re}'_{t,b,2} \right)^{0.3}} \quad (B19)$$

The quantity 1.02 is a pure number.

Equation (B18) is derived by solving the differential equation of heat flow for the support and taking the net heat-flow rate at the support tip as zero; the solution is similar to that for the wire alone and will not be given. The assumption of a uniform support diameter equal to that at the point of wire attachment leads to negligible error because most of the temperature drop in the support occurs within a small distance of that point.

The following quantities are defined:

$$\text{Nu}''_f \equiv \frac{0.2389 i_r^2}{\pi k_f (\bar{\theta}_w - \theta_e)} \quad (B20)$$

$$c \equiv \beta^{1/2} l \quad (B21)$$

$$n \equiv \frac{k_w}{k_f} \left( \frac{D_w}{L_w} \right)^2 (\bar{\theta}_w - \theta_e)^{-1} \quad (B22)$$



$$m \equiv \left( \frac{k_f}{k_w} \right)^{1/2} \frac{L_w}{D_w} \quad (\text{B23})$$

$$b \equiv \Gamma c^{-1} \quad (\text{B24})$$

By use of these definitions, equations (14) and (15), and other relations previously established, the following relations are found to subsist among the several quantities:

$$\text{Nu}_f'' = \text{Nu}_f (1 + \xi) \quad (\text{B25})$$

$$\xi = n \text{Nu}_f^{-1} c (\theta_{w,\infty} - \theta_{w,b}) \quad (\text{B26})$$

$$\bar{\theta}_w = \theta_{w,\infty} - \frac{(\theta_{w,\infty} - \theta_{w,b})}{c} \quad (\text{B27})$$

$$c = m \text{Nu}_f^{1/2} [1 - t (1 + \xi)]^{1/2} \quad (\text{B28})$$

$$\theta_{w,b} = \frac{bc \theta_{w,\infty} + \theta_e}{bc + 1} \quad (\text{B29})$$

From equations (B26) and (B29), it is found that

$$\xi = nc \text{Nu}_f^{-1} \left( \frac{\theta_{w,\infty} - \theta_e}{bc + 1} \right) \quad (\text{B30})$$

The relation

$$(bc + 1)^{-1} = \frac{c(\theta_{w,\infty} - \bar{\theta}_w)}{(\theta_{w,\infty} - \theta_e)} \quad (\text{B31})$$



is then obtained from equations (B27) and (B29).

Combining equations (B30) and (B31) yields

$$\xi = n \text{Nu}_f^{-1} (\theta_{w,\infty} - \bar{\theta}_w) c^2 \quad (\text{B32})$$

or

$$\xi = \frac{n \text{Nu}_f^{-1} (\bar{\theta}_w - \theta_e) c^2}{c (bc + 1) - 1} \quad (\text{B33})$$

when equations (B27), (B29), and (B32) are used.

If equations (B28) and (B33) are used,

$$\xi = \frac{1 - t (1 + \xi)}{bm^2 \text{Nu}_f'' \left[ (1 + \xi)^{-1} - t \right] + m \text{Nu}_f''^{1/2} \left[ (1 + \xi)^{-1} - t \right]^{1/2} - 1} \quad (\text{B34})$$

noting that  $nm^2 (\bar{\theta}_w - \theta_e) = 1$ .

By defining  $B \equiv bm^2 \text{Nu}_f''$  and  $Y \equiv m \text{Nu}_f''^{1/2}$ , it is found that B and Y are the expressions given in equations (25) and (23), respectively, and that equation (B34) becomes equation (22).



## APPENDIX C

## WIRE STRESS AND SUPPORT DEFLECTION

## Aerodynamic Stress

If  $w$  is the uniform transverse load per unit length applied to a hinged thin beam assumed to be bent into a circular arc of which the sagitta  $z$  (portion of radius normal to chord intercepted by chord and arc) is small compared with the arc length  $L$ , the following relation subsists among total tensile force  $T$  and those variables:

$$T = \frac{wL^2}{8z} \quad (C1)$$

For an aerodynamically loaded wire

$$w = C_D \frac{\rho V^2}{2} D_w \quad (C2)$$

Therefore,

$$T = \frac{C_D \rho V^2 D_w L^2}{16z} \quad (C3)$$

If  $\sigma_3 \left( = \frac{T}{A_w} \right)$  is the stress in the wire, then

$$\sigma_3 = \frac{C_D \rho V^2 L^2}{4\pi D_w z} \quad (C4)$$

This relation appears to have first been mentioned in reference 3, except that a factor of 2 is omitted in the denominator of the expression.

The quantity  $z$  must be expressed in terms of the other variables and of the known characteristics of the wire material and supports.



Let  $u$  be the radius of the beam arc;  $\lambda$ , the angle subtended at the center of the circle by the semiarc; and  $L_s$ , the distance between the wire supports.

Then

$$\frac{L}{2} = u\lambda \quad (C5)$$

Now,

$$\begin{aligned} \lambda &= \sin^{-1} \frac{[u^2 - (u-z)^2]^{1/2}}{u} \\ &= \sin^{-1} \frac{(2uz - z^2)^{1/2}}{u} \\ &= z^{1/2} \left(\frac{z}{u}\right)^{1/2} \left(1 + \frac{z}{12u} + \dots\right) \end{aligned} \quad (C6)$$

The last relation follows from the fact that

$$\begin{aligned} \sin^{-1} \left(\frac{2z}{u} - \frac{z^2}{u^2}\right)^{1/2} &\approx \left(\frac{2z}{u} - \frac{z^2}{u^2}\right)^{1/2} + \frac{1}{6} \left(\frac{2z}{u} - \frac{z^2}{u^2}\right)^{3/2} + \dots \\ &= \left[ \left(\frac{2z}{u}\right)^{1/2} - \frac{z}{2u} \left(\frac{z}{2u}\right)^{1/2} - \frac{z^{1/2}}{3^2} \left(\frac{z}{u}\right)^{5/2} - \dots \right] + \\ &\quad \frac{1}{6} \left[ \left(\frac{2z}{u}\right)^{3/2} - \frac{3}{2} \left(\frac{2z}{u}\right)^{1/2} \left(\frac{z^2}{u^2}\right) + \dots \right] \end{aligned}$$



Therefore,

$$L = 2u \lambda \approx 2^{3/2} (uz)^{1/2} \left(1 + \frac{z}{12u}\right) \quad (C7)$$

On the other hand,

$$\begin{aligned} L_s &= 2u \sin \lambda \\ &= 2u \left(\frac{2z}{u} - \frac{z^2}{u^2}\right)^{1/2} \\ &\approx 2^{3/2} (uz)^{1/2} \left(1 - \frac{z}{4u}\right) \end{aligned} \quad (C8)$$

Therefore,

$$\begin{aligned} L - L_s &= 2^{3/2} (uz)^{1/2} \left(\frac{z}{12u} + \frac{z}{4u}\right) \\ &= \frac{2^{3/2}}{3} \left(\frac{z}{u}\right)^{1/2} z \end{aligned} \quad (C9)$$

to a first approximation.

Now,

$$\begin{aligned} u^{-1/2} &= \left(\frac{z}{2} + \frac{L_s^2}{8z}\right)^{-1/2} \\ &\approx \left(\frac{8z}{L_s^2}\right)^{1/2} \left(1 - \frac{2z^2}{L_s^2} + \dots\right) \end{aligned} \quad (C10)$$



If the first term of the right-hand member of equation (C10) is used in equation (C9), the second equation becomes

$$L - L_S = \frac{8}{3} \frac{z^2}{L_S} \quad (C11)$$

The original wire length (after mounting, but prior to imposition of drag load) is designated  $L_1$ .

The decrease in distance between the supports is given by

$$\Delta L_1 = L_1 - L_{S,2} = A_w F (\sigma_3 - \sigma_1) \quad (C12)$$

in which  $F$  in this case is the combined flexibility of the two supports and  $L_{S,2}$  is the distance between the supports during aerodynamic loading.

The change in wire length is given by

$$\frac{\Delta L}{L} = \frac{L - L_1}{L_1} = \frac{\sigma_3 - \sigma_1}{E_w} \quad (C13)$$

Therefore,

$$\begin{aligned} L &= L_1 \left( 1 + \frac{\sigma_3 - \sigma_1}{E_w} \right) \\ &= \left[ L_S + A_w F (\sigma_3 - \sigma_1) \right] \left( 1 + \frac{\sigma_3 - \sigma_1}{E_w} \right) \\ &= L_S + A_w F (\sigma_3 - \sigma_1) + \frac{L_S}{E_w} (\sigma_3 - \sigma_1) + \\ &\quad \frac{A_w F}{E_w} (\sigma_3 - \sigma_1)^2 \end{aligned} \quad (C14)$$



When equation (C11) is used,

$$\frac{8}{3} \frac{z^2}{L_S} = \left( A_W F + \frac{L_S}{E_W} \right) (\sigma_3 - \sigma_1) + \frac{A_W F}{E_W} (\sigma_3 - \sigma_1)^2 \quad (C15)$$

By recalling equation (C4) and dropping the distinction between  $L$  and  $L_S$ , the relation

$$\frac{8}{3} \frac{N^2 L^3}{D_W^2 \sigma_3^2} = \left( A_W F + \frac{L}{E_W} \right) (\sigma_3 - \sigma_1) + \frac{A_W F}{E_W} (\sigma_3 - \sigma_1)^2 \quad (C16)$$

is obtained in which

$$N \equiv \frac{C_D \rho V^2}{4\pi}$$

Now if the quantity

$$\sigma_2 \equiv \left[ \frac{8}{3} \frac{N^2 L^3 E_W}{D_W^2 (L + A_W F E_W)} \right]^{1/3} \quad (C17)$$

(an "exact" form of equation (12)) is defined,

$$\sigma_2^3 = \sigma_3^2 (\sigma_3 - \sigma_1) + \frac{1}{\left( E_W + \frac{L}{A_W F} \right)} \sigma_3^2 (\sigma_3 - \sigma_1)^2 \quad (C18)$$

In arbitrary units, if

$$\sigma_3 \sim 3$$



then

$$\sigma_1 \sim 2$$

and

$$\left(E_w + \frac{L}{A_w F}\right)^{-1} \sim 3.3 \times 10^{-4}$$

therefore  $\sigma_3 \left(E_w + \frac{L}{A_w F}\right)^{-1} \ll 1$  and the second term of equation (C18) may be taken as zero.

The final result is

$$\sigma_3^3 - \sigma_3^2 \sigma_1 - \sigma_2^3 = 0 \quad (11)$$

The preceding treatment neglects variable-temperature effects. These effects are usually of second-order magnitude; however, in the case of high-temperature work (air), the effect of a change of the modulus of the wire support and of the thermal expansion of the mount may be substantial and must be considered. In the preceding expression for  $\sigma_2$ , because  $A_w F E_w \gg L$ , the effect of a change of the modulus of the wire material is nearly always negligible.

#### Deflection of Wire Support

There seems to be no expression in structures literature for the deflection of a conical cantilever beam under a concentrated load.

The assumption that the conical wire support is rigidly held at one end is a good one as the amount of movement at the base is very small in any case. It is observed in practice that the cement used does not develop cracks in the area immediately around the base of the support in the course of ordinary usage even though it is a fairly brittle substance.



In the following relations,  $M$  is the conventional moment of beam theory and  $I$  the (beam) moment of inertia of the cross section. The deflection occurs along the  $y$ -coordinate, taken positive in the upward direction for a horizontal beam. The load  $W$  is assumed to act in the downward direction at a distance  $L$  from the point of support. The horizontal coordinate of any cross section as measured from the point of support taken as the origin is  $x$ .

At the origin, the diameter is  $D_0$ ; it is  $D_1$  at the loading point.

Then,

$$D = D_0 \left(1 - \frac{x}{L}\right) + D_1 \frac{x}{L} \quad (C19)$$

and

$$I = \frac{\pi D^4}{64} = \frac{\pi D_0^4}{64} \left[1 - \frac{x}{L} \left(\frac{D_0 - D_1}{D_0}\right)\right]^4 \quad (C20)$$

Upon writing

$$\frac{D_0 - D_1}{L D_0} \equiv \delta$$

and upon recalling that

$$M = -W(L - x)$$

it follows that

$$y'' \equiv \frac{d^2 y}{dx^2} = - \frac{64W(L-x)}{\pi D_0^4 E_p (1 - x\delta)^4} \quad (C21)$$



or

$$y'' = k_2 \left[ \frac{x}{(1-x\delta)^4} - \frac{L}{(1-x\delta)^4} \right] \quad (C22)$$

where

$$k_2 \equiv \frac{64W}{\pi D_0^4 E_b}$$

Upon integration and imposition of the condition that  $y' = 0$  at  $x = 0$ , equation (C22) becomes

$$\frac{y'}{k_2} = \frac{-1}{2\delta^2 (1-x\delta)^2} + \frac{1}{3\delta^2 (1-x\delta)^3} - \frac{L}{3\delta (1-x\delta)^3} + \frac{(\frac{1}{2} + L\delta)}{3\delta^2} \quad (C23)$$

Upon a second integration and imposition of the condition that  $y = 0$  at  $x = 0$ ,

$$\frac{y}{k_2} = -\frac{1}{2\delta^3 (1-x\delta)} + \frac{1 - L\delta}{6\delta^3 (1-x\delta)^2} + \frac{x}{6\delta^2} + \frac{Lx}{3\delta} + \frac{1}{3\delta^3} + \frac{L}{6\delta^2} \quad (C24)$$

At  $x = L$ , this relation reduces to

$$y = -\frac{2 k_2 L^3}{6 (1 - L\delta)} \quad (C25)$$

Upon recalling the definitions of  $k_2$  and  $\delta$ , the equation finally obtained is



$$F = \frac{|y|}{W} = \frac{64 L^3}{3\pi E_b D_0^3 D_1} \quad (C26)$$

which is equivalent to equation (13) if it is recalled that equation (13) applies in the case of the deflection of a pair of supports.

#### REFERENCES

1. Simmons, L. F. G., and Bailey, A.: Note on a Hot-wire Speed and Direction Meter. R. & M. No. 1019, British A.R.C., Feb. 1926.
2. Bailey, A.: A Directional Hot-wire Anemometer. R. & M. No. 777, British A.R.C., Jan. 1922.
3. Weske, John R.: Methods of Measurement of High Air Velocities by the Hot-Wire Method. NACA TN 880, 1943.
4. King, Louis Vessot: On the Convection of Heat from Small Cylinders in a Stream of Fluid: Determination of the Convection Constants of Small Platinum Wires with Applications to Hot-Wire Anemometry. Phil. Trans. Roy. Soc. (London), vol. 214, no. 14, ser. A, 1914, pp. 373-432.
5. Jakob, Max: Heat Transfer. Vol. I. John Wiley & Sons, Inc., 1949.
6. Durand, W. F.: Aerodynamic Theory. Vol. VI. Durand Reprinting Comm., C.I.T., 1943, pp. 252-253.
7. Boelter, L. M. K., Cherry, V. H., Johnson, H. A., and Martinelli, R. C.: Heat Transfer Notes. Univ. Calif. Press (Berkeley), 1946, pp. XI-15.-XI-19.
8. McAdams, William H.: Heat Transmission. McGraw-Hill Book Co., Inc., 2d ed., 1942, pp. 210-230, 237-246.



9. Burgers, J. M.: Hitzdrahtmessungen. Handb. d. Exp. Phys., Bd. IV, Teil 1, 1931, S. 656-658.
10. Taylor, C. Fayette: A Suggested Method for Measuring Turbulence. NACA TN 380, 1931.
11. Ziegler, M.: On the Directional Effect of the Single Hot Wire Anemometer. Proc. Koninklijke Akademie van Wetenschappen (Amsterdam), vol. XXXV, no. 8, 1932, pp. 1067-1076.
12. Simmons, L. F. G., and Beavan, J. A.: Hot-wire Type of Instrument for Recording Gusts. R. & M. No. 1615, British A.R.C., Feb. 1934.
13. Knoblock, F. D.: A Hot-Wire Anemometer Developed for Full-Scale Airship Measurements. Pub. No. 2, The Daniel Guggenheim Airship Inst., 1935, pp. 58-61.
14. Eckert, E., and Weise, W.: The Temperature of Unheated Bodies in a High-Speed Gas Stream. NACA TM 1000, 1941.
15. Eber: Experimentelle Untersuchung der Bremstemperatur und des Wärmeüberganges an einfachen Körpern bei Ueberschallgeschwindigkeit. Teil 2: Abbildungen. WVA Archiv Nr. 66/57 (Peenemünde), Nov. 21, 1941.
16. Willis, J. B.: Review of Hot Wire Anemometry. Rep. ACA-19, Australian Council Aero., Oct. 1945.
17. Thomas, J. S. G.: Hot Wire Anemometry: Its Principles and Applications. Jour. Soc. Chem. Ind. (London), Trans., vol. XXXVII, no. 11, June 15, 1948, pp. 165T-168T; discussion, pp. 169T-170T.
18. Thomas, J. S. G.: The Hot-wire Anemometer: Its Application to the Investigation of the Velocity of Gases in Pipes. Phil. Mag., vol. XLVI, no. CCXXXIII, 6th ser., May 1920, pp. 505-534.
19. Schubauer, G. B.: A Turbulence Indicator Utilizing the Diffusion of Heat. NACA Rep. 524, 1935.
20. Woldman, Norman E., and Dornblatt, Albert J.: Engineering Alloys. Am. Soc. Metals (Cleveland), 1936.
21. Hoyt, Samuel L.: Metals and Alloys Data Book. Reinhold Pub. Corp., 1943.



22. Anon.: Metals Handbook, 1948 Edition. Am. Soc. Metals (Cleveland), 1948.
23. Everhart, John L., Lindlief, W. Earl, Kanegis, James, Weissler, Pearl G., and Siegel, Frieda: Mechanical Properties of Metals and Alloys. Circular C447, NBS, Dec. 1, 1943.
24. Nemilov, V. A.: Splavy platiny i palladia i ikh primeneniye. Izvestiia No. 19, Sektor platiny i drugikh blagorodnykh metallov, Inst. obshchei i neorganicheskoi khimii, Akad. nauk S.S.S.R. (Leningrad), 1943, pp. 21-44.
25. Anon.: International Critical Tables. Vol. V. McGraw-Hill Book Co., Inc., 1929, p. 225.
26. Schubauer, Galen B.: Effect of Humidity in Hot-Wire Anemometry. Nat. Bur. Standards Jour. Res., vol. 15, no. 6, Dec. 1935, pp. 575-578.
27. Prandtl, L., and Tietjens, O. G.: Applied Hydro- and Aeromechanics. McGraw-Hill Book Co., Inc., 1934, pp. 96-97.
28. de Kármán, Th.: The Problem of Resistance in Compressible Fluids. Quinto Convegno "Volta", Reale Accademia d'Italia (Roma), Sett. 30-Ott. 6, 1935, pp. 3-57.



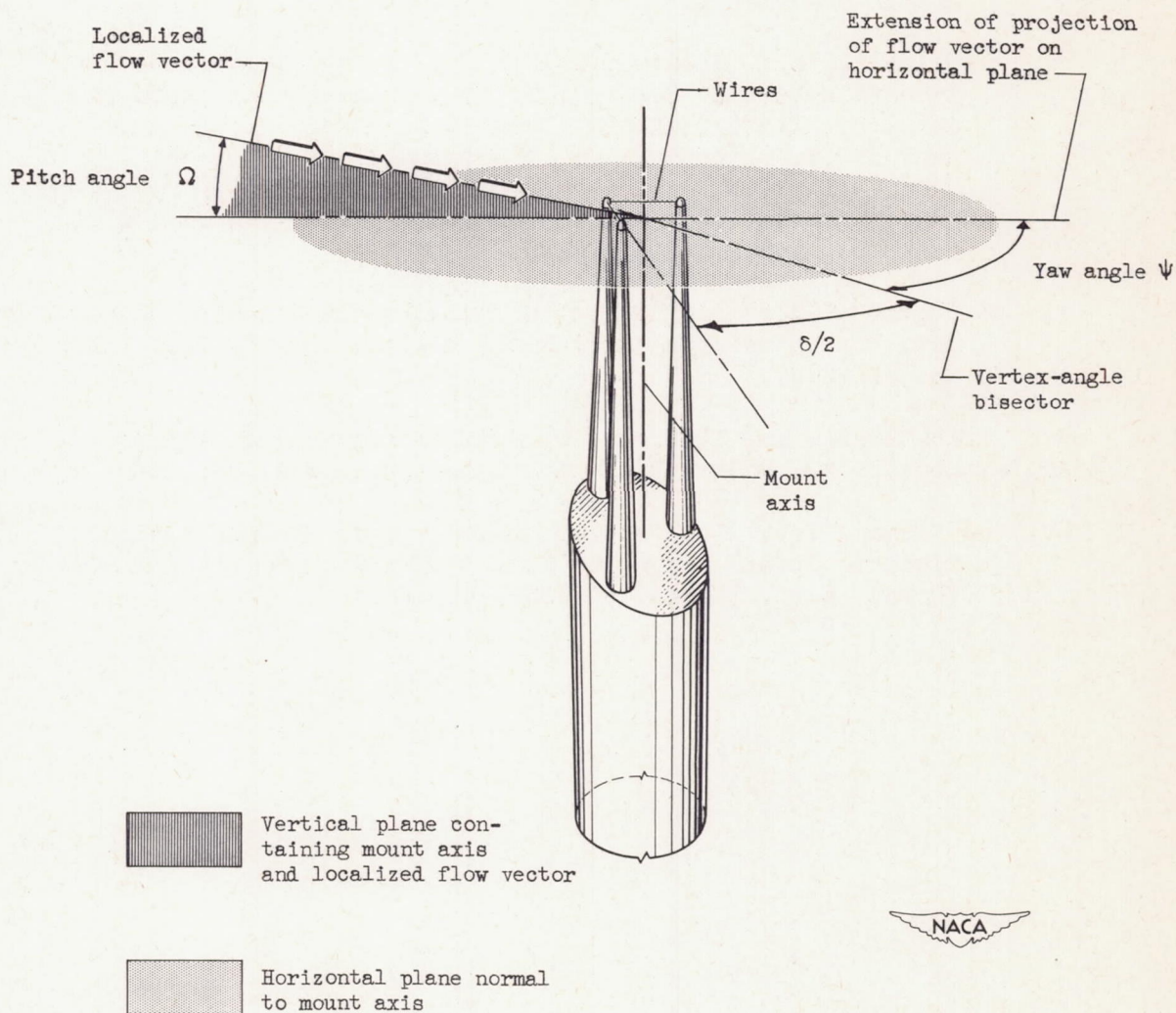


Figure 1. - Geometric relations among mount axis, wires, and flow vector; horizontal V-array.



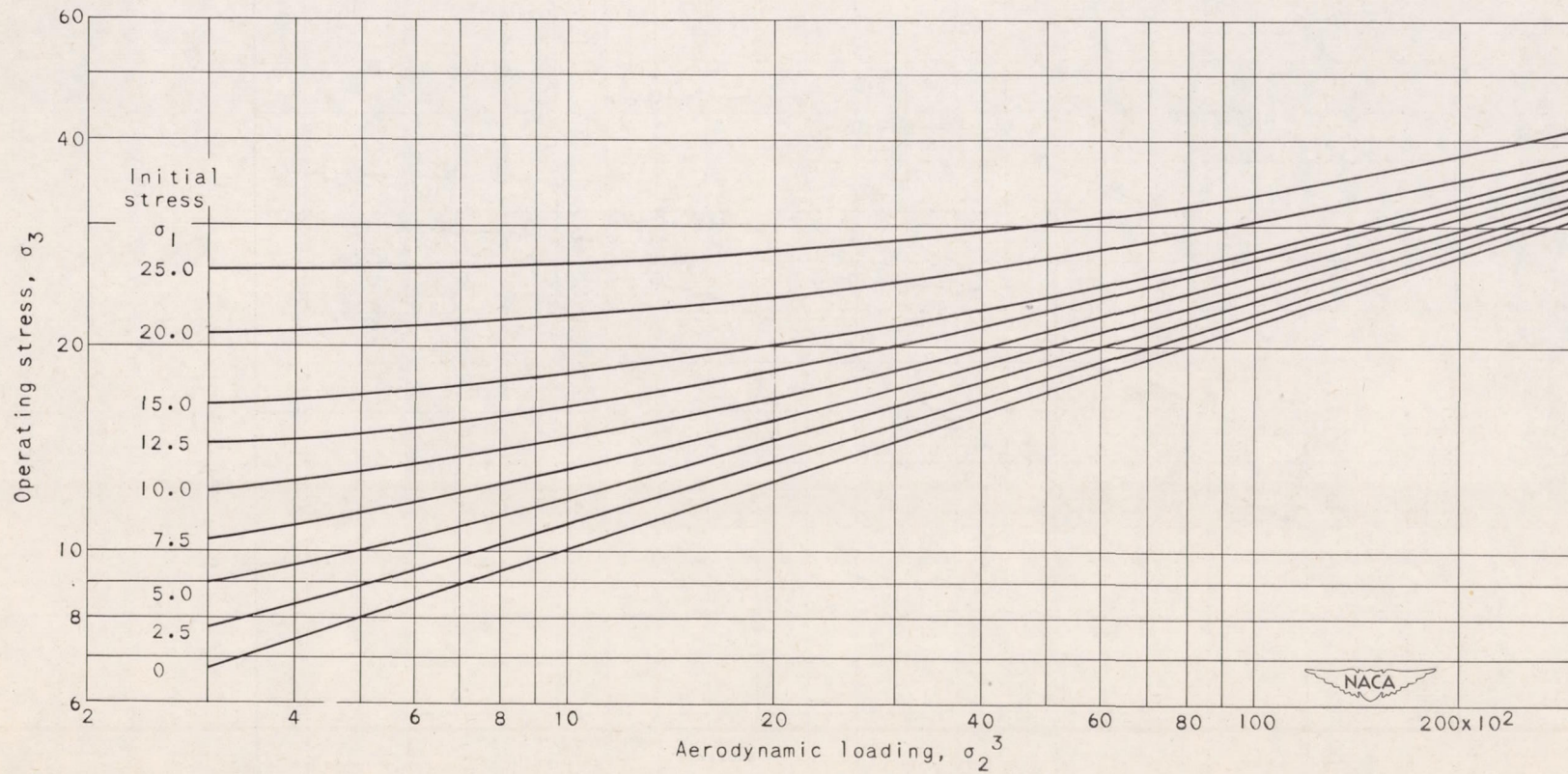


Figure 2. - Stress in wire as function of initial and aerodynamic loading.  $\sigma_3^3 - \sigma_3^2 \sigma_1 - \sigma_2^3 = 0$ .  
Unit of stress arbitrary.



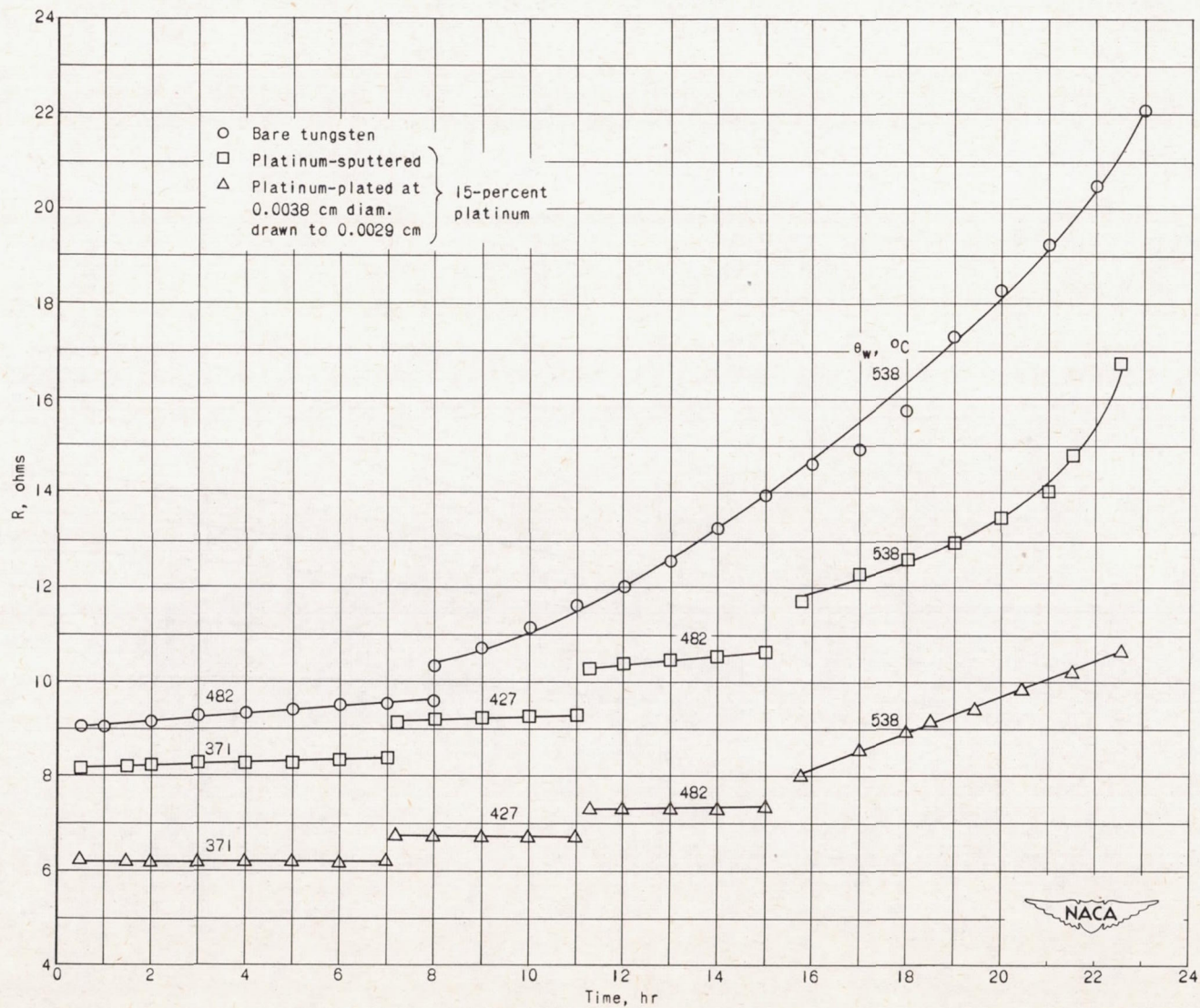


Figure 3. - Oxidation of tungsten wire.



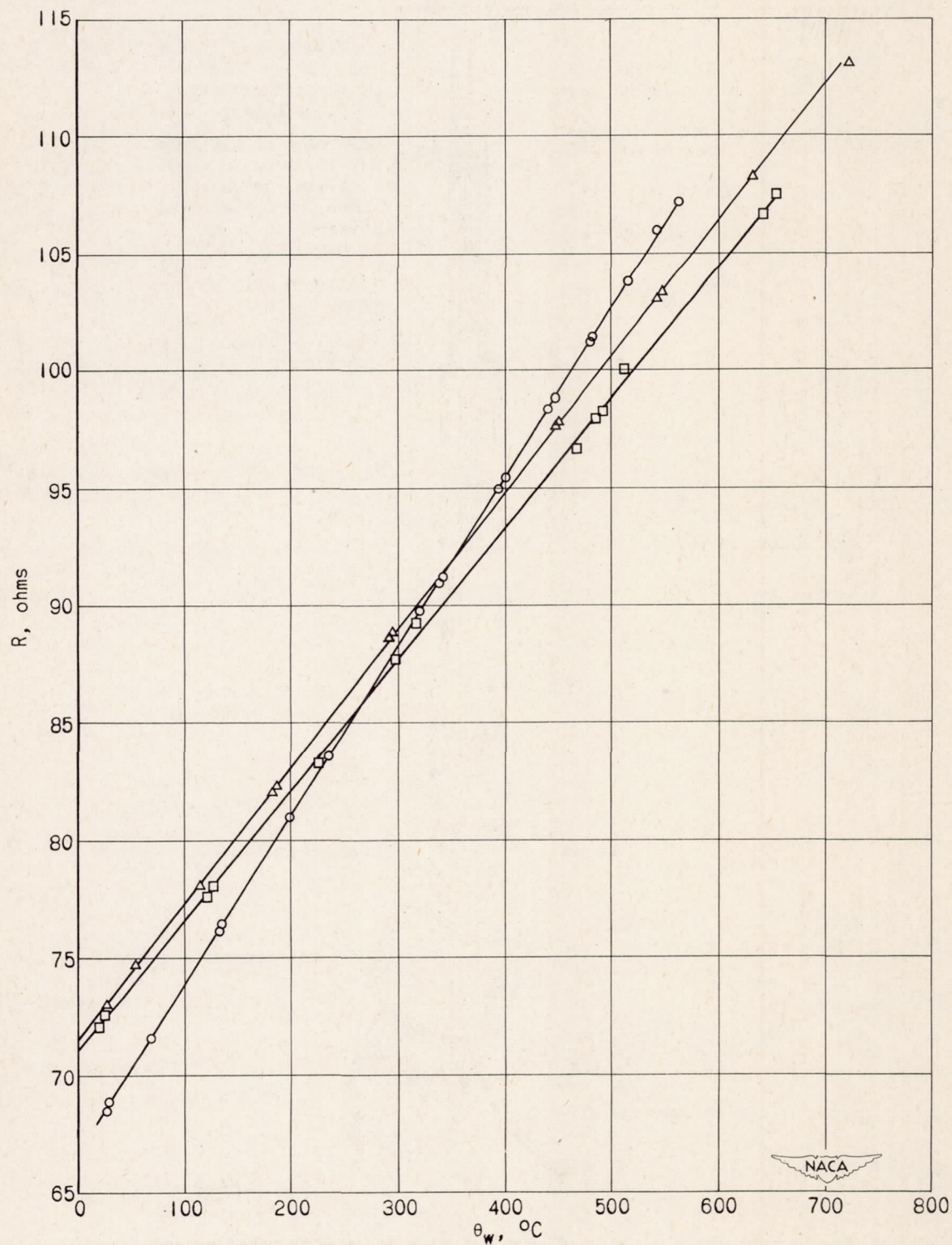


Figure 4. - Variation of resistance of three specimens of 20-percent iridium - 80-percent platinum wire.



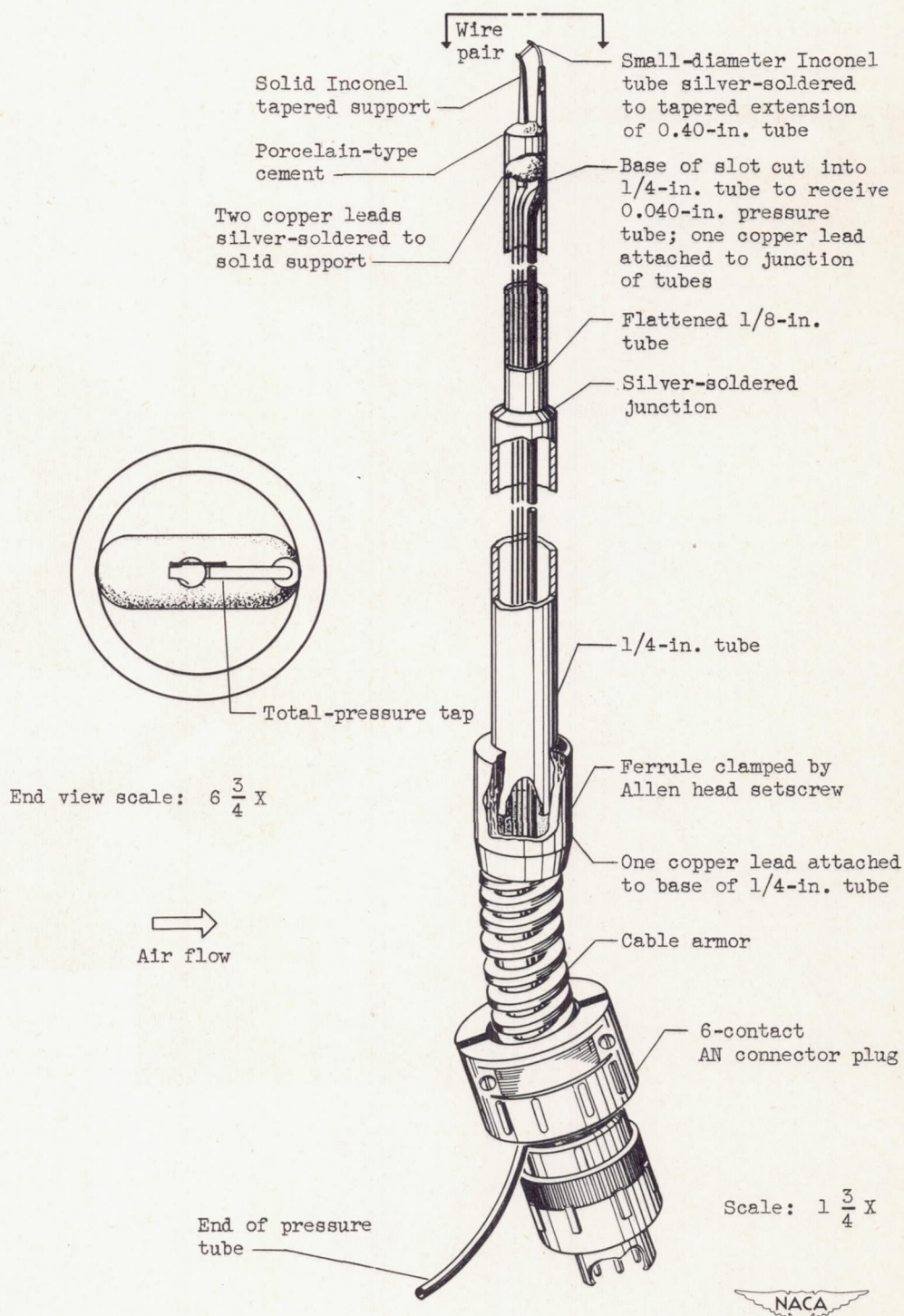


Figure 5. - Construction details of parallel-wire mount with total-pressure tap.



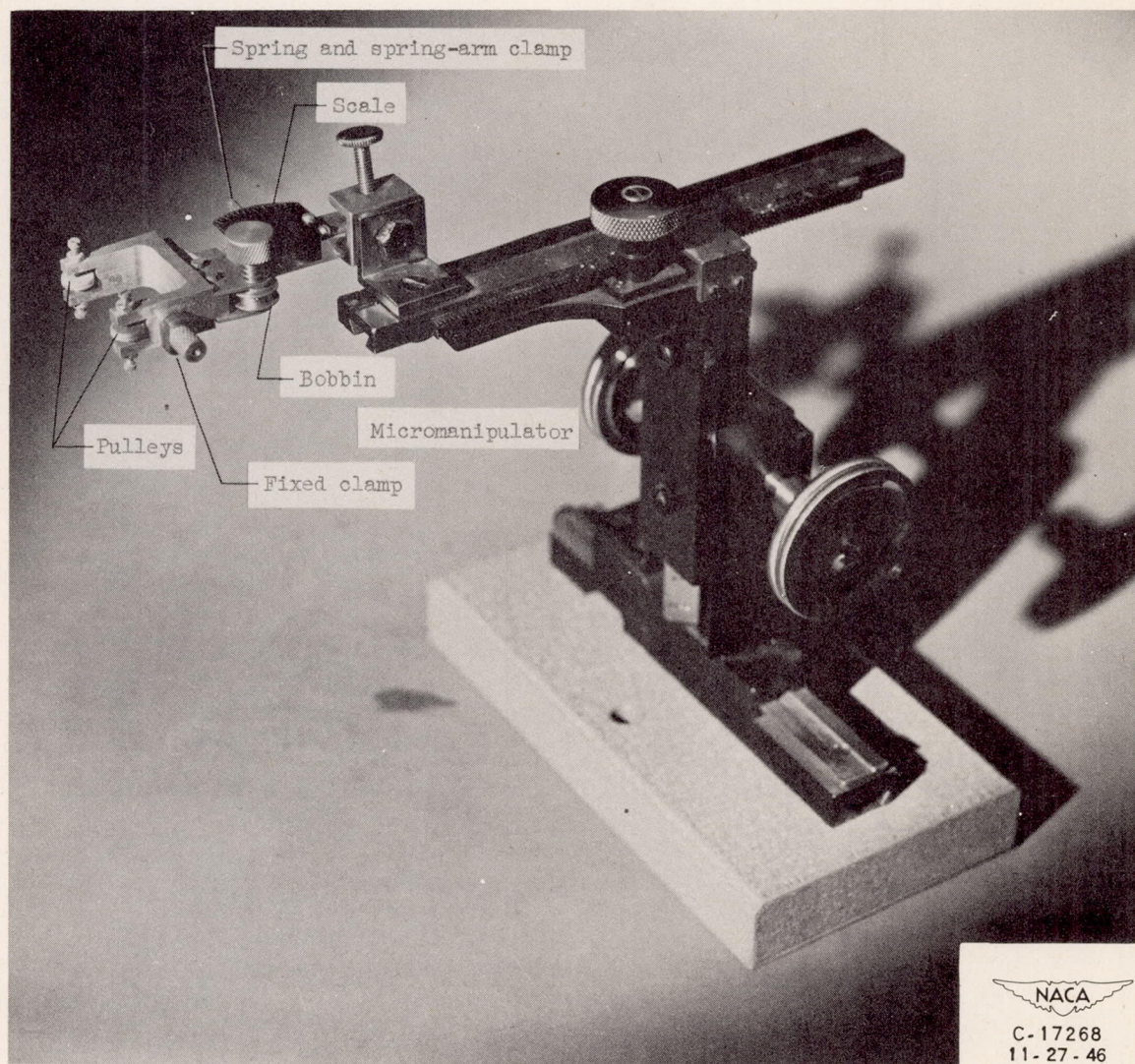
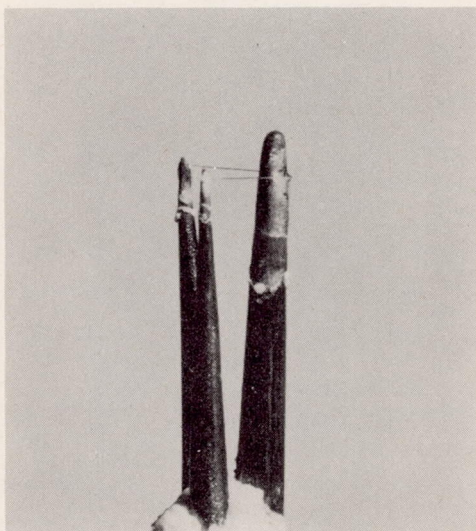


Figure 6. - Mounting jig and micromanipulator.

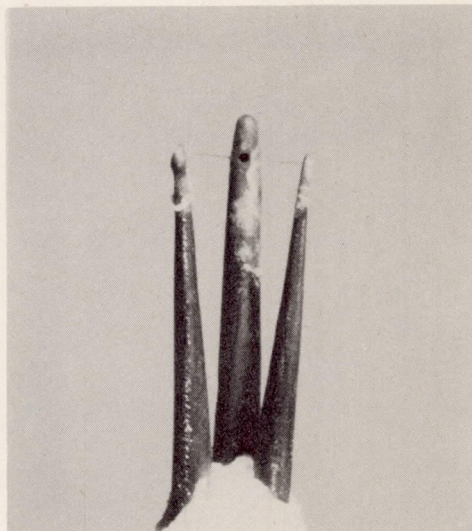




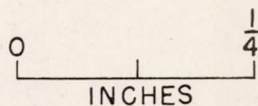




(a) Side view.



(b) Front view.



(c) Top view.

NACA  
C-24411  
9-28-49

Figure 7. - V-array mounts with total-pressure tap.

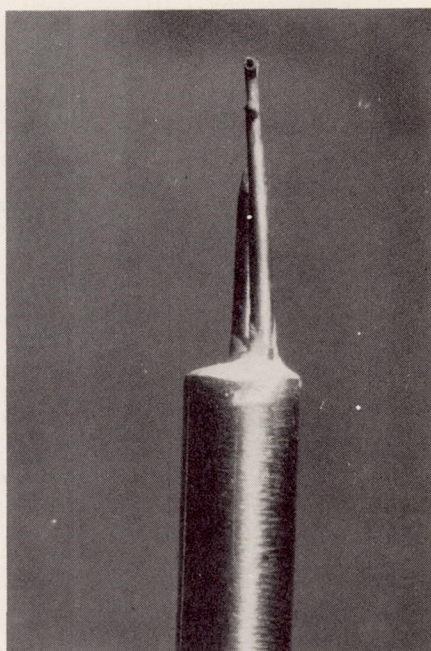
1289





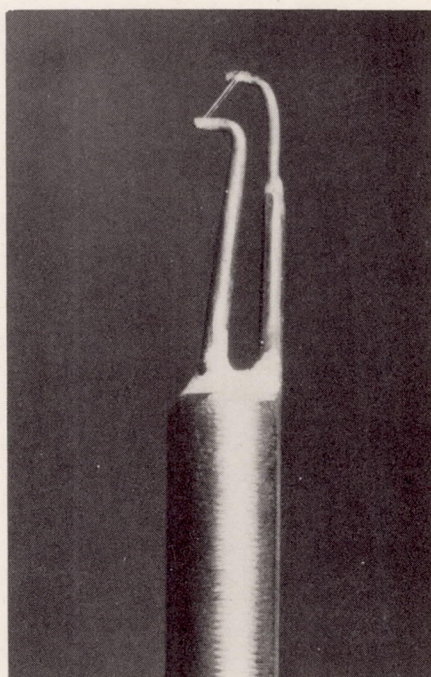


1289



NACA  
C-23108  
3-9-49

(a) Front view.



0  $\frac{1}{4}$   
INCHES

NACA  
C-23109  
3-9-49

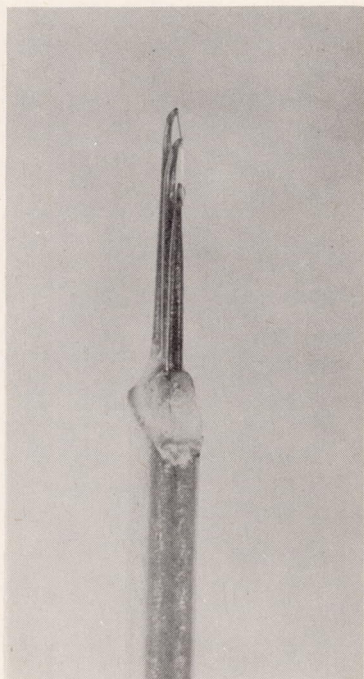
(b) Side view.

Figure 8. - Parallel-wire array mount with total-pressure tap.





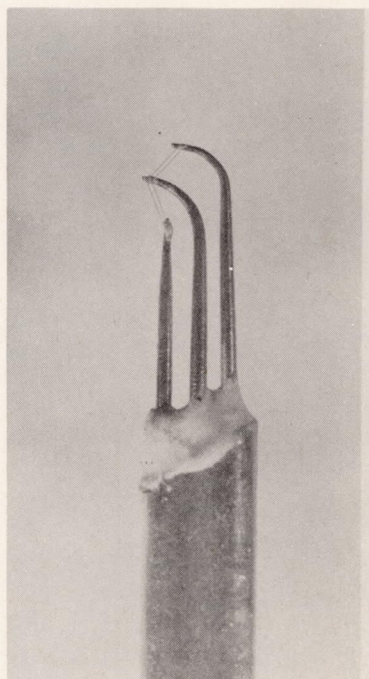




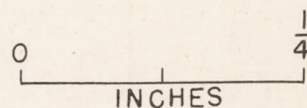
(a) Front view.



(b) Top view.



(c) Side view.



NACA  
C-22424  
10-11-48

Figure 9. - Double parallel-wire array mount.

1289







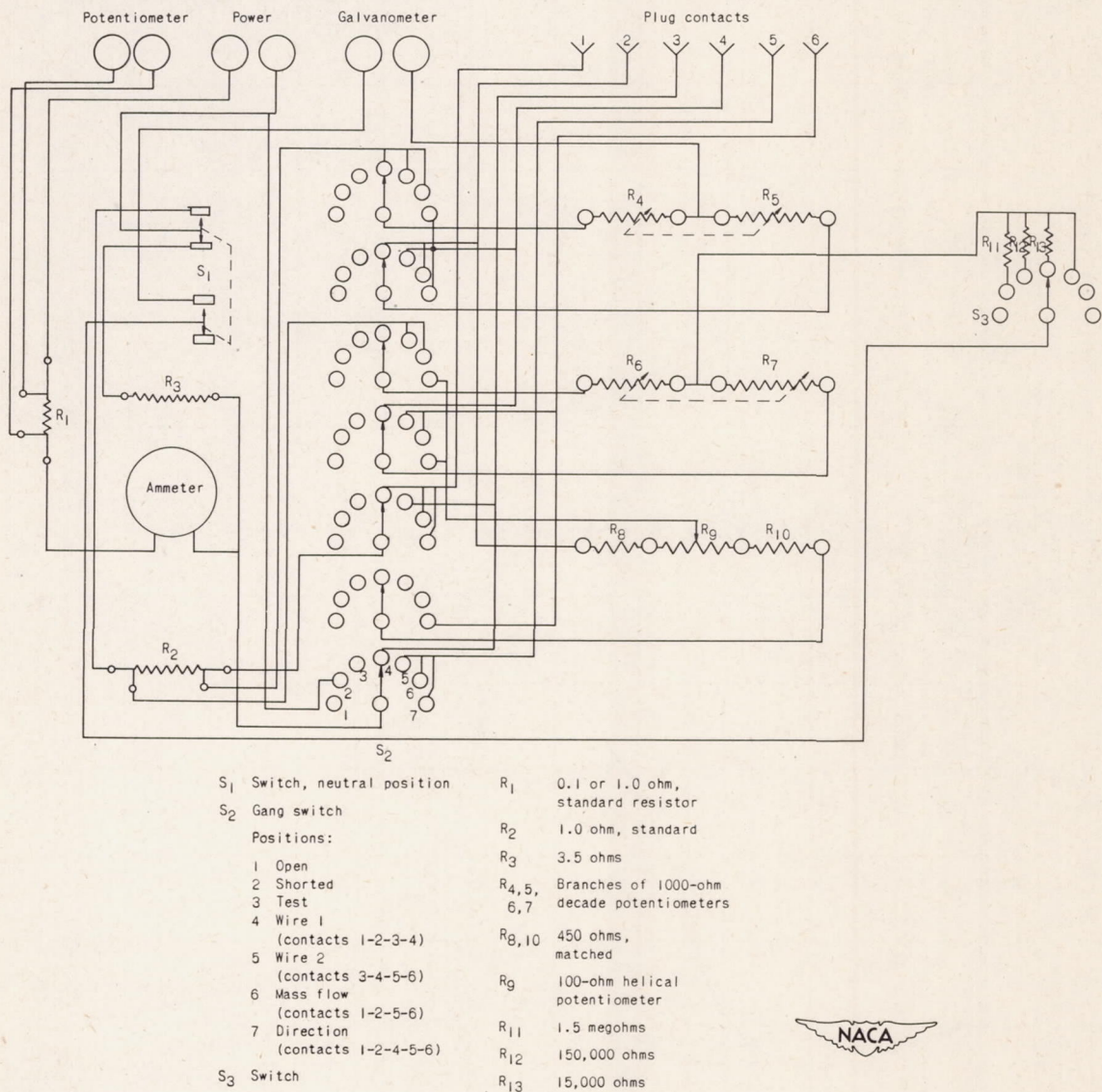
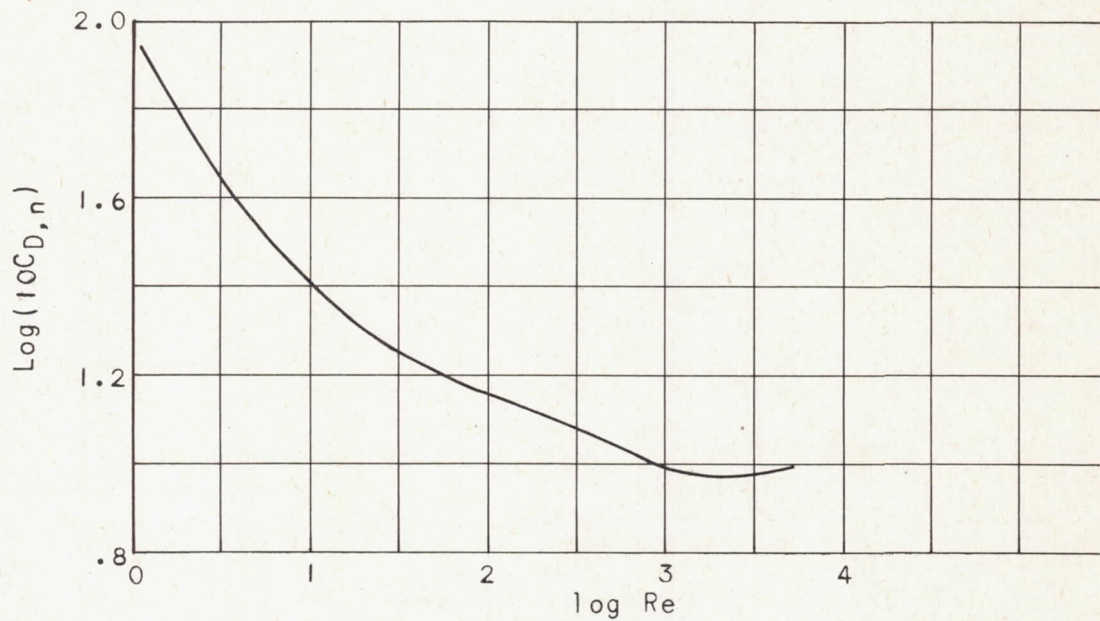
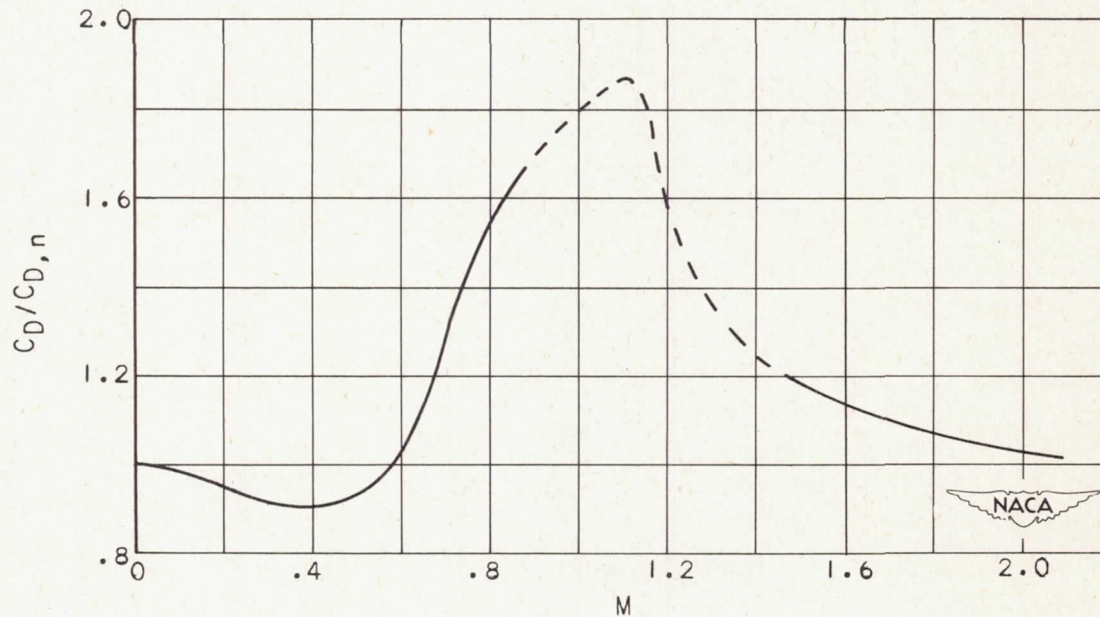


Figure 10. - Bridge circuit.





(a) Experimental data from reference 28.



(b) Experimental data from reference 29.

Figure 11. - Variation of drag coefficient with Reynolds and Mach numbers.



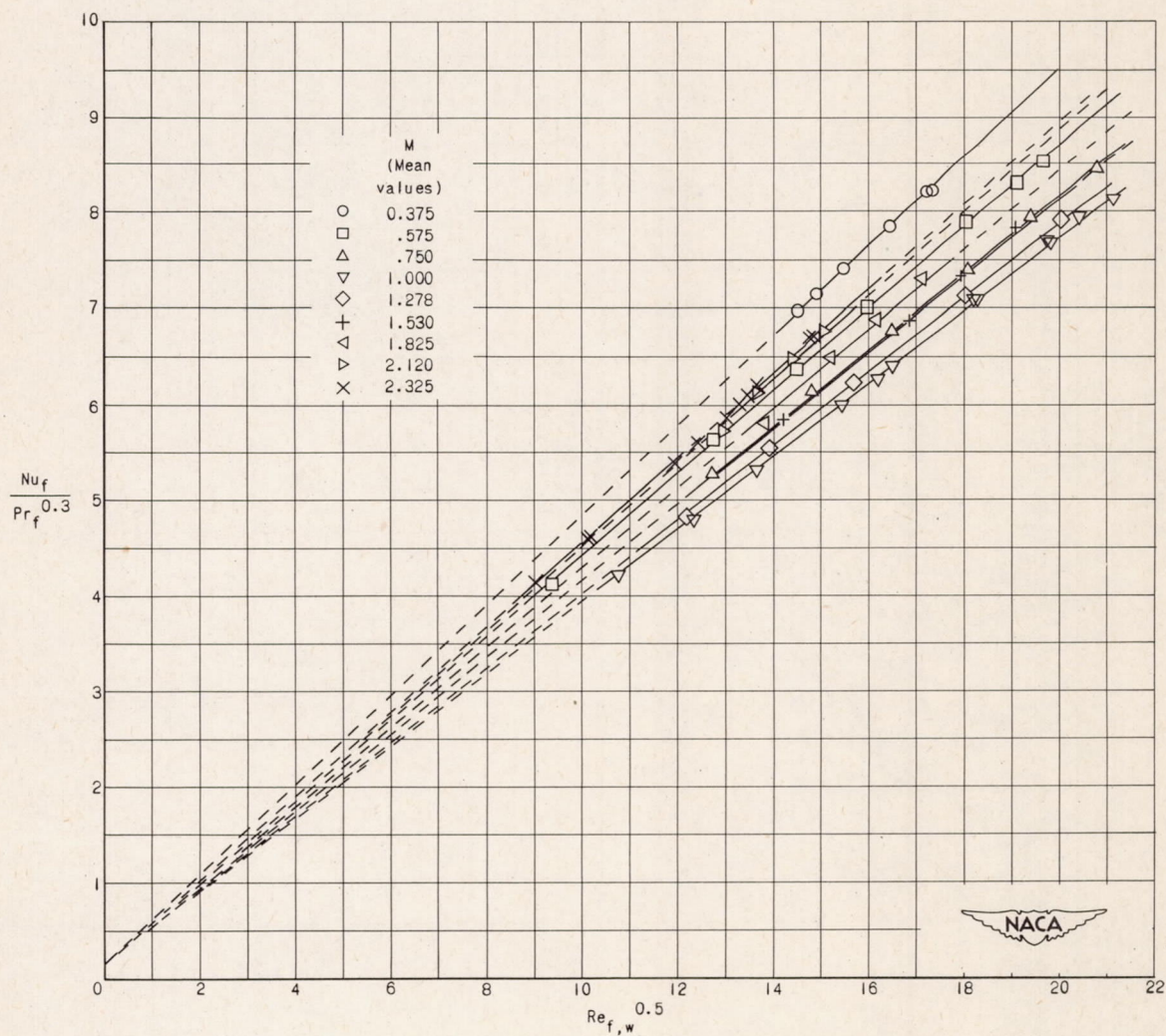


Figure 12. - Heat losses from wire normal to stream at fixed wire temperature. Mean wire temperature, 290° C; wire diameter, 0.0038 centimeter.



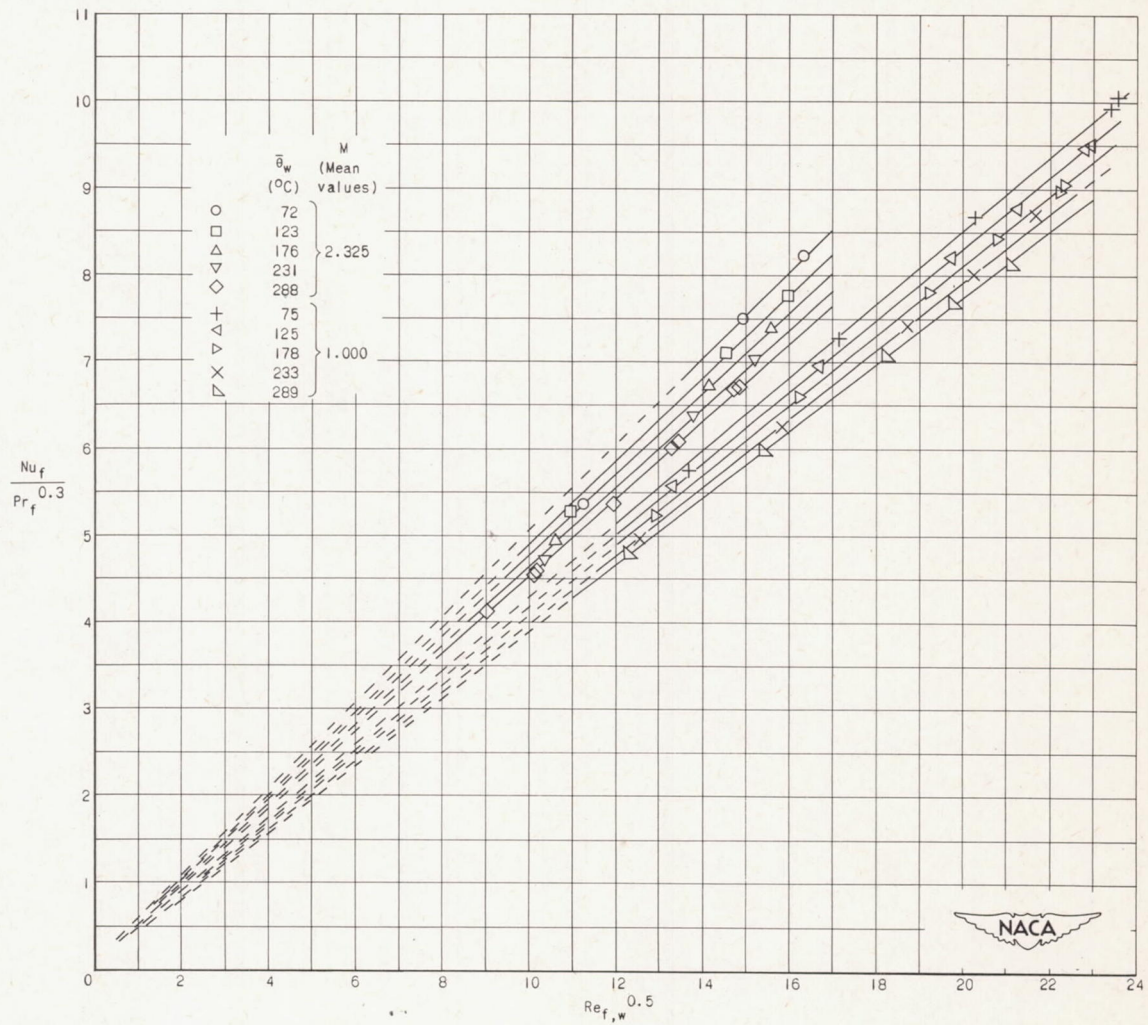


Figure 13. - Heat losses from wire normal to stream at several wire temperatures.



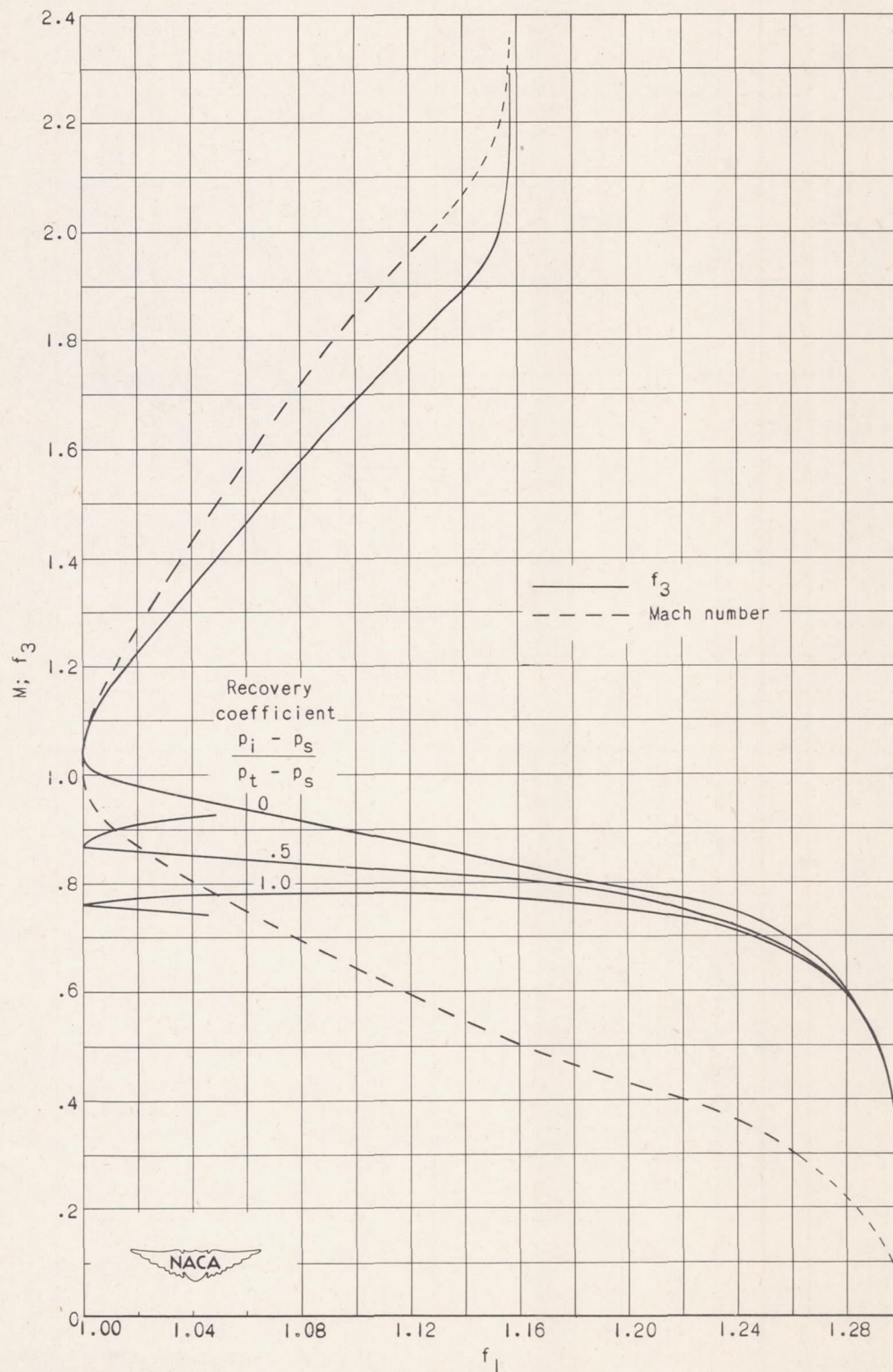


Figure 14. - Relations among Mach number and heat-loss parameters.



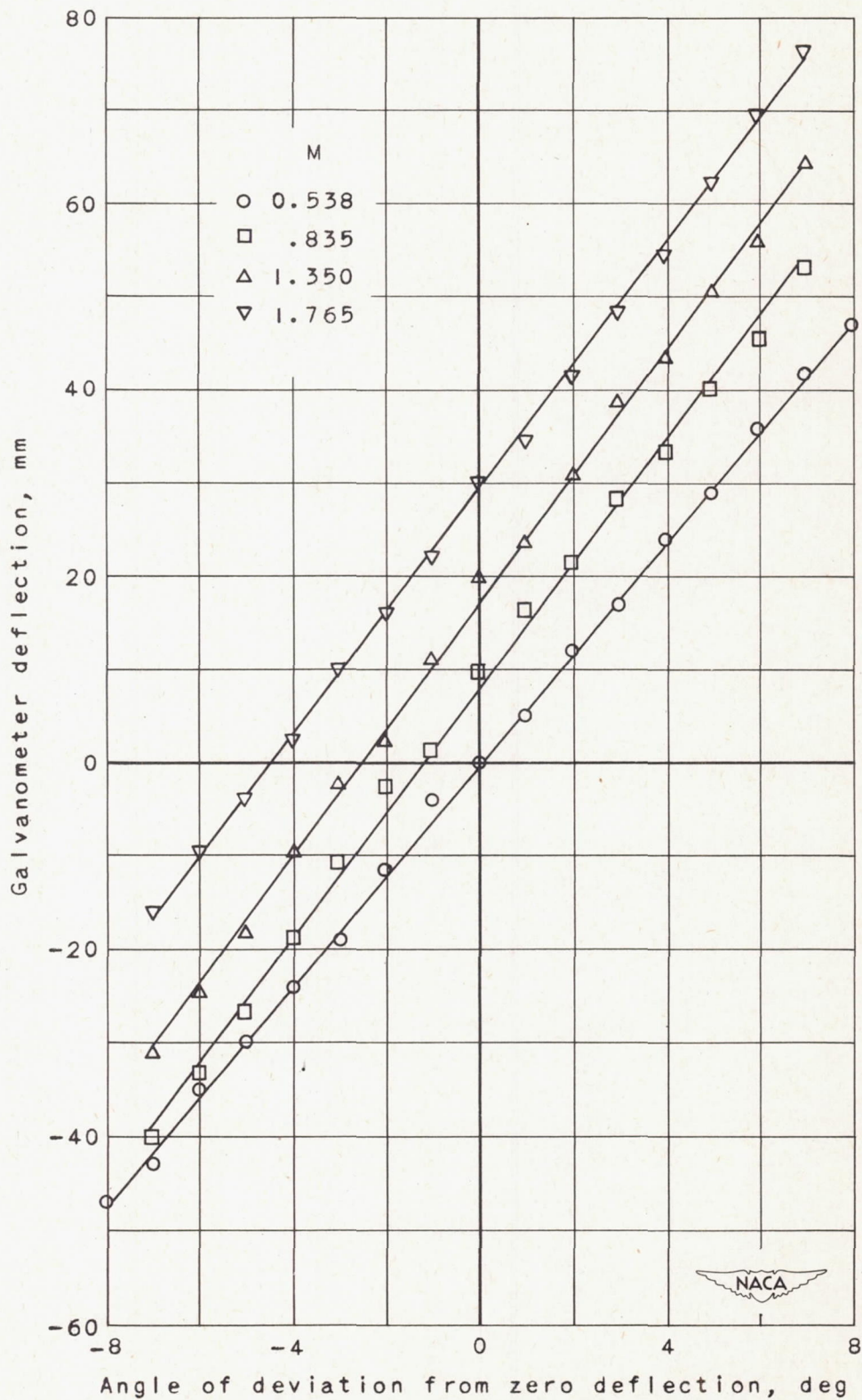


Figure 15. - Yaw characteristics of 90° V-wire.



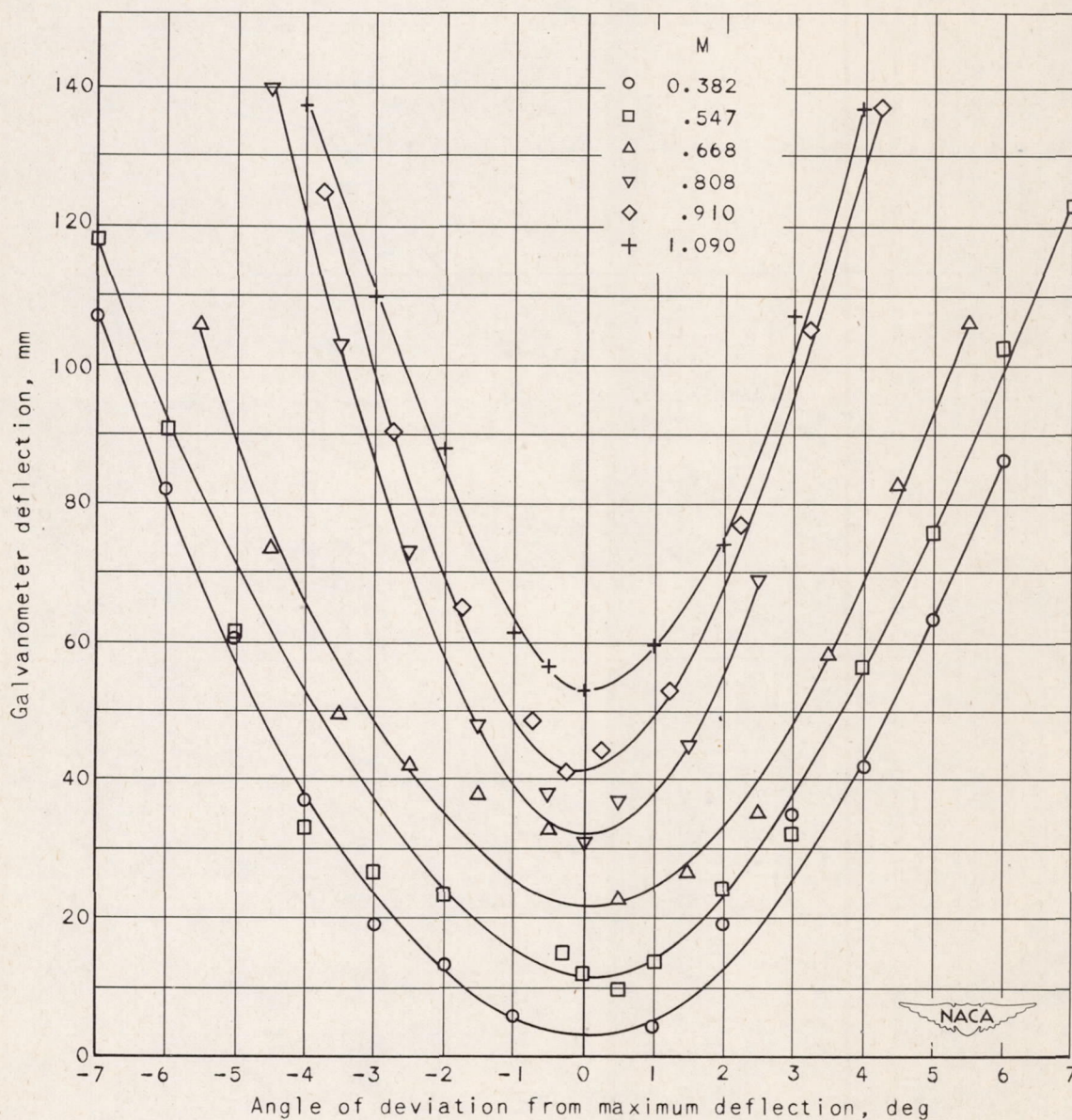


Figure 16. - Yaw characteristics of parallel-wire array.



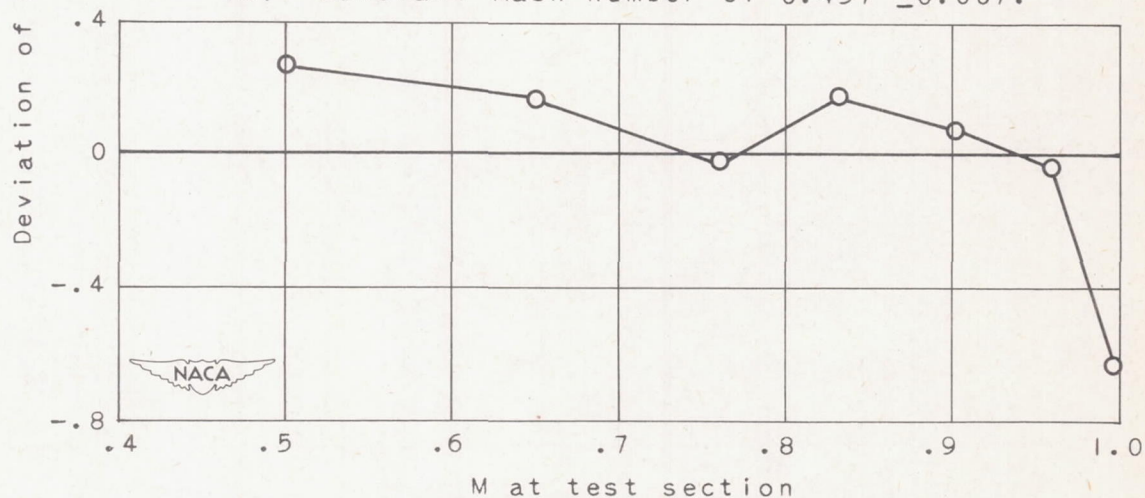
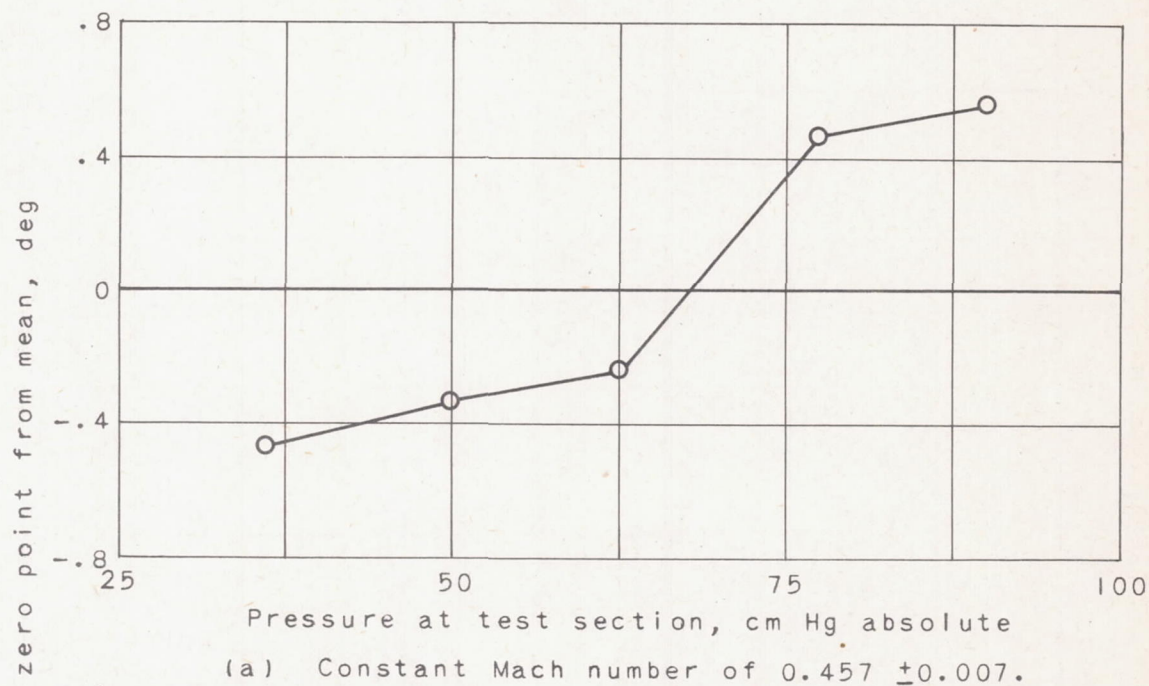


Figure 17. - Angular error of parallel-wire array.



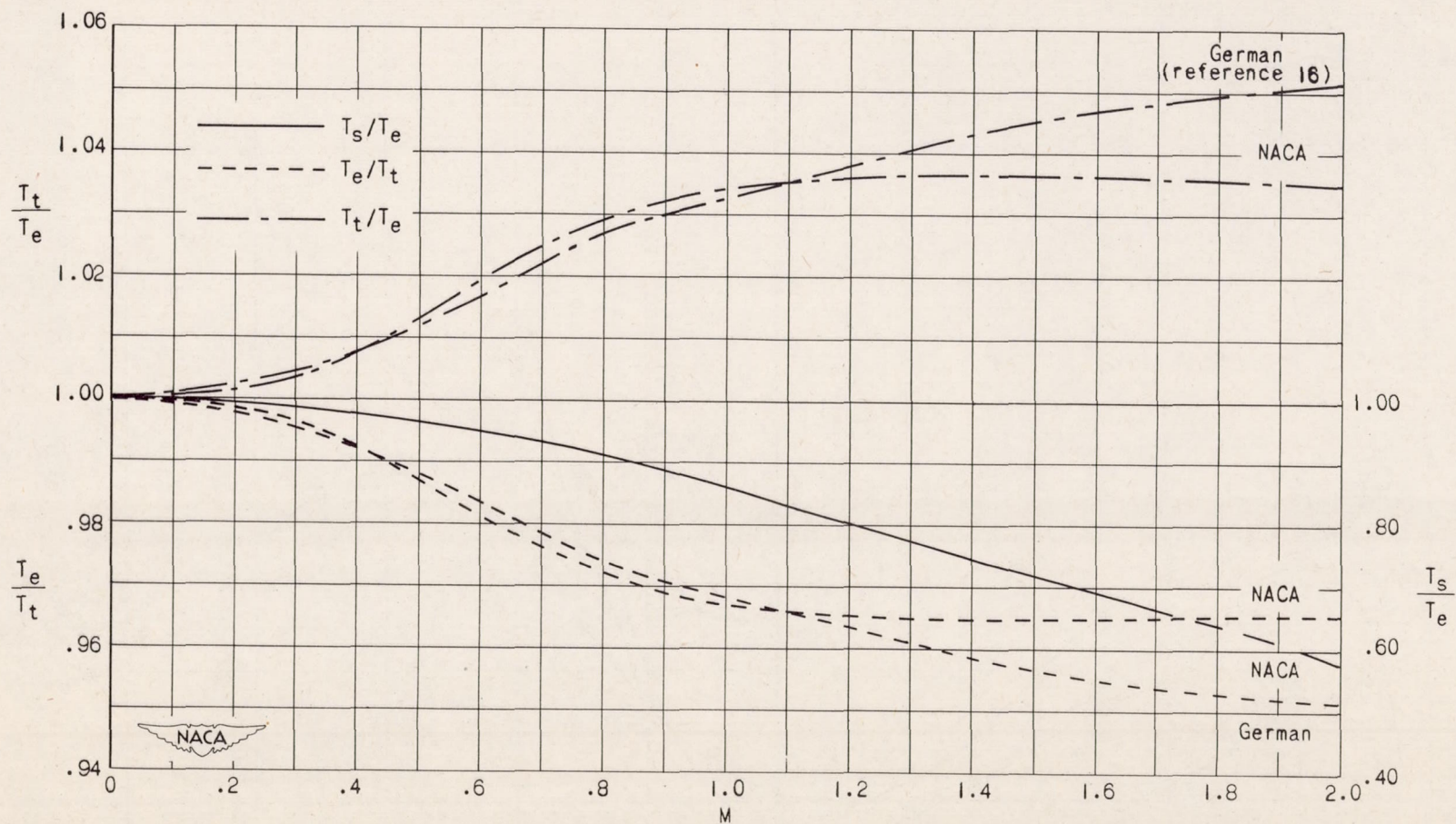


Figure 18. - Recovery ratios for circular cylinder normal to stream.



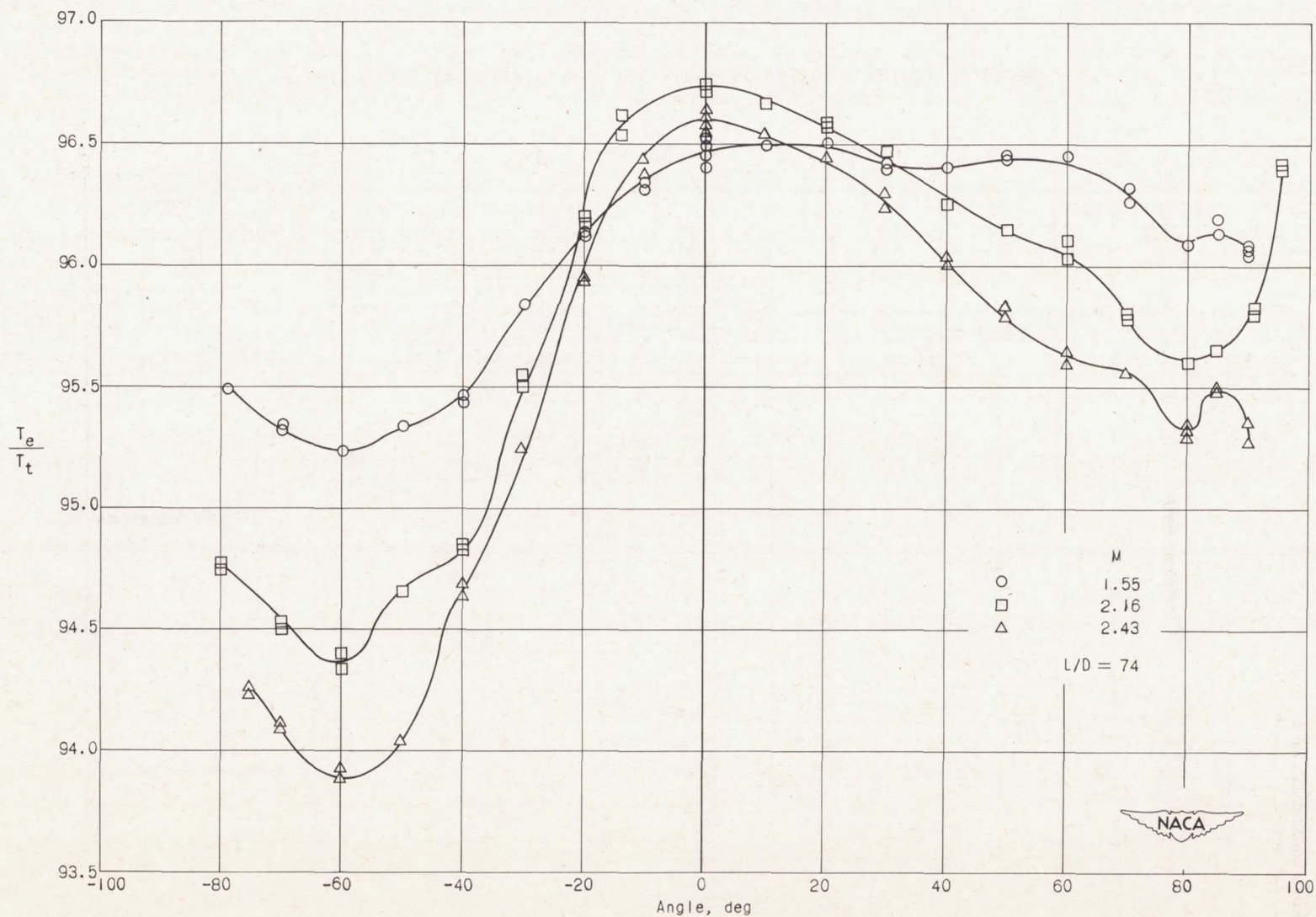


Figure 19. - Variation of ratio of effective to total temperature with angle between stream and normal to wire.